THE USE OF COLOUR IMAGE ANALYSIS FOR ASSESSMENT OF FIRE DAMAGED CONCRETE

SARAH E GUISE

Submitted for the Degree of Doctor of Philosophy

The University of Aston,

Civil Engineering Department

December 1997

THE UNIVERSITY OF ASTON

The Use of Colour Image Analysis for Assessment of Fire Damaged Concrete

Sarah Guise

Submitted for the degree of Doctor of Philosophy, December 1997

Thesis Summary

The aim of this project was to carry out a fundamental study to assess the potential of colour image analysis for use in investigations of fire damaged concrete. This involved:

(a) Quantification (rather than purely visual assessment) of colour change as an indicator of the thermal history of concrete.
(b) Quantification of the nature and intensity of crack development as an indication of the thermal history of concrete, supporting and in addition to, colour change observations.
(c) Further understanding of changes in the physical and chemical properties of aggregate and mortar matrix after heating.
(d) An indication of the relationship between cracking and non-destructive methods of testing e.g. UPV or Schmidt hammer.

Results showed that colour image analysis could be used to quantify the colour changes found when concrete is heated. Development of red colour coincided with significant reduction in compressive strength. Such measurements may be used to determine the thermal history of concrete by providing information regarding the temperature distribution that existed at the height of a fire. The actual colours observed depended on the types of cement and aggregate that were used to make the concrete. With some aggregates it may be more appropriate to only analyse the mortar matrix.

Petrographic techniques may also be used to determine the nature and density of cracks developing at elevated temperatures and values of crack density correlate well with measurements of residual compressive strength. Small differences in crack density were observed with different cements and aggregates, although good correlations were always found with the residual compressive strength.

Taken together these two techniques can provide further useful information for the evaluation of fire damaged concrete. This is especially so since petrographic analysis can also provide information on the quality of the original concrete such as cement content and water / cement ratio.

Concretes made with blended cements tended to produce small differences in physical and chemical properties compared to those made with unblended cements. There is some evidence to suggest that a coarsening of pore structure in blended cements may lead to onset of cracking at lower temperatures. The use of DTA/TGA was of little use in assessing the thermal history of concrete made with blended cements. Corner spalling and sloughing off, as observed in columns, was effectively reproduced in tests on small scale specimens and the crack distributions measured.

Relationships between compressive strength / cracking and non-destructive methods of testing are discussed and an outline procedure for site investigations of fire damaged concrete is described.

Keywords: Concrete, Fire, Durability, Colour, Image Analysis, Cracking, Structural Assessment.

Dedication

To my husband and long term soul mate for his understanding, tolerance and fantastic concrete technology. Without him I doubt whether this PhD would ever have been completed.

ACKNOWLEDGEMENTS

I am deeply indebted to my supervisor Dr. N. R. Short for his invaluable advice, wealth of experience, encouragement and for his immense support and help throughout the research and writing of this thesis.

I am also grateful to Dr. J. A. Purkiss, my associate supervisor, for his guidance and suggestions on this project.

Thanks also go to, the technical staffs of Civil Engineering Department, in particular Mr. C. Thompson, Mr. J. Hollins and Mr. M. Lyons.

Along with thanks to Dr. R. Connolly and Mr. W. Morris of the Fire Research Station for their invaluable advice on furnace designs.

I wish to thank my research colleagues and friends, Dr. M. Webber, Dr. P. Edmunds, Dr. D. Greene and P. Purnell for their help and advice through difficult times.

Finally, I am very grateful to the Engineering Physical Science Research Council (EPSRC) and Civil Engineering Department for their financial support.

LIST OF CONTENTS

LIST OF TABLES

LIST OF FIGURES

CHAPTER 1 INTRODUCTION AND AIMS OF STUDY

When concrete is subjected to high temperatures as in a fire, there is a deterioration in its properties. Of particular importance are cracking, spalling, reduction of elastic modulus and compressive strength of the concrete and reduced yield and tensile strength, ductility, and bond of any steel reinforcement. To determine whether a fire damaged structure can be repaired rather than the more costly alternative of demolition and rebuild, an assessment of structural integrity must be made. As part of this process it is necessary to assess the extent of deterioration of the concrete itself.

Assessment of fire damaged concrete usually starts with visual observation of colour change, crazing, cracking, and spalling. On heating above 300°C, the colour of concrete can change (Bessey, 1950) from normal to red (300-600°C), to whitish grey (600-900°C), and then buff (900-1000°C). The red discolouration results from the presence of iron compounds in the fine or coarse aggregate. Change of colour from normal to red at around 300°C is useful since it coincides with the onset of significant loss of concrete strength (£0% or greater of the original strength) as a result of heating. Thus in practice any concrete which has turned red after a fire is regarded as being suspect of deterioration. Cutting back the concrete should give a good idea as to the depth to which temperatures greater than 300°C have been exceeded. The colour change to red is more prominent with siliceous aggregates; calcareous and igneous aggregates being less susceptible to this effect. Thus just because the concrete is not visibly red does not mean that the concrete is undamaged.

These visual observations may then be supported by various tests which give an indirect indication of the condition of the concrete. These include: core tests, rebound hammer test, ultrasonic pulse velocity test (UPV), Windsor probe, BRE internal fracture test, and the thermoluminescence test. The advantages and disadvantages of these will be discussed

in more detail in Chapter 3. Whilst these tests are valuable aids in assessment, they do not give a complete picture of the extent of deterioration.

Optical microscopy applied to petrographic thin sections has been used extensively in investigations of concrete microstructure for examining features such as : deleterious aggregate reactions, micro-cracking or porosity variations in the cement matrix and other phenomena related to mechanisms of deterioration. Recently this technique has been applied to fire damaged concrete (Riley, 1991) where results suggested that the nature and extent of cracking may be correlated with the actual temperatures attained in the concrete. However, quantification of the crack patterns found was not attempted.

The information gained using optical microscopy may be considerably extended by detailed analysis of the image observed. This may be carried out by analysing images in terms of grey scale or colour using red, green and blue. Recent developments in image analysis utilise a new technique whereby analysis of colour is based on hue, saturation and intensity. This allows greatly improved discrimination of colour threshold and quantification of colour to a high accuracy. This is considered to have considerable advantage for application to concrete sections viewed in reflected or transmitted polarised light.

The aim of the present investigations was to take advantage of these recent developments in colour image analysis and carry out a fundamental study in order to assess its potential for use in investigations of fire damaged concrete. This has involved the analysis and quantification of changes in (i) colour, and (ii) the nature and intensity of cracking.

The objectives of the work were to provide :

(a) Quantification (rather than purely visual assessment) of colour change as an indicator

of the thermal history of concrete.

(b) Quantification of the nature and intensity of crack development as an indication of the thermal history of concrete, supporting and in addition to, colour change observations.

(c) Further understanding of changes in the physical and chemical properties of aggregate and mortar matrix after heating.

(d) An indication of the relationship between cracking and non-destructive methods of testing e.g. UPV or Schmidt hammer.

CHAPTER 2 LITERATURE REVIEW - GENERAL

2.1 REINFORCED CONCRETE

Concrete and steel are the two most commonly used structural materials. They sometimes complement one another, and sometimes compete so that structures of a similar type and function can be built using either of these materials. Steel is manufactured under carefully controlled conditions; its properties are determined by laboratory testing and described in the manufacturer's certificate. When using concrete the situation is totally different. The quality of the cement is usually guaranteed by the manufacturer but it is the concrete, which is the building material. Reinforced concrete is used for structural purposes in buildings for floor slabs to prevent cracking and in beams and columns for added flexural strength and to prevent bursting forces acting on the concrete.

The term concrete refers to the composite mixture formed from Portland cement, water and aggregate. Typically the aggregates form the bulk (70-80%) of the volume of concrete. Other materials, such as admixtures or partial cement replacement materials may be added to the basic constituents.

2.1.1 Cement

The cement is the bonding material in the concrete, the principal constituents of which are Tricalcium silicate or Alite, (C_3S), Dicalcium silicate or Belite, (C_2S), Tricalcium aluminate (C_3A) and Tetracalcium aluminoferrite (C_4AF). The hydration reaction between cement and water is exothermic. The reaction is very complex and the following is a simplified description of the reactions of the individual compounds of the cement with water (Neville, 1995).

(i) Rehydration of calcium sulfate hemihydrate to reform Gypsum.

Hydration of free lime.

Rapid reaction of C_3A with water to form C_3AH_6.

Reaction of C_3A with Gypsum, to prevent flash set of the cement, to form calcium sulfoaluminate (ettringite).

Secondary transformation of ettringite into a monosulfate ($C_3A.CS.H_{16}$).

C_4AF phase occurring over same time scale.

(ii) The alite (C_3S) reacts to form a tricalcium disilicate hydrate (CSH gel) and Portlandite ($Ca(OH)_2$), providing the initial strength.

The belite (C_2S) reacts more slowly but produces identical products to that of alite and increases longer term strength.

2.1.2 Cement Replacement

These constituents are used, as the name suggests, as a partial replacement of cement. Pozzolanic material contains active silica (SiO_2) and in a finely divided form will chemically react with calcium hydroxide to form cementitious compounds in the presence of moisture.

The main cement replacement materials are :

(i) Pulverised fuel ash (pfa) - obtained from pulverised coal used to fire power stations

(ii) Ground granulated blast furnace slag (BFS) - obtained from the 'scum' formed in iron smelting in a blast furnace

(ii) Condensed silica fume (csf) - often called microsilica; very fine particle of silica condensed from the waste gases given off in the production of silicon metal

The CSH production from the pozzolanic reaction is secondary to that from the Portland cement, which results in low early strengths.

2.1.3 Aggregates

With one or two exceptions the aggregates used in concretes can be regarded as inert fillers; i.e. they do not hydrate, and they do not swell or shrink. Aggregates can be obtained either from natural sources, such as gravel deposits and crushed rocks, or specifically manufactured for use in concrete. The three groups of aggregate in terms of their specific gravity are :

(i) Normal density aggregates including, gravels, igneous rocks such as basalt and granite and stronger sedimentary rocks such as limestone and sandstone. All have specific gravities within the range of 2.55 - 2.75 and therefore all produce concrete with similar densities in the range 2250 - 2450 kg/m^3 depending on the mix proportions.

(ii) Lightweight aggregates are used to produce concretes of lower density. The reduced specific gravity is obtained from the air voids within the aggregate particles. Artificial lightweight aggregates are now widely available and include sintered pulverised ash, expanded clay or shale and foamed slag.

(iii) Heavyweight aggregates, e.g. are used when high density concrete is required such as radiation shielding.

2.2 FIRE

In general a fire starts because a material is ignited by a heat source, e.g. cigarette ends, electric sparks, etc. and is able to continue by a supply of combustible material.the flame of a match or the heat of a stove or hot iron. It is known that, if this happens with a wall lining, the fire, depending on the nature of the lining and the circumstances, may spread very rapidly. A contributory cause of the rapid spread of a fire in compartments of a rather limited size, such as offices, living rooms and classrooms, is the accumulation in the enclosure of the heat produced by the burning material. Because of this, other materials in the room may be heated so severely that after a short time they also ignite (Lie, 1972), this is known as flashover.

In order to fulfil Building Regulation requirements it is normal to carry out full scale fire tests on new building constructions or elements of structures to obtain information on their performance. Elements such as walls, floors and roofs must be able to contain a fire within the compartment in which it started and possess sufficient resistance to thermal transmission to prevent excessive temperature increases in other compartments for a specified period. They must also maintain their structural function without excessive deflection, collapse or rupture which would allow the fire to spread to other areas or endanger life.

The temperature-time response in a fire compartment depends on the available combustible material, the air supply available for combustion and the thermal properties of the compartment boundaries. This situation is often referred to as a real fire. However the temperature-time curve generated in a furnace test is governed by the standard to which the test is being carried out (Lie, 1972).

2.2.1 Development of Fires

The development of compartment fires can be broken down into three phases, illustrated in Figure 2.1 (Purkiss, 1996) :

(i) Pre-flashover (growth period) - Temperatures are low and damage relatively small, although the growth period may be extensive.

(ii) Post-flashover (burning period) - The rate of temperature rise throughout the compartment is high, as the rate of heat release within the compartment reaches a peak. The rate of temperature rise continues until the rate of generation of volatiles from the fuel bed begins to decrease as the rate of fuel consumption decreases, or when there is insufficient heat available to generate such volatiles. It is during this period that structural elements are exposed to the worse effects of the fire.

(iii) Decay phase - Once the temperature rise has peaked the decay phase commences. The temperature then begins to decrease.

2.2.2 Fire Resistance

Fire resistance testing is still the most common method of determining the fire resistance of a structural element. Reinforced concrete is one of the best fire resistant materials in structural use and can therefore be used effectively to shield other structural materials such as steel. Fire resistance depends on the actual load level of the concrete, shape and thickness of the structural members, the layout of the reinforcement, the water content and many other factors. Another reason to assess the properties of concrete at high temperatures arises from its various applications in chemical and civil engineering.

2.2.3 Standard Fire Curve

During a fire resistance test a specimen is exposed to heating in accordance with a standard temperature-time relationship. This is to standard BS 476: Pt 20: 1987, using the following equation, for cellulosic type conditions :-

$$\theta_g = 20 + 345 \log(8t + 1) \qquad (2.1)$$

where, θ_g = furnace temperature (°C)

t = time (minutes).

This equation is shown graphically in Figure 2.2. The standard curve gives temperatures of 842°C at 30 mins., 945°C at 60 mins and 1049°C at 120 mins.

2.3 EFFECT ON THE PROPERTIES OF STEEL

The effects of heat on steel are most severe at elevated temperatures, therefore care must be taken to inspect for buckling and deformation. In general temperatures up to 500°C are unlikely to affect mechanical strength properties of the steel significantly and sufficient strength may still be present after heating to higher temperatures. As a result of recrystallisation cold worked steel is more vulnerable than hot rolled.

Temperatures of 500-600°C are critical for reinforcing bars where the strength loss exceeds any potential safety (load) factors. Accepting that temperatures in the concrete surrounding the steel can be estimated, there is no need for a 'direct' determination of steel properties. Also direct determination of steel properties is expensive in that concrete may need cutting away and the structure propped (Illston, 1994).

The effect on the residual yield strength and ductility of steel reinforcement after cooling is for all practical purposes negligible in the temperature range up to 800°C for mild steel and for typical hot-rolled high-yield steels. On the other hand some cold-worked steels may only possess 65% of the original yield strength after cooling from this temperature again due to recrystallisation (Illston, 1994).

If a sufficient length can be removed then ultimate tensile strength, proof stress and modulus of elasticity can be tested mechanically. If this is not possible a sample of a few millimetres should be sufficient for a competent metallurgist to judge if significant effects have occurred by metallographic examination.

2.3.1 Strength of Bond with Reinforcing Steel

For reinforcing steel to carry stresses and fulfil its design purposes there must be sufficient bond between the steel and the surrounding concrete. The bond is adversely affected by high temperatures.

Kasami *et al.* (1975) reported pull-out tests on plain round steel bars in concretes made with ordinary Portland cement and four different gravel aggregates. The 'residual' bond stress was calculated when the slip at the unloaded end of the steel bar was 0.025 mm. It was found that on average, the residual bond strength after cooling from 300°C was approximately 50% of that before exposure to high temperatures.

In a later paper Diederichs & Schneider (1981) attributed the loss of bond strength to differential expansion between the concrete and the corresponding internal stresses set up at the high temperatures. It was concluded that bond strength is reduced as the temperature increases. The percentage reduction is greater than the corresponding reduction in the compressive and tensile strengths. The percentage reduction in bond strength for

deformed bars as temperature is increased is generally less than for plain round steel bars. The differences in the diameters of plain bars had little effect on the percentage reduction in bond strength. Kasami *et al.* (1975) concluded that the type of aggregate affects the bond strength at high temperatures. Work was also carried out by Morley & Royles (1983), it was found that the bond performance was very much dependent upon the concrete strength and the reductions in bond strength with temperature were greater than the corresponding reduction in the concrete compressive strength.

2.4 EFFECT ON THE PROPERTIES OF CONCRETE

In general concrete has good resistance to fire. It is non-combustible, and the length of time under fire that concrete continues to perform is high and no toxic fumes are emitted. The relative criteria for performance of concrete when used as a protective material for steel are load carrying capacity, resistance to flame penetration and resistance to heat transfer.

When considering concrete as a material, the fire will introduce high temperature gradients and as a result the hot surface layers tend to separate and spall from the cooler interior of the body.

2.4.1 Compressive Strength

Strength is probably the most important single property of concrete. Dehydration and transformation reactions, changes in porosity and pore pressures, and differential deformation of hardened cement paste and aggregates that occur at high temperatures may have important effects on the strength of the concrete. The results published by different investigators have indicated wide differences. These differences are due to mix proportions and the nature of materials, including the variety of cements, used in the concrete as well as the different conditions under which the tests are carried out and the age

of the concrete when tested.

2.4.2 Effect of Maximum Temperature and Rate of Heating/Cooling

Generally unsealed concrete specimens made with conventional aggregates generally show a sharp reduction in strength when exposed to temperatures of 300°C and above.

Malhotra (1956) found that heating concrete to temperatures less than 300°C resulted in a less than 10% strength reduction, heating to 500°C gave a 50% reduction and 600°C resulted in a 75% reduction.

Mohamedbhai (1986) examined the effects of exposure time and rates of heating/cooling on strengths of concrete heated to temperatures from 200-800°C. Basalt aggregate concrete was heated to the required temperature, exposure time varied form 1-4 hours and the rate of heating and cooling examined. For slow heating, cubes were placed in an initially cool furnace, while quick heating consisted of samples placed in a preheated furnace to the maximum temperature required. Slow cooling allowed samples to cool in the furnace for 2 hours and then in air, while quick cooling was immediate air exposure. The results in Figure 2.3 indicate that there is variation in the values of residual strength for any furnace temperature, i.e. at 200°C the reduction in strength can range from 8-50%, while at 800°C the reduction varies between 63-77% depending on the exposure time and the rate of heating and cooling. From this work it was concluded that :-

(i) The exposure time beyond one hour had a significant effect on the residual strength of concrete, but the effect diminished as the level of exposure increased. The bulk of strength loss occurred within the first two hours of temperature exposure.

(ii) The residual strengths of concrete after one hour of exposure t 200, 400, 600 and 800°C could be expected to be 80, 70, 60 and 30% respectively, of its unheated strength. The corresponding residual strengths after two or more hours of exposure were of the order of 70, 60, 45 and 25%.

(iii) At temperatures of 600°C and above, the rates of heating and cooling did not produce significantly different results.

Abrams (1971) investigated the strength of concretes heated for a short period of time. He found that specimens that were heated, cooled and then tested had a lower residual strength than those tested in the hot state. It was also reported that the original strength of the concrete had little effect upon the high temperature strength. With the large amount of work existing on high temperature effects on concrete it is not a surprise that different test procedures exist. Abrams' (1971) results agree broadly with those of Malhotra (1956), however the reductions in strength up to 600°C were greater.

Kaplan & Roux (1972) investigated concrete for applications with nuclear reactors. Concrete specimens were exposed to temperatures between 100-400°C, for 6 hours and then cooled. They reported that for a given exposure to a given temperature, concretes of a higher initial strength show a larger drop in residual strength than weak mixes. These results are not consistent with those of Abrams who found the original strength of the concrete to have no effect. Kaplan & Roux reported that a reference mix with an unfired compressive strength of 57.6 N/mm^2 showed a 15% reduction at 100°C, 5% increase at 250°C and a 10% reduction at 400°C. Their conclusion explains that age and the resultant strength at the time of firing and testing affected the results. These problems show the difficulty of fire testing and the large number of factors that can have an effect on the compressive strength of concrete.

The most rapid form of cooling is by quenching the specimen and this can be achieved by immersing, or spraying it with water. Zoldners (1960) found that up to 500°C, the strength of quenched samples was 30% lower than air cooled samples. However, Zoldners obtained reductions for siliceous, calcareous and expanded slag aggregate concretes, at 500°C of 30% but Abrams (1971) reported 50%. It is important to point out that Zoldners did cool some of the specimens by quenching them in water for 5 minutes after their removal from the furnace which would effect strength reduction. The quenched samples had lower compressive strengths than unquenched ones. The quenching produced a severe temperature gradient in the concrete which caused large strength reductions. Above 500°C Zoldners results showed that quenched and unquenched specimens were similar and in some cases quenched concrete was stronger.

In general it has been found that above 300°C the compressive strength of concrete is adversely affected by elevated temperatures. Below this temperature some concretes may show an increase in strength whereas others may exhibit slight decreases, but the variation is normally not less than 10%. The rate of heating and cooling also effects measured strengths with sharp alterations in temperature causing damage to the material.

Nassif *et al.* (1995) identified a new quantitative method of assessing fire damage to concrete by using a stiffness damage test. The stress-strain loops were found to change in characteristics with a sudden increase in the damage index at 320°C correlating well with temperatures of significant strength loss.

2.4.3 Aggregate Type

When considering concrete performance at high temperatures the effects of aggregate must be taken into account. It has been suggested by Philleo (1958), Harada *et al.* (1972) and Cruz & Gillen (1980) that ordinary Portland cement expands up to temperatures of about

150-200°C and shrinks rapidly on exposure to temperatures above this level due to water loss. Normal concrete aggregates however, continue to expand over the whole range of temperatures exposed to. The loss of strength is considerably lower when the aggregate does not contain silica (Neville, 1995).

Abrams (1971) concluded at temperatures above 450°C siliceous aggregate concrete loses a greater proportion of its strength than concretes made with carbonate or expanded shale aggregates but, once temperatures of 800°C and above are reached the differences disappeared, as is shown in Figure 2.4. Unstressed and stressed specimens (load ratio 0.4 of original strength) were tested while hot. This was considered to be due to the abrupt volume change that occurs because of the inversion, at 573°C, of α to β quartz in siliceous aggregate. The applied stress level during heating had no significant effect on compressive strength at a given temperature. The original strength of the concrete also had little effect on the percentage of compressive strength retained after cooling.

Other aggregates may undergo different forms of internal disruption, such as limestones and dolomites. These aggregates undergo calcination of the calcium or magnesium carbonate at elevated temperature. Calcination affects the temperature transmission through the concrete by absorbing available heat to allow the endothermic reaction to occur.

Ingburg (1929) grouped aggregates into four different classes depending on their performance during fire tests on concrete. Group I included calcareous aggregates such as limestones and dolomites and was considered to be the least disruptive group. Group II aggregates included non-quartzose silicate aggregates composed mainly of feldspar. This group did not cause cracking or spalling during tests, it is composed of common aggregates such as basalt, diabase and dolerite. Saemann & Washa (1957) and Harmathy & Berndt (1966) tested unstressed calcareous and lightweight aggregate concretes and

obtained broadly similar results.

Ingburg considered Group III aggregates to be those subject to cracking and spalling in fire tests including igneous rocks with high silica contents than Groups I and II. The group included aggregates such as granites, feldspars and sandstones. Group IV contained rocks that showed the most detrimental effects on concrete. The aggregates contained in this group were quartz, quartzites, chert and flint.

Concrete with a low thermal conductivity has a better fire resistance so, for instance, lightweight concrete stands up better to fire than ordinary concrete. Lightweight aggregates are mainly from products of high temperature furnaces or kilns and after cooling, usually have a good stability during reheating which is probably due to their porous structure and glassy composition.

Weigler & Fischer (1972) heated concretes up to 600°C, the aggregates used were barytes and quartz. At temperatures of 300°C, the unstressed residual strength was 80% of the original. Barytes aggregate concrete was more heat resistant than quartz aggregate. Unstressed specimens tested hot generally had smaller reductions in strength compared to those cooled before testing.

Khoury *et al* . (1986) carried out tests on compressive strength of concrete made with limestone, basalt, siliceous gravel and lightweight aggregates while investigating transient thermal strain. The specimens were heated at either 0.2°C/min (slow) or 1.0°C/min (fast) while unstressed and stressed at 10, 20 and 30% of the original unheated compressive strength. After heating to 600°C the residual strengths of the unstressed specimens were 20, 30, and 40% for limestone, lightweight and basalt aggregate concretes respectively. The siliceous aggregate concrete was so badly damaged it could not be tested. It was suggested that the losses in strength could be due to (i) damage to the aggregate, (ii)

weakening of the bond between the aggregate and cement paste, and (iii) reduction in the strength of hardened cement paste due to an increase in porosity, partial breakdown of calcium silicate hydrates, chemical transformation due to hydrothermal reactions and the development of cracking.

2.4.4 Applied Stress

Malhotra (1956) tested unsealed concrete specimens to determine the compressive strength while hot. The strength was also determined for samples that had been allowed to cool after exposure to high temperatures for comparitive purposes. Before heating commenced the samples were preloaded to 20% of their strength before heating. The mix proportions varied through the procedures, the concrete consisted of an OPC and river gravel. Temperature exposure of less than 200°C effected the compressive strength only very slightly. Higher temperatures the reductions were greater and depended upon the test conditions. A concrete with an aggregate/cement ratio of 6:1, was heated to 500°C. A 35% strength loss occurred for concrete stressed and tested hot, 60% for unstressed hot concrete and 80% loss for unstressed cool concrete. The strength losses for a concrete with an aggregate/cement ratio of 4.5:1 were greater than for a 6:1 concrete.

Abrams (1971) also reported compressive strength measurements for calcareous, siliceous and expanded shale aggregate concrete heated to temperatures from 93-871°C were also reported. The following tests were then performed:

(i) **Unstressed** - unloaded specimen was heated to test temperature and then loaded to failure whilst hot

(ii) **Stressed** - the specimen was loaded in compression and then heated to the test temperature. The load was then increased until failure occurred. Load ratios of 0.25, 0.4 and 0.55 of the unheated strength were applied.

(iii) **Unstressed residual** - the unloaded specimens were heated to the test temperature and allowed to cool. They were then loaded to failure after 7 days.

The strengths were recorded as a percentage of the original compressive strength. The results are given in Figure 2.5 for calcareous aggregate stressed to a 0.4 ratio. For all tests there was a significant decrease in strength at temperatures above 650°C, possibly due to decarbonation of the aggregate. The strengths of the unstressed specimens, tested while hot gradually reduced, at 650°C the reduction was 25% and at 800°C it was 70%.The reduction in strength was always greater for unstressed specimens compared to stressed. The unstressed residual showed the greatest losses. The results for the other aggregates tested also indicated that specimens stressed had smaller reductions than ones which were unstressed when heating. This may have been due to crack formation being inhibited during restrained heating (Purkiss & Bali, 1988).

Schneider (1986) drew the following conclusions on high temperature influence on strength characteristics:

(a) Original strength of concrete has little effect on strength-temperature characteristics, agreed by Abrams (1971), but Kaplan & Roux (1972) disagreed.

(b) Water/cement ratio within the practical range of usage for concrete hardly influences the high temperature-strength characteristics of concrete, agreed by Malhotra (1956).

(c) Aggregate/cement ratio has a significant effect on the strength of concrete exposed to high temperatures. The reduction being proportionally smaller for lean mixes than for rich mixes, agreed by Malhotra (1956).

(d) Different types of aggregate influence the strength-temperature characteristics. The decrease in strength of calcareous and lightweight aggregate concretes occurs at high temperatures compared to siliceous concretes. The type of aggregate seems to be one of the main factors influencing the high temperature strength, agreed by Abrams (1971) and Ingburg (1929).

(e) Type of cement has little effect on a strength-temperature characteristic, agreed by Carette *et al.* (1982).

(f) Maximum size of aggregate seems to be a second order factor as investigations of mortars and and various concretes demonstrate, agreed by Davis (1967).

(g) Sustained stress during the heating period influences the shape of the strength-temperature relationship significantly. It is evident , that the stressed strength is higher than the unstressed strength. The stress level itself has little effect on the ultimate strength as long as the stress ratio is greater than 0.2 of the original concretes strength, agreed by many investigators including Abrams (1971), Khoury *et al.* (1986), Malhotra (1956) and Weigler and Fischer (1972).

In general, the application of compressive stresses to concrete during heating is beneficial in terms of residual strength probably due to closing of microcracks in areas in compression, although there is an upper limit.

2.4.5 Flexural Strength

Concrete is normally designed to act in compression, but it also undergoes flexural stresses in structural elements. Concrete experiences flexural stresses in situations such as beams or slabs.

The flexural strength of concrete subjected to elevated temperatures shows greater losses than the compressive strength under identical conditions. Zoldners (1960) confirmed this by testing fired beams after cooling in flexure and the resulting beam ends in compression. At 400°C the flexural strength was between 45 and 60% lower than for the compressive strength. Aggregates that performed well in compression did not act similarly in flexure. Expanded slag aggregate maintained 71% of its unfired strength after exposure to 600°C, but had only 16% of its normal flexural strength after 400°C. This was explained by Zoldners that the reduction in flexural strength is dependent upon the development of microcracking. Kaplan & Roux (1972) tested siliceous aggregate concrete beams for flexural strength in the hot state. Their results showed that the maximum temperature and the mix proportions of the concrete were important factors for reduction of flexural strength. Mixes with a higher water/cement ratio were affected to a greater extent than mixes with lower ones. At 400°C high water cement ratios lost between 15 and 30% of the original concrete strength, whilst lower ratio mixes lost between 5 and 10%.

2.4.6 Tensile Strength

Direct tensile testing is normally impracticable and tensile splitting tests are normally carried out. The tensile splitting test induces a tensile stress in a cylinder loaded at diametrically opposite points and an apparent tensile strength obtained. The bond between cement paste and aggregate has a significant effect on the tensile strength of concrete and is affected by the aggregate rock and surface roughness and the water cement ratio of the mix

(Hsu & Slate, 1963).

Sullivan (1979) reported that tensile strength is more likely to be sensitive to deterioration at high temperatures than compressive strength, this was sustained by Harada *et al.* (1972). He observed that tensile strength of concrete deteriorates at a faster rate than compressive strength but otherwise showed similar variations as temperatures increases.

Harada *et al.* reported tests on concrete made with sandstone and limestone aggregate. The reduction of tensile strength was greater for the limestone aggregate concrete, with strength ratios of 55, 45 and 30 % at 220, 320 and 420°C compared to strength ratios of 85, 75, 60, and 50% at 150, 250, 350 and 450°C for sandstone aggregate concrete.

To conclude tensile reduction strength reduction - the strength does not always decrease as might be expected on initial consideration of microcracking effects. The type of aggregate has a significant effect. Evidence exists that concretes made with siliceous aggregate perform better than those with calcareous aggregates (Harada *et al.*, 1972), although Zoldners (1960) reported with contrary results.

2.4.7 Changes in Microstructure

2.4.7.1 Differential Thermal Analysis

These experimental techniques are use for characterising materials by measuring changes in one or more physico-chemical property as a function of increasing temperature. The two chief techniques are differential thermal analysis (DTA) in which energy changes are measured, and thermogravimetry analysis (TG) in which weight changes are measured. In DTA the measurement is made by the continuous monitoring of the temperature difference (ΔT) between a sample and thermally inert reference material, normally achieved using an

opposed thermocouple system, suitably amplified.

DTA curves provide information on the physical and chemical behaviour of materials, e.g.

Physical Changes : Melting, freezing, sublimation and vaporisation. Crystalline and glass transition phenomena, measurement of specific heats.

Chemical Changes : Decomposition, dehydration, degradation (e.g. oxidation studies), and solid-state reactions.

The characteristics of thermal analysis, namely its simplicity, speed of operation, amenability to routine procedures, quantitative (TG) or semi-quantitative potentialities, ability to be used in the direct identification and estimation of compounds or minerals make it a valuable technique in the physico-chemical studies of silicate, calcareous and similar building materials and their constituents.

2.4.7.2 Porosity

The strength of concrete is influenced by the volume of all voids in the concrete: entrapped air, capillary pores and gel pores; and is a primary factor influencing the strength of the cement paste. Work reported by Rossler & Oddler (1985) in Neville (1995) found a linear relationship between strength and porosity although the effect of pores smaller than 20 nm in diameter was found to be negligible. Consequently, in addition to total porosity, the effect of pore size distribution on strength must be considered.

Although the pore size is, for convenience expressed as a diameter, all the pores are by no means cylindrical or spherical in shape, The 'diameter' represents a sphere with the same ratio of volume to surface area as the totality of pores. The method of mercury intrusion in

the studies of the pore system assumes that pores become narrower with depth while, in fact some pores have a constricted entrance; this distorts the value of porosity measured by mercury intrusion.

When hardened cement paste is exposed to increasing temperatures it first experiences desiccation or drying out of the pore system followed by decomposition of the hydration products and destruction of the gel structure. Rotasy *et al.* (1980) reported that gradual heating caused destruction of the gel pore structure of the cement mortar - the total pore volume increased and the distribution of pore sizes was affected. The total pore volume for all pores larger than 4 nm, was 0.071 cm^3/g for dry control portland cement mortar specimens. After heating to 300, 600 and 900°C the volumes had increased to 0.074, 0.110 and 0.131 cm^3/g respectively. The small increase in pore volume on heating to 300°C was considered to be due to structural changes resulting from the desiccation and dehydration processes occurring mainly in pores of radii less than 4 nm, which would not be detected by mercury intrusion. The significant increase in total pore volume caused by heating to 600°C was probably due to an expansion of the pores or to the formation of microcracks.

Fischer (1970) noted that in concrete containing quartz aggregate there was no clear indication of any change in porosity when alpha-quartz transformed into beta-quartz, i.e. between 500 and 650°C. The porosity of unloaded heated specimens increased more than when heated under a load. Concrete that was cooled after heating and then stored in air in the laboratory did not tend to re-establish lower porosity. However, after saturation in water at 20°C, the porosity of previously heated concrete specimens was slowly reduced to that which existed before being heated. This is probably due to rehydration of the cement paste.

2.4.8 Cracking

At high temperatures the thermal incompatibility of aggregate and cement paste causes stresses in concrete which frequently lead to cracks, particularly in the form of surface crazing. Experience (Schneider, 1989) suggests that such cracks concentrate at positions where, before the fire, incipient cracks were present owing to drying shrinkage, flexural loading, etc.

Cracks occur in every reinforced concrete cross-section when exposed to a heating process, this may be for a number of reasons. Schneider suggests that stresses resulting from the different thermal elongation of the cement matrix and the aggregates are important for crack development. Microcracks are present at 100°C, but as the coefficients of thermal elongation diverge with increasing temperature the importance of the cracks grow with increasing temperature. The strength of the concrete is directly connected to these cracks.

Stresses also arise from the differential thermal elongation of the concrete and the reinforcing steel. These stresses start to become important as temperatures reach 400°C for normal dense concrete, and significantly lower temperatures for lightweight aggregate concrete. This type of cracking appears near the reinforcement. Stresses are also present due to different temperature rises where the size and shape of a concrete cross-section are changing. Corners and edges of cross sections are susceptible for such cracks.

Non-linear temperature gradients within the cross-section will produce stresses in the concrete. Cracks formed from this type of stress form in the inner part of the cross-section, however stresses from the mechanical loading may strongly influence their occurrence and position. When the concrete begins to cool stresses will occur if the free re-contraction is hindered. Sudden cooling for example, with a fire extinguishing hose

stream will cause sudden re-contraction of the concrete which has been affected by the water, and this leads to cracks near the surface.

The crack formation of the kinds described above decrease with cooling and redeformation of the structure. However they may not close totally. With monolithic structures, thermal deformation of structural members exposed to a fire causes stresses in the surrounding assembly, which is not directly effected and remains cool. Thus, with strong exposure, cracks may occur in these regions. This fact needs to be taken into account, mainly when the damage of the heated part of the structure indicates a strong fire attack. It should be considered that hidden cracks may cause an increased long-term deformation of a re-adjusted concrete structure.

2.4.9 Spalling

The occurrence of spalling under fire has been observed under laboratory and natural fire conditions. Spalling may be categorised into four distinct types; aggregate, corner, surface and explosive spalling.

Aggregate spalling has been found to be a form of shear failure of aggregates local to the heated surface. The susceptibility of any particular concrete to the aggregate spalling can be quantified from parameters which include the coefficients of thermal expansion of both the aggregate and the surrounding mortar, the size and thermal diffusivity of the aggregate and the rate of heating. Corner spalling, which is significant for the fire resistance of concrete columns, is a result of concrete losing its tensile strength at elevated temperatures.

Surface spalling is the result of excessive pore pressures within heated concretes. An empirical model has been developed by Connolly (1995), which attempts to quantify pore pressures and proposes a material failure model. The dominant parameters are rate of

heating, pore saturation and concrete permeability.

Explosive spalling is very detrimental to a concrete elements and may be caused by either of two distinct mechanisms. Either excessive pore pressures can cause explosive spalling or the thermally induced stresses or applied load stresses exceed the tensile strength of the concrete.

2.5 SUMMARY

It is evident from field investigations and tests carried out in the laboratory that subjecting reinforced concrete to elevated temperatures leads to its degradation. This is particularly significant at temperatures above 300°C.

The nature of the degradation process is complex and is governed by :

(i) The properties of the reinforcement which alter according to the steel composition, fabrication process and heat treatment.

(ii) Reinforcement - concrete bond characteristics

(iii) The properties of the concrete which in turn are influenced by mix design etc.

(iv) Load under heating.

A difficulty arises when trying to compare a wide range of reinforced concrete types. Tests have been developed and whilst these may not truly represent the situation of real fires never the less they do allow increased understanding of behaviour.

Figure 2.1 Development of a compartment fire, Purkiss (1996)

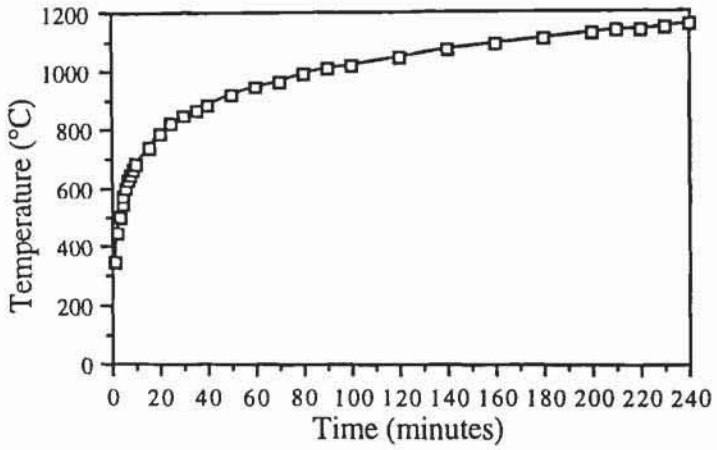

Figure 2.2 Standard fire curve (BS 476: Pt 20: 1987)

Figure 2.3 (a)Maximum and (b) minimum residual strengths of concrete cubes after a cycle of heating and cooling at different rates, Mohamedbhai (1986)

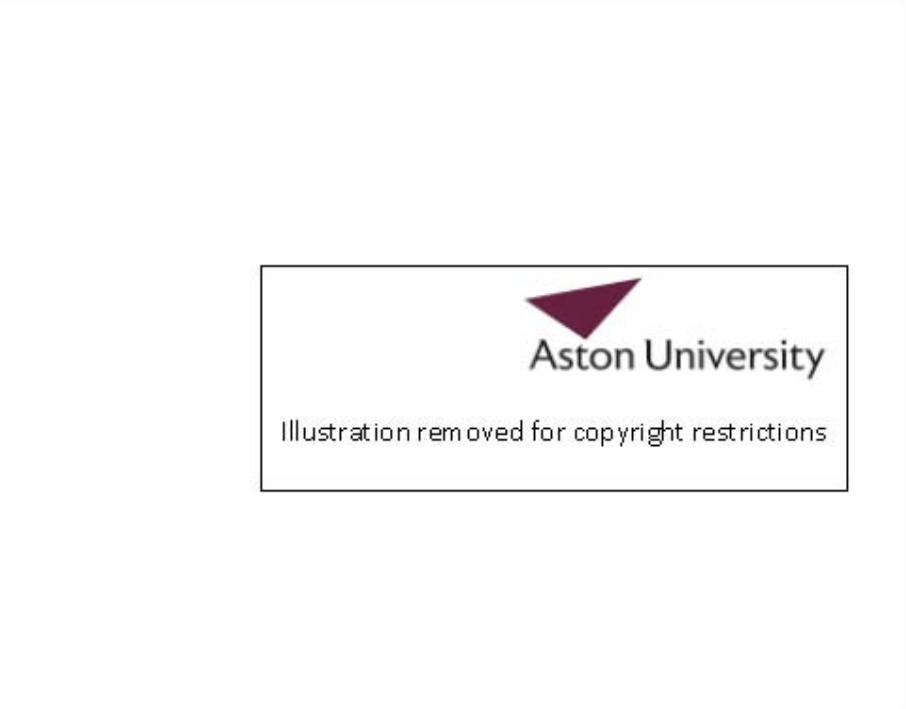

Figure 2.4 Effect of aggregate type on compressive strength of specimens during stress free heating and loaded while hot, (a) Expanded shale aggregate light weight concrete, (b) Calcareous aggregate concrete and (c) Siliceous aggregate concrete (Abrams, 1971)

Figure 2.5 Strength ratio of calcareous aggregate concrete under various conditions as a function of temperature, Abrams (1971)

CHAPTER 3 LITERATURE REVIEW - ASSESSMENT

Assessment of fire damaged concrete usually starts with visual observation of colour change, crazing, cracking and spalling. These visual observations may then be supported by various tests which give an indirect indication of the condition of the concrete.

3.1 COLOUR

3.1.1 Early work on concrete

The colour of concrete can change permanently as a result of heating and therefore in theory may be used to indicate the maximum temperature attained during a fire and its duration. Bessey (1950) found that on heating above 300°C , the colour of concrete can change from normal to pink (300-600°C), whitish grey (600-900°C), and buff (900-1000°C). In addition various types of aggregate were heated up to 1000°C. All of the quartz sand and sandstones (except the pure colourless quartz sands) showed a significant colour change at 250-300°C. It was noted that whilst the colour change from yellow or brown to a pink or reddish brown was well known, but the temperature at which this occurred had not been previously recorded. The colour change was found to be very sharp; at 200°C no colour change was present even after 18 hours; at 250°C the colour develops slowly and is fully developed in 18 hours; at 300°C it is fully developed in 2 hours. As the original yellow colour of many sands is due to the presence of small quantities of iron compounds it seemed logical to conclude that the colour change was most also dependent upon the presence of these compounds either in the stone or coating the sand grains. In the paper by Bessey (1950) there is a review of the literature concerning the effect of temperature on hydrated iron oxides. The more important findings were recorded as follows (see Bessey, 1950 for references):

Fischer discovered that limonite ($Fe_2O_3.nH_2O$)) decomposed with a colour change from yellow to red at 300°C.

Williams & Thewlis found lepidocrite (γ-$Fe(OH)_2$) was converted to the γ-oxide at 250°C.

Posjnak & Merwin found that Goethite (α-FeO(OH)) lost very little water below 250°C , but was almost completely dehydrated at 300°C.

Hansen & Brownmiller in examining precipitated ferric oxide hydrogel ($Fe_2O_3.H_2O$) found that it had no structure, as judged by X-ray diffraction after heating at 200°C, but that after heating to 300°C it had a structure similar to haematite (Fe_2O_3).

Therefore it was concluded that the colour change in various sands and sandstones corresponded well with the dehydration of iron compounds and that such transformations are a reliable indication that the sample has been heated to a temperature of at least 250-300°C.

In addition, Bessey also investigated the effect of temperature on the colour of flint and limestone aggregate, and similar changes were found. However the initial colour of the flint and limestone determined the amount of red colour developed. Bessey found no change of colour on heating igneous rocks which is in contrast to tests carried out by Baguant and reported in Smith (1983) for a basalt aggregate. These results showed changes in the colour of basalt sand from grey to pinkish grey when heated to 400°C, to brownish grey at 600°C and finally to reddish brown at 800°C. The colour only became apparent after cooling, possibly due to the adsorption of moisture by the aggregate.

Ahmed (1992) reported that heating limestone concrete, no changes in colour were seen for temperatures up to 200°C. However at 400°C the colour of the concrete changed to a light pink and at 600°C a dull grey colour developed.

In addition to observation of colour change on heating aggregate particles further observations (Bessey, 1950) were made after heating concrete made with these aggregates. For example flint gravel concrete slabs were heated from one face and then broken open to observe the colour change at various depths into the concrete.

Four distinct temperatures were noted:

(i) At 300°C a red colouration replaced the normal grey of the concrete, and the boundary of colour change was easily distinguishable. With different sands it was found to vary in intensity and in some cases needed a practised eye and suitable lighting to determine the depth affected.

(ii) At a temperature between 500-600°C, the flint aggregate had become cracked and friable. At around this temperature a second colour change was observed, the development of a whitish grey colour. This change in colour was explained by the reaction of ferric oxide with lime, forming calcium ferrites of lower pigmenting power. The change of colour will be a relatively slow reaction and the temperature at which the red colour disappears may therefore depend upon the time of exposure at the maximum temperatures. The range of variation may be taken as approximately 550-700°C.

(iii) At temperatures over a 1000°C the colour of concrete can change again, from a whitish grey to a buff shade, but the change is not as obvious as the changes at lower temperatures.

(iv) Sintering of the concrete occurs at temperatures above 1200°C and depends upon the amount of iron oxide present.

Chew (1993a) investigated the extent of damage by a fire at the lower ground floor of a multi-storey building. Observation of laboratory specimens, as well as those from actual sites that had been subjected to a temperature of above 300°C all showed some kind of colour change. However, Chew reported that in many cases difficulties were found in the determination of the boundary where colour change diminished (i.e. not affected by the heat).

The change of colour from normal to pink is important since it coincides approximately with the onset of significant loss of strength due to heating. Therefore any pink discoloured concrete should be regarded as being suspect.

Most of the previous work concerned with the colour change of aggregate or concrete after exposure to high temperatures did not attempt to quantify the change. Generally observations of colour to identify the exposure temperature have only been made by a practised eye. Thus any change has been defined as in an arbitrary manner rather than by comparing the colours to a defined colour chart. Visual observation as a technique for colour change also has its problems when assessing boundaries, i.e. those areas that have changed colour to red compared to other areas that have not.

Colour definition is more obvious with some aggregates than others. Thus just because an aggregate is not red does not imply that the concrete is undamaged. This can be extended to the opposite effect, e.g. high strength concrete, where the aggregate may have changed colour to red but the concrete is not damaged.

3.1.2 Colour Theory

The concepts involved in understanding colour and its measurement are quite complex, see e.g. Clulow (1972), Berger-Schunn & Saltman (1994) , and only a brief description is given here.

The human eye is sensitive to electromagnetic radiation of wavelengths in the range approximately 380-770 nm. Radiation at the longer wavelengths in this range is recognised as red, changing to yellow, green, cyan, and blue as the wavelength decreases, Figure 3.1 For measurement purposes the primary colours - pure red, green and blue have standard wavelengths of 700.0, 546.1 and 435.8 nm respectively. Combination of these colours give rise to e.g. yellow (red + green); cyan (green + blue); magenta (red + blue).

Different colours can be described and quantified in terms of their components by the use of what are known as colour spaces. There are numerous forms of these but they can, more or less, be divided into two groups which represent specific colours either as combinations of other colours e.g. the primary colours red, green and blue (RGB) or in terms of hue, saturation and intensity (HSI).

3.1.2.1 RGB Colour Space

The RGB colour space is widely used in cameras and monitors since it is simple and good for generating and displaying images. Separate signals for red, green, and blue are obtained and then the resultant colour is defined by the percentage of red, green and blue that are present as its constituents. For image display systems this becomes a range of 0-255 of brightness where 0 means no component of the primary colour in the resultant colour and 255 means the resultant colour has a full component of the primary colour (In

terms of computer storage the 255 is equivalent to 1 MByte of information).Thus a specific colour must be expressed in terms of all three components and examples are given below in Table 3.1.

Table 3.1 RGB components and resultant colours

Component			
R	G	B	Resultant Colour
255	0	0	Red
0	255	0	Green
0	0	255	Blue
255	255	0	Yellow
0	255	255	Cyan
255	0	255	Magenta
255	255	255	White
127	127	127	Mid-Grey
0	0	0	Black

This system is often visualised as the colour cube as shown in Figure 3.2, where three orthogonal axes represent the brightness or intensity of each primary colour. A line equidistant from each axis follows the line from black to white. A disadvantage of this system is that people do not think of colour in terms of combinations of red, green and blue. In addition manipulation is more difficult since red, green and blue values have little significance independently and processing becomes computationally intensive.

3.1.2.2 HSI Colour Space

In this type of colour space the components hue, saturation and intensity may be defined as follows as follows:

Hue: Denotes the kind of colour i.e whether it appears as red or yellow or green or cyan or blue etc. It is the attribute by which the eye distinguishes different parts of the spectrum and is measured in terms of wavelength. The hue of a specific colour may then be represented by its position on a horizontal circle, Figure 3.3. The zero on this circle depends on the measuring system used. In the present work the instrument defines pure red as the zero and hue may be quantified as an angle. For computer purposes the 0-360° range is re-scaled to fit the 0-255 instrument display.

Table 3.2 Definition of hue in terms of the instrument display

Hue	Wavelength (nm) (approximate)	Circle (°) Angle	Instrument Display Level
Red	700	0/360	0 & 255
Yellow	580	60	42.5
Green	546	120	85
Cyan	480	180	127.5
Blue	435	240	170
Magenta	700+	300	212.5

Saturation: Refers to the degree to which a pure colour is diluted with white. e.g. a bright/deep red not diluted with any white is said to be highly saturated. As white is added the colour changes to light red, to pink and then white (completely desaturated). Colours may be matched by diluting a standard with white. In HSI colour space the circumference of the circle represents 100% saturation with 0% at the centre (Figure 3.3).

Intensity: This is a colour neutral value and represents the extent to which a material reflects light i.e it describes the relative brightness or darkness. Thus in bright light red has a high intensity but as the light dims the intensity decreases and the red becomes darker and darker until it fades to black. In HSI colour space it is represented by an axis perpendicular to the circle plane (Figure 3.3).

The full model is then represented by a double cone. It may also be simplified to a double hexcone (a six sided cone) and can then be visualised as viewing the RGB colour cube along the diagonal axis passing through the black and white corners. Either way, a specific colour is defined in terms of Hue, Saturation and Intensity by its position on the surface of the cone.

3.2 NON-DESTRUCTIVE TESTS

These tests give direct information about the concrete in the actual structure, they are termed in-situ tests. Although traditionally called non-destructive tests, some minor damage to the structure may be involved, although its performance or appearance must not be impaired. An important feature of non-destructive tests is that they permit re-testing at the same, or nearly the same, location so that changes with time can be monitored. The tests can be categorized into those that assess the strength of the concrete in situ, and those that determine other changes in e.g. stiffness as a result of sub critical sized flaws and cracks that do not directly affect strength.

Neville (1995) quotes that strength can only be assessed, and not measured, because the non-destructive tests are, for the most part, comparative in nature. The following descriptions of tests are taken from Bungey (1989) and Concrete Society (1990).

3.2.1 Core Test

The most direct method of estimating the strength of in-situ concrete is by testing cores cut from the structure. However it should be remembered that in the case of fire damaged concrete a strength gradient will exist along the core and little information is available of the influence of this on core behaviour.

A major problem with core testing is that normal sampling is usually carried out at the exposed face, which in the case of a fire damaged structure will include the damaged surface. Contact of the damaged surface of the concrete with the plattens of the testing machine during loading may then give premature failure. Tests on the strength of fire damaged regions of a structure are more difficult since there is a steep temperature gradient, and the affected depth may be quite shallow. This may require the diameter of the core to be reduced to obtain a reasonable length to diameter ratio and this correspondingly reduces the accuracy of the test.

3.2.2 Rebound Hammer Test

The rebound hammer is one of the oldest non-destructive tests available beyond the traditional hammer. It was devised in 1948 by Ernst Schmidt it is often referred to as the Schmidt hammer test. This test is based on the principle that the rebound of an elastic mass depends on the hardness of the surface against which the mass impinges.

In the rebound hammer test, a spring loaded mass has a fixed amount of energy imparted to it by extending the spring to a fixed position; this is achieved by pressing the plunger against the surface of the concrete under test. Upon release, the mass rebounds from the plunger, still in contact with the concrete, and the distance travelled by the mass, expressed as a extension of the initial extension of the spring, is called the rebound number.

The rebound number is an arbitrary measure because it depends on the energy stored in the particular spring and on the size of the mass. The test is sensitive to local variations in the concrete especially if large aggregate particles are near by. Due to the local variability in the hardness of concrete over a small area, the rebound number should be determined at several locations in close proximity. Neville (1995) reports that ASTM C 805-85 states that readings should not be closer than 25 mm, and BS 1881: Pt 202: 1986 recommends testing on a grid pattern with a spacing of 20 to 50 mm within an area not larger than 300 by 300 mm; this reduces operator bias.

The test is not generally suitable for use on spalled surfaces and even on flat surfaces is somewhat variable, Concrete Society (1990). The explanation for this is perhaps due to skin hardening effects that appear to occur sometimes on damaged concretes.

3.2.3 Ultrasonic Pulse Velocity

The ultrasonic pulse velocity (UPV) test involves measurement of the time taken by an ultrasonic pulse to travel a measured distance through the concrete. The equipment includes transducers which are placed in contact with the concrete, a pulse generator with a frequency between 10 and 150 Hz, an amplifier, a time measuring circuit, and a digital display of the time taken for a longitudinal wave to travel between the two transducers.

The velocity of the ultrasonic pulse through a sample of concrete is a complex function of different rates of propagation through individual components. For a given aggregate and cement content of the mix, the ultrasonic pulse velocity of the concrete is affected by changes in the hardened cement paste such as a change in the water/cement ratio, which affects the modulus of elasticity of the hardened cement paste. It is only within these limitations that the ultrasonic pulse velocity test can be used to assess the strength of

concrete. There is a further limitation arising from the fact that the pulse travels faster through a water-filled void than through an air-filled one. In consequence, the moisture condition of the concrete affects the pulse velocity while the strength in situ is not affected.

Despite the limitations of this test, it has considerable merit of giving information about the interior of the concrete element. The test is used to detect cracking, voids, deterioration due to frost or fire and the uniformity of concrete in similar elements. Watkeys (1955) tested various Ham River aggregate concretes and found that a correlation existed between the maximum temperature reached by the concrete and the reduction in UPV due to heating. He found the general relationship between the pulse velocity and the strength to be independent of the rate of heating but the decrease to be dependent upon the maximum temperature attained. The post firing treatment had a great influence on the value of the ultrasonic pulse velocity and changed the relationship with strength especially when severely damaged specimens were soaked in water. Watkeys found the samples with the lowest residual UPV showed greater fluctuations in measured values. This was due to the variable nature of cracking damage that can occur in fire damaged concrete resulting in large variations in measured pulse velocities due to small changes in the transducer application pressure.

Zoldners (1960) tested concretes made with gravel, limestone and sandstone aggregate. In all cases the pulse velocity reduced with increasing temperature until at about 700°C it was between 20 and 50% of its unfired value. Concretes made with limestone aggregate showed the smallest reductions in UPV while sandstone and gravel behaved similarly. Smith (1983) tested various concretes made with different UK aggregates, such as Siliceous Gravel, Dolerite, Basalt and Granite.

The results obtained by Smith (Figure 3.4) are similar to those obtained by Zoldners and Watkeys. At 300°C 88.1, 78.8, 81.8 and 78.8% of the unfired UPV for Gravel, Dolerite,

Granite and Basalt respectively existed. These results showed the gravel aggregate concrete to be more fire resistant at this temperature and exposure than the other aggregates. Whilst at 600°C the percentage of unfired UPV for the above aggregates was 37.7, 13.2, 23.1 and 20.8% respectively. These results showed that the influence of aggregate is not important until temperatures in excess of 500°C are reached.

3.2.4 Windsor Probe

The Windsor probe test was developed in the USA about 25 years ago but has not received much attention in the U.K. The test involves firing a steel probe into the surface of the concrete. The length of probe left exposed is measured and can be correlated with compressive strength. The test has been found to be very quick and simple and to give low within-test variation. It is suitable for both vertical and horizontal surfaces and can be used on spalled surfaces provided they are reasonably flat. The direct correlation with strength is considered to be slightly better with this test than with other methods (Concrete Society, 1990).

3.2.5 BRE Internal Fracture Test

The BRE internal fracture test involves drilling a hole in the concrete into which a wedge anchor is placed. The torque required to pull the anchor out gives an indication of the strength by reference to a calibration chart. The within-test variation has found to be wide (Concrete Society, 1990); with the result that direct determination of strength is less reliable. Its usefulness improves when it is possible to compare fire damaged and non-damaged concrete in the same area. A reasonably flat surface approximately 100 mm in diameter is required to support the ring of the test apparatus. A chiselled surface would be sufficient although due to its increased size more preparatory work is required compared to the Windsor probe which is generally considered to be a more convenient test.

3.2.6 Thermoluminescence

Thermoluminescence (TL) is the emission of visible light that occurs on heating many minerals (e.g. quartz sand, feldspars, lithium fluoride, and diamond). This light output occurs in addition to the normal red hot glow that occurs as the specimen heats up but at lower temperatures (200 to 500°C normally) and it is dependent on the samples' thermal and radiation history (Smith, 1983).

The basis of the technique for investigation of fire damaged concrete is the measurement of the residual TL in small samples of mortar drilled from the concrete.

Placido (1980) and later Smith (1983) first investigated TL and its reduction when assessing fire damaged concrete. Smith (1983) found that heating samples to 200°C reduced the measured TL. The rate of loss with time was reported to reduce, so that the greatest reduction in TL for any given temperature occurs during the initial stages of heating. Large changes in the measured TL were observed for specimens heated to temperatures in excess of 300°C. However, there are disadvantages (Smith):

The sensitivity is reduced when heating for periods in excess of 3 hours at 300°C or in excess of 1 hour at 400°C.
At temperatures of 400°C or above no residual TL could be measured.

Chew (1993b) described the TL technique by asking to visualizing a glass of water. Imagine that if water is flowing into a glass at a very slow rate, the amount of water in the glass will increase with time, symbolizing the accumulation of TL in grains over the years. If the glass is subjected to a high temperature, water will evaporate, symbolizing the loss of TL when subjected to a high temperature. It follows that using the relationship between

temperature and the loss of TL - by measuring the residual TL left in a sample of concrete with appropriate normalization and calibration - the temperature history of the sample can be estimated.

Chew (1993b) confirmed that the greatest reduction in TL occurs in the initial stages of heating, but he also reported that the differences between the exposure times of 3, 4 and 5 hours was difficult to detect. He used a self-normalizing technique similar to that of Smith (1983) to interpret the TL results. These were a set of standard curves for momentary temperatures of 100 to 500°C. Table 3.3 presents a set of results taken from Chew (1993b) showing the effect of time of exposure on estimated maximum temperature using self-normalization.

From the data it is obvious that the self normalizing technique would overestimate an actual exposure of, e.g. 300°C. If the duration of heating was 5 mins. the estimated temperature would be 330°C whilst if the duration was 3 hours the estimated temperature would be 470°C, a difference of 140°C! Chew also attempted to correlate compressive strength with the TL signal, but found the sensitivity of concrete to exposure times to be greater than the sensitivity of the TL. He therefore concluded that a significant under estimation of the reduction in the strength of the concrete would be made and attempted to be overcome this problem by suggesting a curve of maximum temperature estimated using TL with the residual strength of the concrete. However this curve would be limited to the methodology, types of materials, and range of variables used in the experiment.

3.2.7 Dynamic Modulus of Elasticity

In addition to the above tests, determination of the dynamic modulus of elasticity has been found to be useful in laboratory investigations. The dynamic modulus of elasticity (E_d) is determined by means of vibration of a concrete prism specimen, with a negligible stress

being applied. Because of the absence of a significant stress no microcracking is induced in the concrete and there is no creep. In consequence, the dynamic modulus refers to almost purely elastic effects. This test will determine the progressive changes in the state of a concrete specimen. This can be done by determining the fundamental resonant frequency of the specimen at appropriate stages of the investigation, from this frequency the dynamic modulus of the concrete can be calculated.

The vibration is usually applied in a longitudinal (flexural) mode. A specimen, typically a 500 mm long by 100 mm square cross-section prism, is clamped at its centre with an exciting unit placed against one end face of the specimen and a pick-up against the other. The exciter is driven by a variable frequency oscillator with a range of 100 to 10 000 Hz. The vibrations propagated within the specimen are received by the pick-up, amplified, and their amplitude is measured by an appropriate indicator. The frequency of excitation is varied until resonance is obtained at the fundamental (i.e. lowest) frequency of the specimen, this is indicated by the maximum deflection of the indicator.

The density (ρ) of the concrete is given as,

$$\rho = \frac{W_A}{l\ b\ d} \times 10^9 \qquad \text{unit} = kg/m^3 \qquad (3.1)$$

and the dynamic modulus of elasticity (E_d) as,

$$E_d = 4\ n^2\ l^2\ \rho\ 10^{-12} \qquad \text{unit} = MN/mm^2 \qquad (3.2)$$

where W_A = Weight of concrete in air (kg) l = length of specimen (mm)

b = breadth of specimen (mm) d = depth of specimen (mm)

n = Fundamental resonant frequency vibration (Hz)

The reduction in elastic modulus on heating specimens to elevated temperatures, was shown by Lie (1968), where a reduction of 40% occurred at 300°C increasing to 85% by 600°C when compared with control values. There are conflicting views as to whether the compressive strength or the modulus of elasticity reduce faster on heating. Harmathy & Berndt (1966) found that the greatest reduction in elastic modulus of concrete occurred at temperatures between 200°C and 315°C. Saemann & Washa (1957) also found the elastic modulus reduced more rapidly than compressive strength. In their tests the elastic modulus first decreased on heating, then increased at about 150°C before decreasing again more rapidly. However, Sullivan & Poucher (1971) did not find any increase on heating using the initial tangent method of measurement. The E_d values dropped for both mortar and concrete as the temperature increased. The ratio of E_d before treatment to E_d after treatment decreased rapidly between 20 and 100°C. The E_d value was reasonably constant between 100 and 300°C and decreased again above 300°C.

3.3 SUMMARY

From the preceeding discussion it is evident that the range of tests are useful in evaluating the state of fire damaged concrete. However, a number of problems still remain :

For instance, determination of colour change is by subjective visual assessment. The review of colour theory and measurement suggests that it should be possible to overcome this problem by using modern instruments and software instruments giving quantitative values.

In addition whilst the non-destructive methods can be used as an indicator of the degree of cracking, utilisation of petrographic techniques should enable direct measurement of cracking thus giving a clearer indication of the damage.

Table 3.3 Effect of time of exposure on estimated maximum temperature using self - normalization techniques when measuring the thermoluminescence

Thermal Exposure, °C/time	Maximum temperature by self-normalizing, °C
100 / 5 min	170
100 / 30 min	220
100 / 1 hr	230
100 / 3 hr	260
100 / 5 hr	260
100 / 24 hr	280
200 / 5 min	220
200 / 30 min	250
200 / 1 hr	280
200 / 3 hr	310
200 / 5 hr	310
200 / 24 hr	330
300 / 5 min	330
300 / 30 min	380
300 / 1 hr	400
300 / 3 hr	470
300 / 5 hr	470
300 / 24 hr	500
400 / 5 min	470
400 / 30 min	500

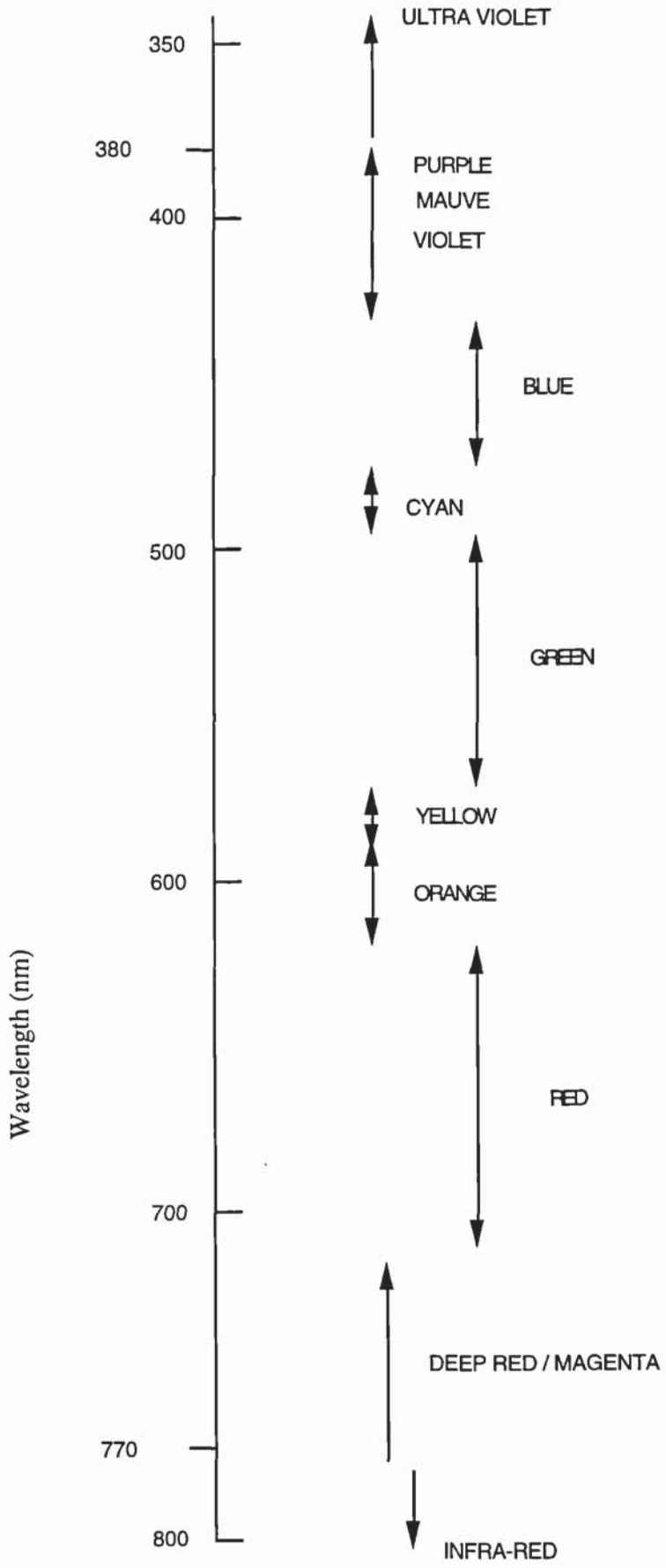

Figure 3.1 Visible Components of the Electromagnetic Spectrum

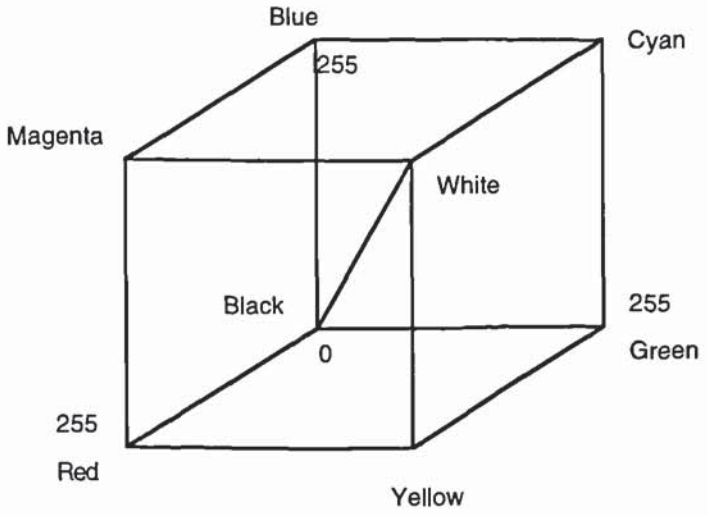

Figure 3.2 RGB Colour Cube

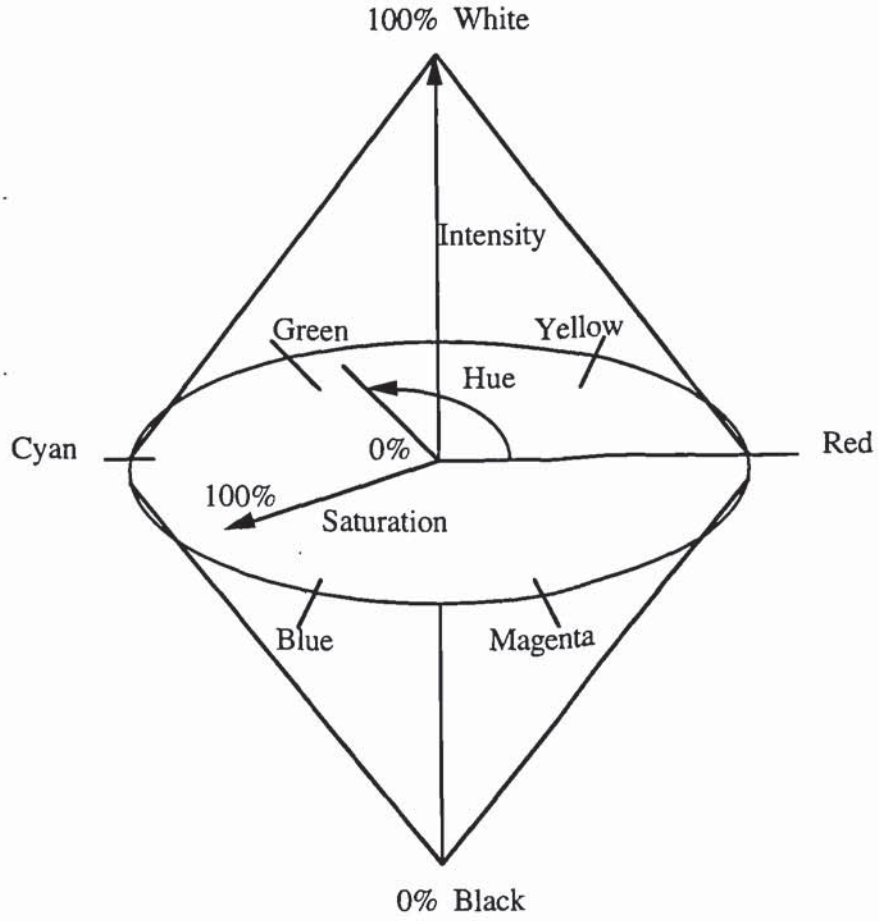

Figure 3.3 HSI Colour Cone

Figure 3.4 Residual UPV after 1 hour temperature exposure (Smith, 1983)

CHAPTER 4 EXPERIMENTAL

This chapter details the experimental procedures to be used and commences with details of the materials.

4.1 MATERIALS

4.1.1 Cements

An ordinary Portland cement (OPC), and blended cements, OPC + 30% pulverised fuel ash (PFA) and OPC + 50% ground granulated blast furnace slag (BFS), were used. The chemical compositions of the various materials expressed in percentages by weight of the constituent oxides are given in Appendix 1.

4.1.2 Aggregates

The coarse aggregates were chosen from those used in the UK and were known to show a range of behaviour with regard to colour change and spalling after heating. These were (i) siliceous gravel, (ii) crushed limestone, (iii) crushed granite and (iv) Lytag. The fine aggregate was a medium zone quartz sand from the St. Albans area. All of the aggregates were oven dried prior to mixing. Further details are given in Appendix 2.

The siliceous gravel and quartz sand were from the same source as those used by Connolly (1995) in a project carried out at the Fire Research Station in collaboration with Aston University. Since it was known that the aggregate showed a distinct colour change on heating the work from the projects would be comparable.

4.2 CONCRETE MIX DESIGN

The mix designs and details of quality control for the individual mixes are given in Appendix 3. The concrete mix was a 1 : 2.1 : 4.2 - cement : sand : coarse aggregate (except for the Lytag mixes). Mixes were designed to give equivalent workability (50mm $^{+/-}$ 25mm) by varying the water/cement ratio between 0.62 - 0.66, and 60 day cube strengths were typical of good quality structural concrete. Quality control was maintained by measuring slump and fresh wet density (BS 1881 : Pts 102 & 107 : 1983).

4.3 MIXING AND CASTING OF TEST SPECIMENS

The aggregate was added to a pan mixer with approximately half of the water and mixed for 2 minutes and then left for 8 minutes. The cement was then added and mixed in for 30 seconds followed by the rest of the water and the mixing continued for another 30 seconds. Finally the concrete was left to mix for a further 3 minutes, giving a total mix time of 14 minutes.

The concrete was then added to oiled moulds in three layers, vibrating each layer to remove any air, and the cast surface trowelled flat. If specimens were to have thermocouples cast into them they were added at this stage by measuring the required position and forcing a hole into the concrete with a screwdriver, placing the thermocouple and then gently vibrating to allow the concrete to move around the thermocouple. The type K thermocouple used consisted of Chromel (Ni-Cr) and Alumel (Ni-Al) wire spot welded at the end. The wires were threaded through a ceramic sheath to ensure they were separated until the soldered tip was reached.

Samples were cast for four series of experiments.

Series A Samples were heated and allowed to equilibrate at a series of different temperatures. Two 500 x 100 x 100 mm beams and four 100 mm cubes were heated to each temperature. In total forty nine sets of specimens were produced.

Series B A concrete cylinder was heated at one end face so as to establish a thermal gradient along its axis. In total eighteen cylinders (300 mm length x 150 mm diameter) and twelve 100 mm cubes were cast.

Series C **(i)** Samples were heated to equilibrate at different temperatures under an applied load.

(ii) Samples were heated to equilibrate at different temperatures, allowed to cool and then placed under water to assess any autogenous healing of cracks.

Each heating procedure used one 150 x 50 mm cylinder. In total fifteen cylinders and four 100 mm cubes were cast.

Series D A limited number of samples were cast and heated in such a manner as to try and induce spalling (no oven drying). Samples were fabricated as 500 x 100 x 100 mm beams containing reinforcing steel. In total eight beams were cast.

4.4 CURING AND CONDITIONING OF TEST SPECIMENS

The specimens were cured under plastic for 24 hours and then demoulded. They were marked with reference numbers and placed under water at 20°C. At 60 days the specimens were removed from the water tanks, dried at 105°C for 48 hours to reduce the possibility

of explosive spalling when heated (except for Series D where spalling conditions were required) and then subjected to their specific heating regimes.

4.5 THERMAL TEST REGIMES

4.5.1 Series A - Heating to Equilibrium Temperatures

Two beams and four cubes were heated to each equilibrium temperature whilst the two other cubes cast at the same time were crushed for control purposes. This enabled a direct comparison of strength within the individual mixes. Samples were heated and allowed to equilibriate at temperatures of 175, 200, 250, 300, 350, 400, 450, 500 and 700°C, in a proprietary muffle furnace capable of giving temperatures above 1200°C. The rate of heating was equivalent to temperature rises of approximately 60°C/min. The samples were heated to the required temperature to establish a uniform temperature gradient through the sample and held at this temperature for around 45 minutes, the total length of heating was around 3 hours.

The position of the specimens in the furnace was kept the same throughout the experiments. The beams were stood vertically on a thermal insulation block and the four cubes were placed on top of each other to keep the heat transmission through the concrete equivalent in the different samples. One of the beams had two thermocouples embedded 50 mm into the concrete. The position of these were 25 mm and 50 mm from one end face of the beam. Thermocouples were also attached to the surfaces of the beams and cube, with a refractory cement. The thermocouples were then connected to a 'squirrel' datalogger (Grant model no. 32-6K) and temperature readings were logged every 30 seconds. After the heating regime was completed data from the logger were down-loaded to a PC spread sheet package. The samples were left to slowly cool in the furnace overnight.

The following tests were carried out on samples equilibriated at each temperature level :

Compressive Strength

The compressive strength was tested in accordance with BS 1881: Part 116: 1983. The equipment used to load the specimens was a Denison (model no. T73) testing machine. The 100 x 100 mm specimens were loaded at a rate of 13 ± 5 kN/min.

Flexural Strength

The flexural strength was tested in accordance with BS 1881 : Part 118 : 1983. The equipment used to test the beams was a Denison (model no. T60) with four point loading.

Surface Hardness (Schmidt Hammer)

The surface hardness of the concrete was measured using a Schmidt hammer to BS 1881: Part 202: 1986. A grid was drawn along one of the sides of a beam, adjacent to the cast surface. The test points were 25 and 75 mm in from the edge of the beam and at distances of 100, 200, 300 and 400 mm along the beam. The tests were then repeated on the side of the beam directly opposite, so in total there were 16 test points. The results are given as an average with maximum and minimum values disregarded.

Dynamic Modulus of Elasticity

The dynamic modulus of elasticity was tested in accordance with BS 1881: Part 209: 1990. The equipment used was an Erudite Resonant Frequency tester (model no. SCT4/1821). The tests were performed along the length of beam specimens.

Ultrasonic Pulse Velocity

The velocity of ultrasonic pulses transmitted through the concrete specimens were measured using a standard PUNDIT. The test was carried out in accordance to BS 1881: Part 203: 1986. The pundit equipment can measure pulse transit times in three ranges, these are :

(i) 0.1 to 99.9 μs in units of 0.1 μs

(ii) 1 to 999 μs in units of 1 μs

(iii) 10 to 9990 μs in units of 10 μs

The equipment was calibrated using a 26.3 μs steel calibration bar before each days' test. Measurements were made to an accuracy of ± 0.1μs. All tests were carried out at 20°C and the couplant used was Castrol Water Pump Grease, applied in a very thin layer. The ultrasonic pulse velocity measurements were made using the direct transmission method between the two end faces of the beam.

Differential Thermal Analysis (DTA) and Thermal Gravimetric Analysis (TGA)

These techniques were used to determine any effects of the imposed high temperatures on the hydrated cement component of the concrete. The techniques allow direct identification and estimation of quantity of compounds or minerals within the cement.

Experimental procedure

Samples of concrete were pulverised with a hammer and then ground using a pestle and mortar. Passing through a 150 μm sieve removed most of the aggregate although the powder probably still contained a small amount of fine sand. Samples were then stored in a desiccator until analysis.

About 35-40 mg of powder were subject to simultaneous DTA/TGA using a Thermal Sciences Ltd STA 1500 thermobalance. Heating was carried out at 20°C / min in air. The data manipulated using Trace Software V400 in association with Stanton Redcroft.

Mercury Intrusion Porosimetry (MIP)

This technique was used to determine the size and distribution of pores within specimens that had been exposed to different temperatures. The intrusion tests were carried out using a Micrometrics Poresizer Model 9310 from Micrometrics Ltd., Dunstable, Bedfordshire. Pieces of mortar of approximately 5 mm in size were obtained from the concrete specimens. The samples were treated with propan-2-ol to displace any free water and then evacuated over several days to remove the solvent.

A weighed quantity of sample (~5g) was placed inside the chamber of a glass cell, which had a glass capillary stem surrounded by a metal sheath. The glass cell was then placed within the porosimeter and evacuated to 50 μm Hg pressure to remove residual moisture and gases. The chamber and capillary were then filled with mercury and hydrostatic pressure gradually applied up to 200 N/mm^2, so as to force the mercury into the pores of the sample.

The volume of mercury intruded into the sample was measured by the change in capacitance of a cylindrical coaxial capacitor formed by the outer metallic sheath around the penetrometer stem and the inner capillary of mercury which was reduced as mercury was forced into the pores of the sample. The pore radius was calculated using the Washburn equation:

$$P = \frac{-4 \upsilon \cos\theta}{d} \qquad (4.1)$$

assuming a contact angle of 117° between the mercury and the pores, based on the work of Winslow & Diamond (1970), where :-

P - applied pressure

d - pore diameter

υ - surface tension of mercury (485 dynes / cm)

θ - contact angle between mercury and the pore walls (117°)

4.5.2 Series B - Effect of a Thermal Gradient

During an actual fire, temperatures within a concrete section do not generally reach equilibrium values. A thermal gradient is established with only the temperature of the outside layers being drastically increased, whilst the temperatures of the inner concrete may be comparatively low. Initially it was proposed to expose a selection of concrete surfaces to heat flux levels of 80, 110 and 140 kW/m^2 representative of low, medium and high intensity fires.

4.5.2.1 Furnace Design

A furnace was designed to establish a temperature gradient along the axis of a standard concrete cylinder of dimensions 300 mm length x 150 mm diameter see Figures 4.1 (a) and (b). The outside casing was of steel construction enclosing refractory furnace blocks. The electric heating disc came from Kanthal Furnace Products via the Fire Research Station where similar discs had been used. It was known that these heating discs were capable of producing heat flux levels up to 150 kW/m^2 and could withstand temperatures of 1400°C.

The electrical heating disc consisted of coiled wire sunk into a spiral on a ceramic backing disc of diameter 150 mm. The heating disc was fixed at the one end of the heating enclosure and then locating steel pegs were fixed in front of this to prevent the concrete specimens touching the heating disc and damaging it. After performing test runs it was found that a mesh cover over the heating disc was required for protection to stop pieces of concrete falling on to the electric element.

The furnace had a removable section to gain access into the main body of the enclosure. The removable portion had holes drilled through the casing of the furnace to allow thermocouples to be threaded through and temperature readings logged. The heating compartment was lined with a vacuum formed board, capable of withstanding temperatures up to 1260°C. The board minimised conduction heat losses where the two halves of the compartment were fixed together.

4.5.2.2 Calibration of Heat Source

The heat flux levels produced by the heating discs were calibrated using a Gardon heat flux meter. The meter was manufactured by Medtherm and had been calibrated by the Building

Research Establishment Radiometer Calibration Service. A heat flux meter measures the total incident heat flux falling on its surface, i.e. both radiative and convective heat flux.

A calibration arrangement was set up to represent the heating compartment as in the experiment. The calibration used a concrete disc of approximately 80 mm thickness with the flux meter mounted in the disc with its measuring face flush with the concrete surface. The concrete disc had been cast with left over concrete from other castings so it had the same material properties of the specimens to be used in the experimental programme.

During the calibration three measurements were taken;

(i) temperature on the surface of the concrete disc

(ii) power flow to the heating enclosure

(iii) total heat flux

The calibration procedure was carried out twice. In further experiments recalibration was only carried out if anything had changed. This occurred several times when the heating disc was replaced due to damage from spalling. During the calibration, it took approximately 10 minutes for the temperature readings and heat flux of the concrete surface to stabilise. The plot of heat flux with increasing electrical input is given in Figure 4.2 This figure enabled power setting to be set for equivalent target heat flux levels of 80, 110 and 140 kW/m^2.

4.5.2.3 Heating

A series of thermocouples were embedded in the cylinders at approximately 0, 20, 40, 55, 85 and 110 mm from the end face to be heated. This enabled a temperature profile along the axis of the cylinder to be determined. The concrete cylinder was placed in the chamber

and the thermocouple wires were threaded through the casing and attached to the datalogger. A fire exposure of 80 kW/m^2 was performed first, and this heat flux level applied for 1 hour. The medium fire exposure of 110 kW/m^2 was found to be very extreme and this was applied for only 40 minutes. The concrete surface was damaged and had become crumbly, so it was decided not to perform the higher exposure of 140 kW/m^2. The heated specimens were left to cool in the furnace overnight. The upper casing was removed after the heating was completed to aid the cooling procedure.

4.5.3 Series C (i) - Applied Compression During Heating

The application of compressive stress during the heating of concrete samples does reduce strength loss and the loss in elastic modulus, Purkiss & Bali (1988). The mechanism of this phenomenon is not known but is likely to be a result of crack formation, caused during unrestrained heating, being inhibited. Therefore the influence of constant compressive load applied to samples during heating cycles has been investigated. The equipment used was that reported by Bali (1984) with minor alterations.

4.5.3.1. Furnace Design

The main frame of the rig consists of three triangular crossheads connected by three prestressed vertical members. A screw-jack is mounted below the crosshead and is fixed by means of tensioned high steel bolts. Previously a dynamometer placed under the centre cross head was attached to a threaded portion of the lifting screw of the jack. This was removed when problems were encountered with the dynamometer during calibrations. Consistent results were not achieved for load and hence it was decided to manually load the samples by means of a ram. The specimen was placed between two rigid smooth plattens.

The furnace was designed to hold cylindrical specimens of dimensions 150 x 50 mm (approximately 1 : 3 diameter to length ratio). Each cylinder was cast with a thermocouple embedded in the centre of the sample. The coarse aggregate size was reduced to 10 mm to avoid problems of homogeneity caused by a large aggregate to specimen size ratio. The samples after curing but before drying were paralleled so that the faces were completely flat, thus avoiding ambiguities when the load was applied.

4.5.3.2 Loading

The rig was simplified from its original design. The inbuilt datalogger and control system and the gears were disconnected. The method of applied load was altered, a ram (24 - 203 kN) was installed under the crosshead and the platten lifted by pumping up the ram.

4.5.3.3 Calibration of Loading System

The ram was calibrated using a Denison machine (model no. T42). The calibration was repeated three times to obtain an average reading. The results of the calibration are given in Figure 4.3. The rig was found to weigh 1.8 kN on the ram gauge and this was taken into account when applying the load to the concrete sample.

The applied load to the specimen was determined from 0.35 of the compressive load at 60 days. The average compressive strength was found directly to be 51.5 MPa. Taking into account the weight of the rig a total of 19.5 kN was applied. The load was applied first and then the furnace switched on.

4.5.3.4 Heating

The furnace was constructed in two halves so that the whole of the cylinder was encapsulated. The split furnace was made of refractory material consisting of Gibcrete 1300 and this was housed within welded steel plates. Any additional insulation was obtained by inserting loose wool fibres between the welded steel plates and the refractory elements. The loose fibre was manufactured by MacKechnie Refractory Fibres Limited.

The temperature of the furnace was controlled by a series of Type K thermocouples connected to the Eurotherm temperature controllers with a maximum temperature of around 950°C. Two thermocouples are inserted into the furnace, one each side to monitor the test temperature and connected to the controller. The temperature of the furnace, surface and inside of the concrete was also measured via an independent logging system.

The furnace was set to a temperature of 530°C and a maximum rate of 10. The samples were soaked at 500°C for 1 hour. During the experiment the applied load needed to be fine tuned depending on whether the specimen was expanding or shrinking. The load was maintained for 1 hour after the furnace had been turned off, the sample was left in the furnace to cool overnight. Control samples were heated using the same procedure as above with the applied load absent.

4.5.4 Series C (ii) - Autogenous Healing of Cracks

This set of experiments were performed to see whether the damage caused whilst heating could be healed if samples were subsequently immersed in water. The samples were heated and cooled using the same procedure as above for the control samples and were then immersed in water for either 3 or 14 days.

4.5.5 Series D - Heating to Produce Spalling

In these experiments attempts were made to induce spalling similar to that found in a wider ranging project which had been carried out at Fire Research Station in collaboration with Aston University (Connolly, 1995). It had been reported that corner spalling was the natural manifestation of tensile strength loss at high temperatures and the complete degradation of bond between the aggregate and the cement matrix.

The beams used were cast plain and reinforced with either 6 or 8 mm steel bars. Cages were made for the reinforcement so that they would fit into the 500 x 100 x 100 mm beams with a minimum cover of 25 mm of concrete. Two beams were heated together in the muffle furnace (see Series A - Equilibrium Heating) at one time.

It has been suggested (Dougill, 1971) that thermal shock may increase the possibility of spalling. The furnace was set to 800°C and left to heat. After approximately 1 hour when the furnace had reached 700°C, the door was opened and two beams were quickly placed inside. After between 20-60 minutes, the furnace was switched off and the samples were left to slowly cool in the furnace overnight and then observations made.

4.6 COLOUR AND CRACK DENSITY MEASUREMENTS

4.6.1 Preparation of Polished Sections for Colour Measurement

To prepare samples for observation in reflected light the following sequence of operations were carried out.

(i) Sections 10 mm thick and 80 x 50 mm in area (the largest size possible for polishing) were cut from control and heated cubes.

(ii) These sections were then dried in an oven at 50°C.

(iii) After drying the sections were impregnated with clear resin (Epofix) using a Logitech IU-20 vacuum impregnation unit and then stored overnight to ensure the resin had fully cured.

(iv) The top face was then polished using 15 and 9 μm diamond grinding fluids, followed by cleaning with propan-2-ol in an ultrasonic bath.

(v) The bottom face was then ground parallel to the top polished face on a milling machine.

(vi) Finally the top face was polished for 10 minutes on a lapping plate using 9 μm grinding fluid.

4.6.2 Preparation of Thin Sections for Crack Density Measurements

To prepare samples for observation in transmitted polarised light the following sequence of operations were carried out.

(i) The procedures were the same as above up to step (iv) except for impregnation a fluorescent low viscosity resin (Epothin) was used.

(ii) A glass slide was ground flat on one side using 15 μm fluid and the ground slide face glued to the top face of the sample using epoxy 301 two-part adhesive and then clamped using a spring loaded jig to cure overnight.

(iii) The following day the slide was held onto the arm of a CS10 saw under vacuum and the excess of sample was cut off leaving approximately 0.5 mm of sample thickness on the slide.

(iv) The sample was then polished until it was about 50 μm thick with 15 μm grinding fluid and then subsequently using a 9 μm fluid.

(v) Finally the sample was cleaned and the cover slip glued on using a fast setting adhesive and UV lamp.

4.6.3 Colour Measurement using the Image Analysis Workstation

Colour measurement was carried out using a Sight Systems Image Analysis and Processing System (JVC KY-F 3CCD) which incorporated Freelance software from Sight Systems.

Polished concrete samples were placed under the macro-lens of a video camera, Figure 4.4. The room was blacked-out and the surface of the sample illuminated. Operational parameters were kept constant as follows:

Lens - concrete surface distance = 165 mm
Angle of illumination = 45°
Light Meter reading at surface of sample = 15/16 Ev
Diaphragm of macro-lens = 5.6

An area of 50 x 80 mm was viewed and displayed on the monitor. This image area was then divided into 512 x 512 pixels (i.e. 262144 in total), and the hue, saturation and intensity levels of each of these pixels was determined. Results were displayed as, the frequency of occurrence at each of the 0-255 levels.

The results from an image area of 50 x 80 mm include different aggregates and mortar matrix. Subsequently areas consisting only of individual aggregate particles and the mortar matrix were also examined.

4.6.4 Crack Density Measurements

The 80 x 50 mm thin sections were examined in filtered transmitted light using an Olympus (BH2) microscope at a magnification of x40. At this magnification the observed area is 10 x 10 mm and any cracks were easily visible. It had been hoped that the image analysis would have automatically given the required data for crack density by measuring the fluorescent yellow dye incorporated into the resin. However it was found that the resin had not penetrated all of the measurable cracks. This may have been due to a poor vacuum inside the impregnation unit when the thin sections were being prepared and / or that the cracks were discrete rather than continuous. Furthermore it was evident that the fluorescent resin had not only impregnated cracks but had also been smeared over most of the mortar matrix during polishing.

Consequently, photographs (x6) were taken of each 10 x 10 mm area on the 80 x 50 mm slide. The visible cracks were then traced onto paper from the photographs and the crack lengths measured using a map measurer pen. Crack density is then expressed in terms of mm of crack length per cm^2. For each 80 x 50 mm section the crack value denotes an average of the 40 different photographs.

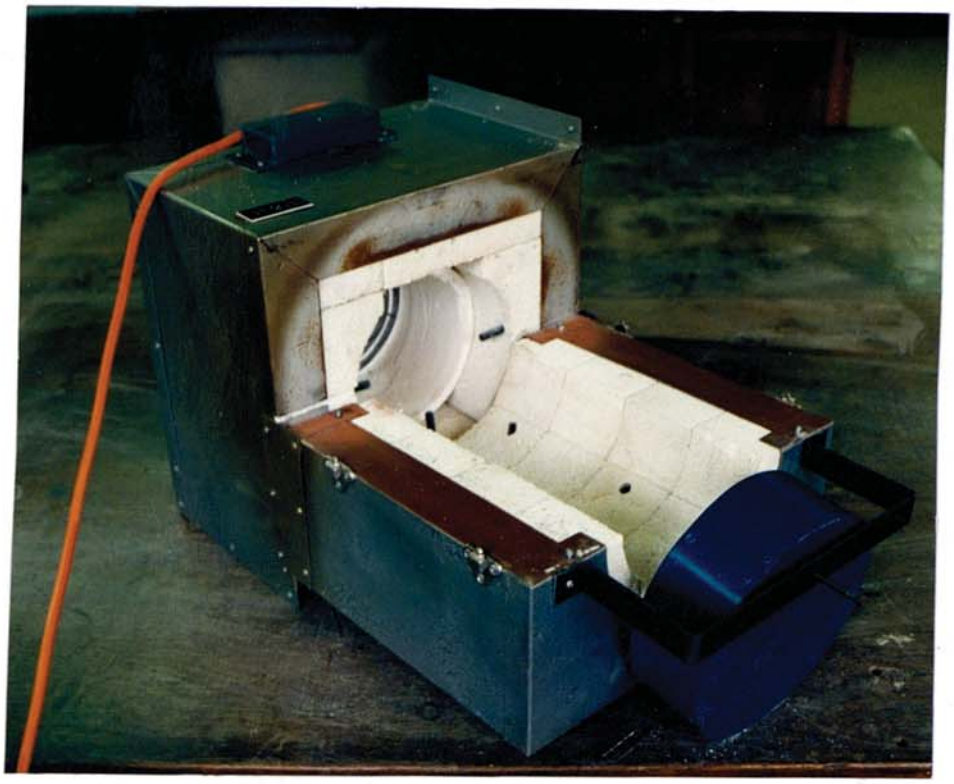

(a)

(b)

Figure 4.1 (a) Photograph of purpose built furnace to produce thermal gradients in concrete cylinders, (b) Photograph of electrical element

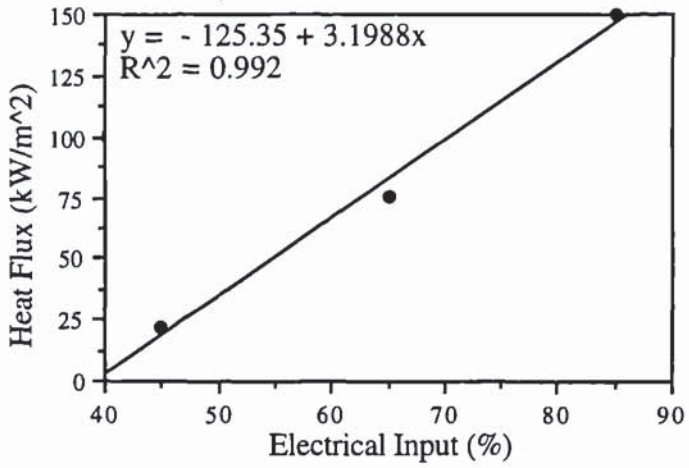

Figure 4.2 Calibration of electrical heating element for target flux

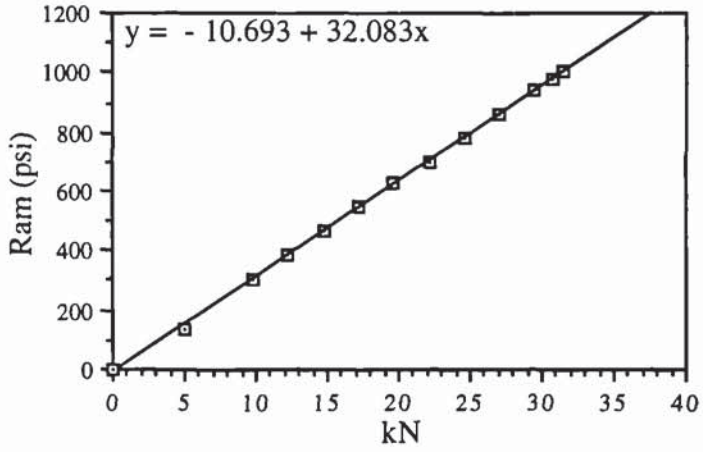

Figure 4.3 Calibration of load for applied load experiments

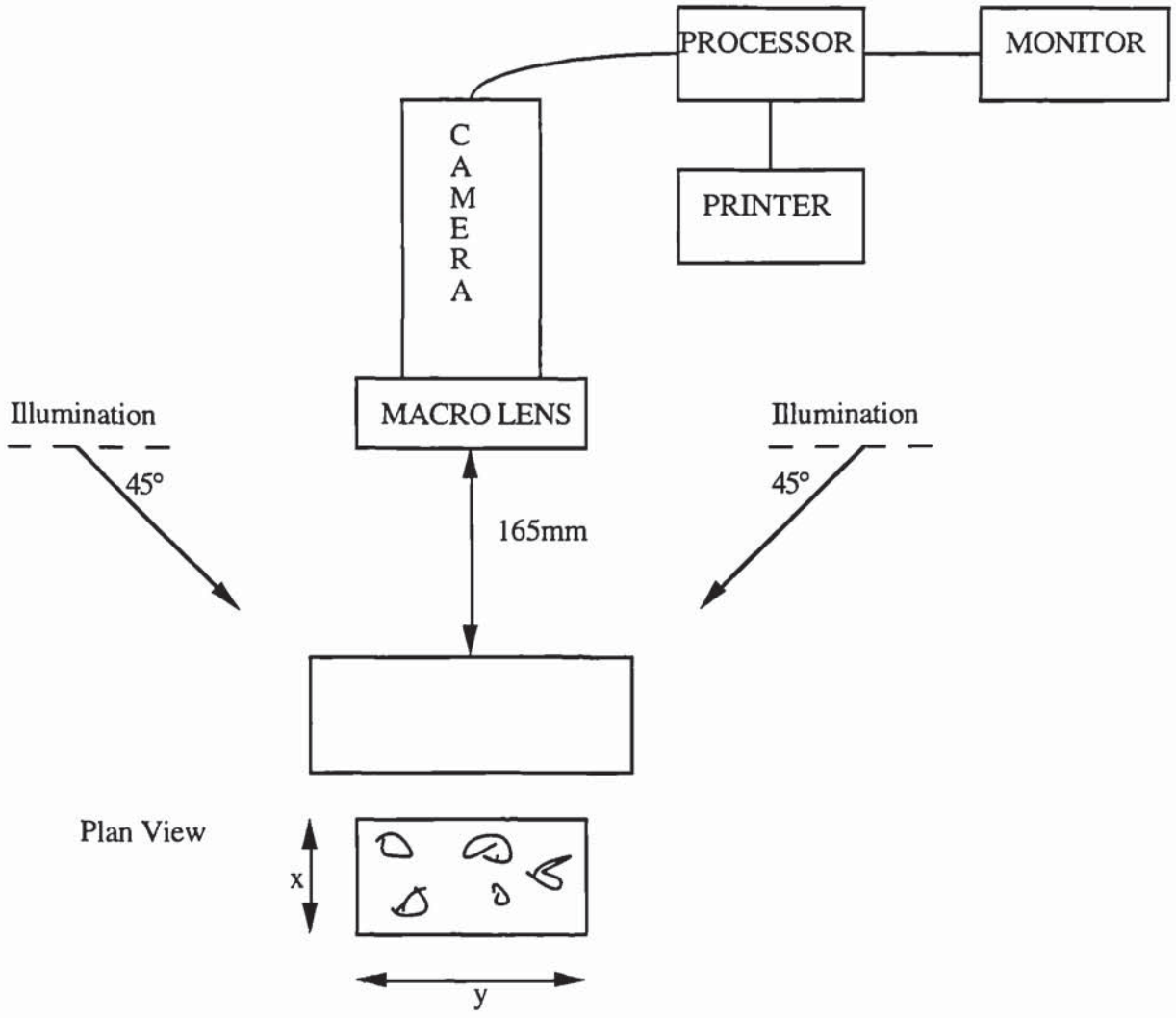

Figure 4.4 Arrangement of Image Analysis equipment for colour measurement using the macro-lens

CHAPTER 5

RESULTS AND DISCUSSION: THE THAMES VALLEY AGGREGATE CONCRETE SAMPLES HEATED TO EQUILIBRIUM TEMPERATURES

The results presented in this chapter are for samples of concrete made with the Thames Valley aggregate and OPC, OPC / PFA or OPC / BFS.

5.1 COLOUR CHANGE

A photograph of a polished cross-section of an unheated OPC concrete control sample is shown in Figure 5.1(a) and it is evident that the different components of the concrete exhibit a range of colours. This is also the case for an OPC concrete sample which has been heated to 350°C, Figure 5.1(b). A difference in colour between these two specimens is discernible - many of the components of the heated concrete having turned red or moved to a deeper red colour. Figure 5.2 (a) shows unheated OPC / PFA concrete and Figure 5.2 (b) shows concrete exposed to 350°C. Figure 5.3 (a) & (b) shows OPC / BFS concrete that is unheated and heated to 350°C. When comparing photographs 5.1 (a) & (b), 5.2 (a) & (b) or 5.3 (a) & (b) you are able to see a distinct colour change to red for the concrete heated to 350°C compared to the unheated concrete.

Initially measurements of colour were made for each of the sample areas, 50 x 80 mm as shown in the photographs in Figures 5.1, 5.2 & 5.3 (a)&(b), thus including a range of colours. Essentially the analyser records an image of this area and divides it into 512 x 512 pixels, i.e 262,144. The Hue, Saturation and Intensity for each pixel was then determined.

5.1.1 Hue

The results presented in Figure 5.4 (a) show the frequency of occurrence for the hue levels from 0 to 255 for the OPC samples shown in Figure 5.1. Figure 5.4 (b) shows the hue levels for the OPC/PFA samples shown in Figure 5.2 and the hue levels for the OPC / BFS samples shown in Figure 5.3 are presented in Figure 5.4 (c).

In order to preserve the clarity of the information when showing all the levels, it has been necessary to aggregate them in sets of 10 i.e 0-9, 10-19 etc. It is evident that, for both control and fired samples for the three cements, Figures 5.4 (a), (b), (c), the frequency of response is concentrated in the 0-50 hue levels and is particularly predominant in the 10-29 levels. By reference to Figure 3.3 it can be seen that this is representative of colour in the red-yellow region. For the OPC samples, Figure 5.4 (a), heating to equilibrium temperatures of 350°C caused a shift in the frequency so that for levels 20-29 there is drop in frequency of occurrence from 178,000 to 56,000; whilst in the 10-19 levels there is an increase from 76,000 to 203,000.

For the OPC/PFA samples, Figure 5.4 (b), there is a drop in frequency of occurrence in the 20-29 levels from 206,000 to 180,00 and in the 10-19 levels there is an increase from 19,000 to 73,000. The shifts are not as distinct as found for the OPC samples but are never-the-less discernible. For the OPC/BFS samples, Figure 5.4(c), the frequency of occurrence in the 20-29 levels drop from 260,000 to 106,000 and in the 10-19 levels increase from 30,000 to 109,000.

The shifts described above together with the photographs for all types of concrete; OPC, OPC/PFA and OPC/BFS, demonstrate a distinct change in colour on heating to a more pure red.

5.1.2 Saturation

The results presented show the frequency of occurrence for the levels of saturation from 0 to 255. It is evident that, for the OPC cement, Figure 5.5 (a), for both control and fired samples, the frequency of response is concentrated in the 30-150 levels. It is evident that heating to equilibrium temperatures of 350°C has caused a shift in the frequency so that there is a decrease in the levels 30-80 and an increase in the levels 90-119. Thus the colour is now more saturated.

Similar results were obtained for the PFA blended cement, Figure 5.5 (b) whilst with the BFS blended cement, Figure 5.5(c) the shift was not as pronounced.

5.1.3 Intensity

Figures 5.6 (a),(b),(c) show the frequency of occurrence for the levels of intensity from 0 to 255 for OPC, OPC/PFA and OPC/BFS for blended cement concretes. All three plots show a shift towards lower intensity levels for concrete heated to 350°C compared to the control concrete, i.e they become darker.

Strictly an actual colour, and colour change, should be defined in terms of all three components, hue, saturation and intensity. However, since the major changes occur in values of hue (and this is what people perceive visually) it was decided to present subsequent results only in terms of this parameter. Colour changes occurring on heating are then expressed as frequency of occurrence in the 0-19 levels as a percentage of the total frequency in all levels.

5.1.4 Measurement of Hue for the 0-19 Levels on the different aggregate constituent and mortar matrix for concrete made with TVA before and after firing at 350°C

Various components of the Thames Valley aggregate, such as flint, quartz and sandstone, and the mortar of the OPC concrete were identified and described in terms of colours by matching them with the colour plates given in Kornerup & Wanseker (1963). Subsequently the frequency of occurrence for Hue in the 0-19 levels was measured for each of the individual components. These were then expressed as percentages of the total frequency of occurrence for that particular piece of aggregate or area of mortar seen in Figure 5.7 and the results are given as follows in Table 5.1:

Table 5.1 Percentage (%) Hue found for the different aggregate constituents and mortar matrix for concrete made with TVA before and after firing at 350°C

Code	%	S01/A (control)	%	S01/F (heated to 350°C)
a	0.2	Grey flint with brownish yellow edge	99.7	Reddish brown flint with pale red edge
b	1.3	Dark grey flint	52.3	Grey flint
c	0	Light grey flint	99.4	Reddish brown flint
d	5.5	White flint & brownish orange streaks	48.6	White flint & light brown areas
e	4.4	Orange flint	83.9	Pale red flint
f	64.6	Pale red veined quartz	99.4	Reddish orange veined quartz
g	5.2	Brownish orange sandstone	98.7	Reddish brown sandstone
h	5.1	Yellowish grey Mortar	57.7	Brownish grey Mortar

Averages for whole polished sections were

16.8% 69.7%

These results show that the colour of the individual components vary widely and the effects of temperature are different. The colour of flint (a - e) in the control samples varied widely. There were examples of aggregate which are completely grey but are different in shades and others which have a brownish-yellow colour around the edge. These aggregates then exhibit a different change in colour when they have been exposed to equilibrium temperatures. The concrete tested is one that has been exposed to 350°C. In this sample the flints vary in colour from what seems unchanged to others that are very red. The veined quartz aggregates (f) do not appear to change colour as distinctly, changing from a pale red to a reddish orange. The mortar (h) changes from yellowish grey to brownish grey when heated and hence the measured hue for the 0-19 level increases.

5.1.5 Colour Change in Slag Blended Cements

It is known (ACI Committee 226, 1987) that concretes made with Blast Furnace Slag blended cements may develop a dark blue-green colouration. This colour is associated with release of sulfide ions into the concrete pore solution as the glassy slag dissolves during reaction with alkalis. Exposure to air allows oxidation of the sulphides to take place and the colouration diminishes with age.

This aspect was investigated as a final year project, Henstock (1995). To emphasise colour changes in the cement matrix, a mortar with a 3 : 1 sand : cement ratio was used rather than the concrete. It was found that a curing period of 28 days was required to allow development of the colour shown in Figure 5.8(a). (Note : Such colour colour is not developed with curing times of 7 days). A light coloured zone is observed around the dark core, formed as a result of surface oxidation. Action of heat on the cube accelerates

the oxidation process and the dark core retreats uniformly to the centre of the cube, Figure 5.8(b) and is then eliminated 5.8(c). The kinetics of the oxidation process is a function of temperature and time of heating. The higher the temperature the faster the dark core retreats since the rate of oxidation increases. The increased time of heating at a given temperature also results in the reduction of the size of the core.

5.1.6 Hue Measurement for 0-19 Level for Samples Heated to Equilibrium Temperatures

After examining the full plots of hue for concrete heated to 350°C, Figures 5.2 (a), (b) & (c), the levels which showed the most change compared to the control sample could be identified. This was found to be in the range from 0-19. Measurements of hue for each concrete; OPC, OPC/PFA and OPC/BFS heated to temperatures of 175°C, 250, 300, 350, 400, 450, 500 and 700°C were then taken and expressed as a percentage of the total frequency of occurrence:

$$(Fd / Fa)\ 100 \qquad (5.1)$$

where, Fd = Total frequency of occurrence in the 0 - 19 levels

Fa = Total frequency of occurrence in the 0 - 255 levels i.e the whole area.

Figure 5.9 shows the % hue in the 0-19 levels for OPC, OPC / PFA and OPC / BFS samples before and after heating. It is evident that the red colour started to develop significantly for all samples soaked in the temperature range 250-300°C. The development of this red colour is thought to be as a result of transformations in the composition and / or structure of hydrated iron oxides present in the aggregate. This colour develops quickly at 350°C whilst only very slowly at 250°C (bearing in mind the soaking time at equilibrium temperature of 45 minutes). Soaking at temperatures in the range 350-500°C shows little

change in red colour, after which the concrete becomes less red with the colour moving to a whitish-grey (which was not analysed). Figure 5.10 shows photographs of an OPC concrete heated to 350°C (a) and 500°C (b). Figure 5.10 (a) shows the maximum development of red colour that occurred for this concrete whilst Figure 5.10 (b) shows how the colour of the concrete has shifted to a more whitish grey colour after being exposed to 500°C.

It should be noted that the values plotted represent a mean red colour for a sample cross-sectional area of 50 x 85 mm. Within this area there are differences in colour between the mortar matrix and the various components of the siliceous gravel, as discussed earlier.

The control samples made with the blended cements have a higher base-line red colour compared to control samples made with OPC. In spite of this, the relative changes in colour are very similar. This observation demonstrates that development of red colour is not related to the iron oxide content of the cements since these vary widely, see Appendix 1.

Overall the results clearly demonstrate that this technique can be used to quantify colour changes in some concretes as a result of heating and is a considerable improvement on using subjective visual assessment. However this may not be true for all concretes, as referred to in chapter 7.

5.2 EFFECT UPON MECHANICAL PROPERTIES

5.2.1 Reduction in Compressive Strength

Figure 5.11 shows that for concrete made with plain OPC, there is a slight reduction in the compressive strength of samples soaked at temperatures up to 350°C. Soaking at temperatures greater than 350°C leads to a substantial reduction in strength. Comparing Figure 5.11 with Figure 5.9 it is evident that the substantial change in strength loss coincides with the full development of red colour. The concretes made using blended cements initially show an increase in strength indicating some effect of accelerated hydration. However, substantial reduction in strength occurs at 350°C, and is coincident with full development of the red colour. Thus the full development of a red colour may be used as an indication of significant loss in compressive strength.

5.2.2 Reduction in Flexural Strength

Figure 5.12 shows that significant drops in flexural strength occur at temperatures between 200 and 300°C, although the result for the OPC sample heated to 175°C does not exist. It is known that flexural tensile strength drops faster than compressive strength (Zoldners, 1960). Since the decrease in flexural strength occurs before the maximum development of red colour, which has been shown to coincide with the substantial loss in compressive strength, the two parameters of flexural strength and colour change cannot be correlated.

5.2.3 Reduction in Surface Hardness

Figure 5.13 shows similar trends for all three cements in that there is a slight reduction in surface hardness up to 350°C and significant reduction at temperatures greater than 350°C

which mirrors the results of compressive strength. The reduction in compressive strength indicates the increase in cracking and therefore the significant reduction in surface hardness can also be used as an indicator that the amount of cracking has increased.

5.2.4 Reduction in Dynamic Modulus of Elasticity

Figure 5.14 shows dynamic modulus reduces linearly with increasing temperature to 450°C. So that by heating to 300°C the residual values are only approximately 20% to those of the unheated samples. The effect of the high temperature on the dynamic modulus seems to be more detrimental than Lie (1968) reported, where he found a 40% reduction at 300°C. The greatest reduction in elastic modulus occurs at temperatures around 200-250°C which compares favourably with Harmathy and Berndt (1966). At temperatures over 450°C the dynamic modulus decreases rapidly. The severity of the decrease in dynamic modulus may be effected by the way the results have been calculated using BS 1881: 209: 1990, where the value is taken to the nearest 500 MN/mm^2, hence values of 249 MN/mm^2 or below are rounded down to 0 MN/mm^2. There is no correlation between these parameters and the residual compressive strength, Figure 5.11.

5.2.5 Reduction in Ultrasonic Pulse Velocity

Classification of the quality of concrete on the basis of pulse velocity may be taken as follows, Greig (1982), Table 5.2:

Table 5.2 Typical Preliminary Damage Classification of UPV based upon a flint concrete with an undamaged UPV of 4.35 km/s

Pulse Velocity (km/s)	Quality of Concrete
> 4.35	Undamaged remote from fire
>3.90	Undamaged, within normal range
3.90 - 3.70	Some damage
3.70 - 3.50	Damaged, tensile strength may be reduced by large amounts. Compressive strength probably affected but possibly not significantly.
3.5 - 3.0	Tensile strength may be reduced by more than half. Compressive strength may be affected significantly.
< 3.0	Severe reduction in tensile strength. Compressive strength most probably affected significantly.

In this context the unheated samples have pulse velocities at 4.5 km/s and would therefore be considered in excellent condition. Samples heated to 175 - 250°C have pulse velocities between 3.0 - 3.5 km/s would therefore be in doubtful condition, whilst samples heated to 300°C have pulse velocities of about 2.5 km/s and therefore are in a poor condition. In relation to the compressive strength results, such a classification is probably overestimating the damage. Furthermore, the technique does not detect the more significant compressive strength deterioration at temperatures greater than 350°C.

Figure 5.15 shows the pulse velocity decreases almost linearly with increasing temperature. The cement type seems to have no significant influence on this relationship.

The mechanical properties of pulse velocity (the effect of time to transit a waveform through a material), dynamic modulus (the enforced elastic vibration of a material) and flexural strength will be affected by any material degradation including micro- and macro-cracks due to loss of bond and thermal incompatibility, e.g. between aggregate and matrix phases. Thus both of these measurements will show immediate decrease on heating. Compressive strength measures the mechanical response of a (cracked) matrix, when the cracking is negligible, i.e. below temperatures of 300°C, see section 5.3, the application of load closes any micro-cracks with little extra damage to the specimen and thus measured strengths may not be much reduced. With the onset of macro-cracking, about 350°C the initial portion of loading causes extra damage by trying to overcome the effect of the cracks before the reduced strength core starts taking load and gives much reduced strengths.

Figure 5.16 shows the correlation of normalised UPV with normalised compressive strength. The R^2 values are 0.815, 0.639 and 0.673 for the OPC, OPC/PFA and OPC/BFS concretes respectively and therefore the R values are 0.902, 0.799 and 0.820. These R values represent a reasonable correlation of UPV with compressive strength. There does not appear a significant difference between the three types of cement blends.

The correlation of normalised UPV with normalised flexural strength is shown in Figure 5.17. The R values show a better correlation, with values of 0.948, 0.985 and 0.977 for the OPC, OPC/PFA and OPC/BFS concretes than for those of compressive strength with UPV. There does appear to be a small difference between the three cements. The intercepts range from 0.389 for the OPC concrete to 0.488 for the OPC/BFS concrete. The slopes of the best fit line also differ slightly. Therefore it is apparent that there is a slight difference between the three cement blends. This may be due to the property of flexural strength being dependent upon the bond between the aggregate and the cement and the cement replacement effecting this.

The correlations of normalised UPV with normalised dynamic elasticity show a more significant difference between the three cement blends. The intercepts range from 0.246 for the OPC/BFS to 0.418 for the OPC and the slopes from 1.017 to 1.267 respectively. Since the dynamic modulus of a concrete depends on its actual composition differences are to be expected, although these are not very large.

5.2.6 Differential Thermal Analysis (DTA) & Thermo-Gravimetric Analysis (TGA)

During heating of cementitious materials a series of endothermic reactions may occur and include (Table 5.3):

Table 5.3 Temperatures at which endothermic reactions occur when heating cementitious material

dehydration of CSH gel	100 - 120°C
decomposition of ettringite	130 - 160°C
dehydration of $Ca(OH)_2$	450 - 550°C
decomposition of $CaCO_3$	750 - 850°C
α to β quartz transition in siliceous aggregate	573°C

Figures 5.19 and 5.20 show typical DTA and TGA thermograms for samples taken from the Thames Valley Aggregate concrete made with (a) OPC, (b) OPC/PFA and (c) OPC/BFS cements. Each figure shows results from unheated (control) samples and those heated to 350 or 500°C. Considering first the DTA thermograms for the OPC cements, Figure 5.19(a). In the case of the unheated sample it is evident that a series of endothermic reactions occurs including: dehydration of CSH gel (100-120°C), dehydration of calcium

hydroxide (450-500°C) and decomposition of calcium carbonate (750-850°C). Firing at 350°C results in the disappearance of the CSH gel endotherm but not the calcium hydroxide or carbonate endotherms. Firing at 500°C results in a small diminution of the calcium hydroxide endotherm but does not eliminate it. The kinetics of decomposition may be such as to require much longer periods of firing at 500°C for its elimination. Thus when examining fire damaged concrete, the absence of this endotherm would indicate temperatures in excess of 500°C had been reached during the fire.

TGA thermograms for the OPC cements are shown in Figure 5.20(a). Unheated samples show gradual loss in weight up to 400°C corresponding with gradual dehydration of the CSH gel. Two discontinuities then occur at around 450 and 750°C, these corresponding with the dehydration of calcium hydroxide and decomposition of calcium carbonate. Since these reactions occur during firing, the subsequent weight loss is much less for the samples which have been heated to 350 and 500°C.

Thus if assessing fire damaged concrete made with OPC cements the CSH gel and calcium hydroxide DTA peaks and TGA weight losses may be used as markers.

In the case of the blended cements, Figures 5.19(b) and (c), the CSH gel and calcium hydroxide DTA endotherms are much smaller when compared with those found for the unblended cement. TGA traces are virtually the same regardless of temperature, Figures 5.20(b) and (c). These observations reflect the different hydration characteristics of blended cements e.g. consumption of calcium hydroxide as a result of the pozzolanic reactions. Thus it may be concluded that the use of DTA/TGA would be of little use in assessing the thermal history of concrete made with blended cements.

5.2.7 Porosimetry

The changes in pore size distribution on heating the three cement matrices are shown in Figures 5.21(a)-(c). In the case of the OPC matrix there is little change at temperatures of up to 350-400°C. At higher temperatures the total porosity increases and there is a coarser pore structure. With the blended cements changes occur at lower temperatures so that even at 250°C a coarsening of the pore structure occurs. This may be related to the slower hydration found when using blended cements. The coarsening of pore structure in the blended cements due to the larger size of the cement replacements may also be responsible for the onset of cracking at slightly lower temperatures, Figure 5.22(b) (c), compared to unblended cement, Figure 5.22(a).

5.3 CRACK DENSITY

Figures 5.22 (a), (b) & (c) show the effect of temperature on the crack density (mm of crack length per cm^{-2}) for the OPC, OPC/PFA and OPC/BFS concretes. Each of the points on the graphs is an average of the crack lengths measured in 40, 10 mm squares covering a 80 x 50 mm section.

Looking at the photographs in Figure 5.23, it is evident that some minor cracking is evident in the control specimens, e.g. shrinkage cracks and defects in the aggregate, Figure 5.23(a). This explains the the baseline of cracking that exists in Figures 5.22(a), (b) & (c). Increased cracking due to thermal effects start at temperatures around 250-350°C and this increase can be seen in Figure 5.23(b). Crack density then increases linearly with increase in temperature, and at 500°C it is obvious from Figure 5.23(c) that the density of cracks has increased greatly.

Increase in cracking owing to the application of heat starts at 250°C for the OPC/PFA, 325°C for the OPC and 350°C for the OPC/BFS concretes, as shown by the intersection points in Figures 5.22 (a), (b) & (c).

The temperatures for the onset of increased cracking for the OPC and OPC/BFS concretes are very similar to those found for the substantial drop in compressive strength as shown in Figure 5.11. In the case of the OPC/PFA blended concrete cracking appears to start at a slightly lower temperature in relation to the drop in compressive strength. At the moment no explanation can be given for this.

The correlation between the temperatures for the onset of increased cracking and the full development of colour as shown in Figure 5.9 is not as obvious. This may be because the cracking in the concrete is a physical change while the colour development is a chemical change and these two properties are therefore not dependent upon each other, unlike the physical changes of compressive strength and cracking.

Comparison of crack density, with residual compressive strength at equivalent temperatures show good correlations (R^2 : 0.92, 0.88, 0.95 for OPC, OPC/PFA, OPC/BFS concretes respectively) as can be seen from Figure 5.22(d). The results show that within experimental error there is no distinct difference between the cements, most points lie on or close to the linear line. Therefore the use of blended cements does not seem to increase the concretes resistance towards fire.

5.4 SUMMARY

The experimental investigations with Thames Valley aggregate concrete and different cement blends have shown that the colour change of a concrete after fire exposure can be quantified. The heating of the concrete to equilibrium temperatures has allowed a calibration of temperature versus colour change to be developed.

The compressive strength is effected by exposure to heat and significant reductions correlated well with the maximum development of red colour. Other tests that have been used for fire damaged concrete such as UPV and dynamic modulus failed to determine the significant strength reductions and showed the effect of heat to be more gradual. Surface hardness testing using the Schmidt Hammer proved to be useful in determining the increased cracking in the concrete due to heat exposure.

The effect of different cement blends on the concretes susceptibility to heat showed some difference. Generally the OPC concrete was more resistant to higher temperatures compared to the OPC / PFA and OPC / BFS blends, although the difference was not substantial.

(a)

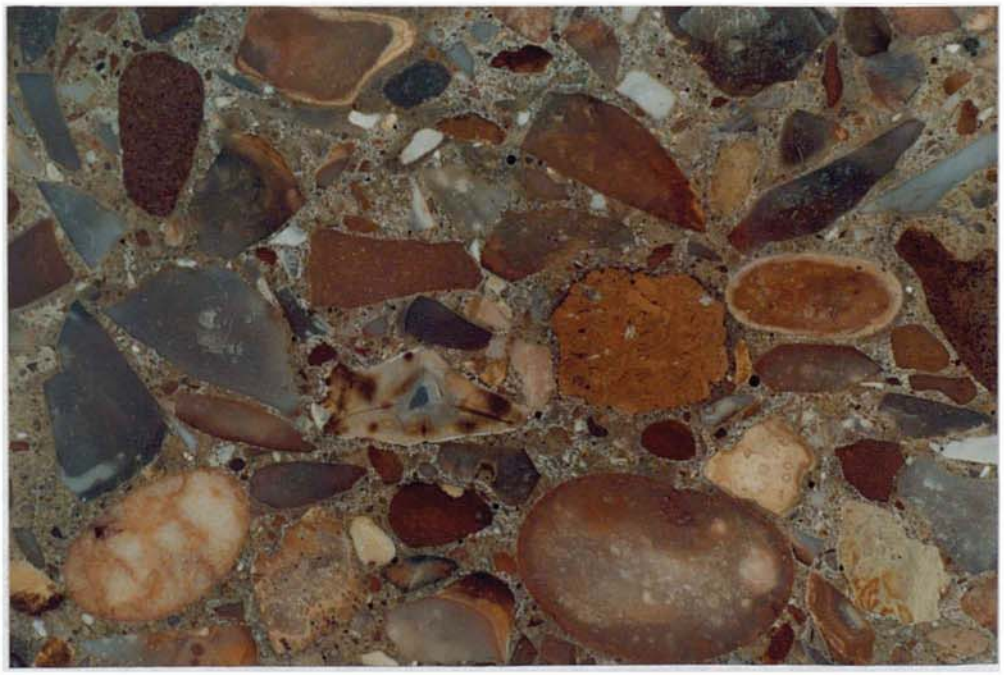

(b)

Figure 5.1 Photographs of polished cross section of (a) an unheated OPC concrete and (b) heated to 350°C (x 1.6)

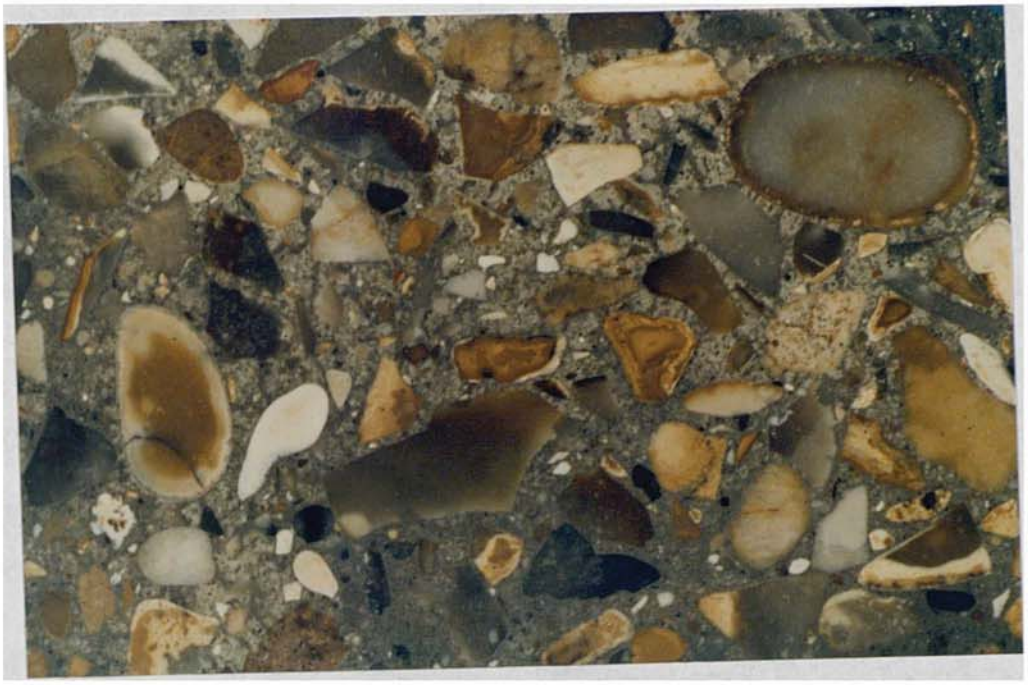

(a)

(b)

Figure 5.2 Photographs of polished cross section of (a) an unheated OPC/PFA concrete and (b) heated to 350°C (x 1.6)

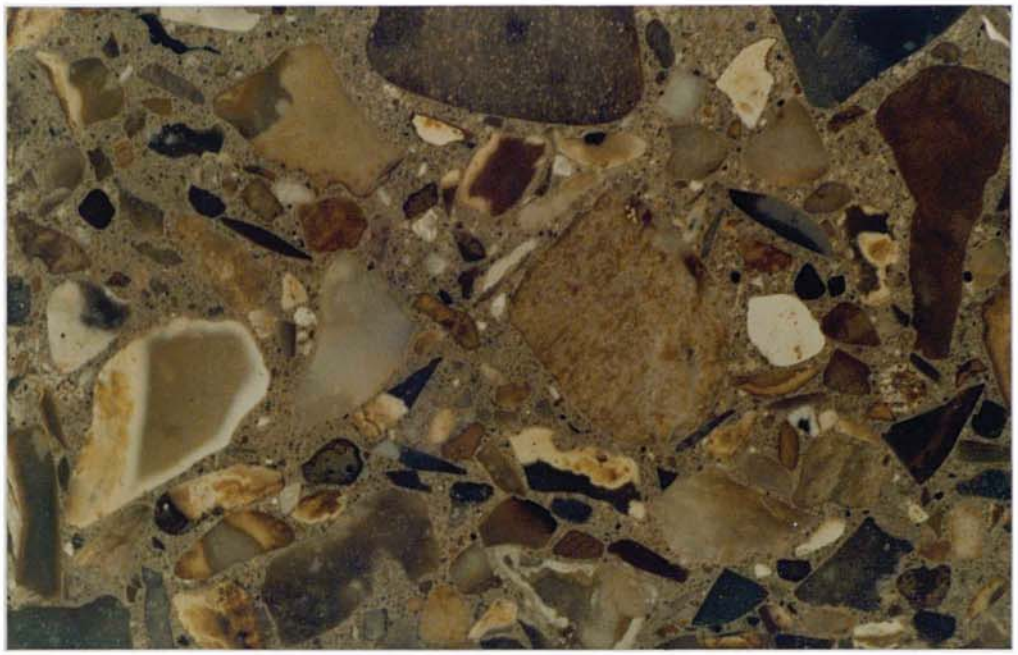

(a)

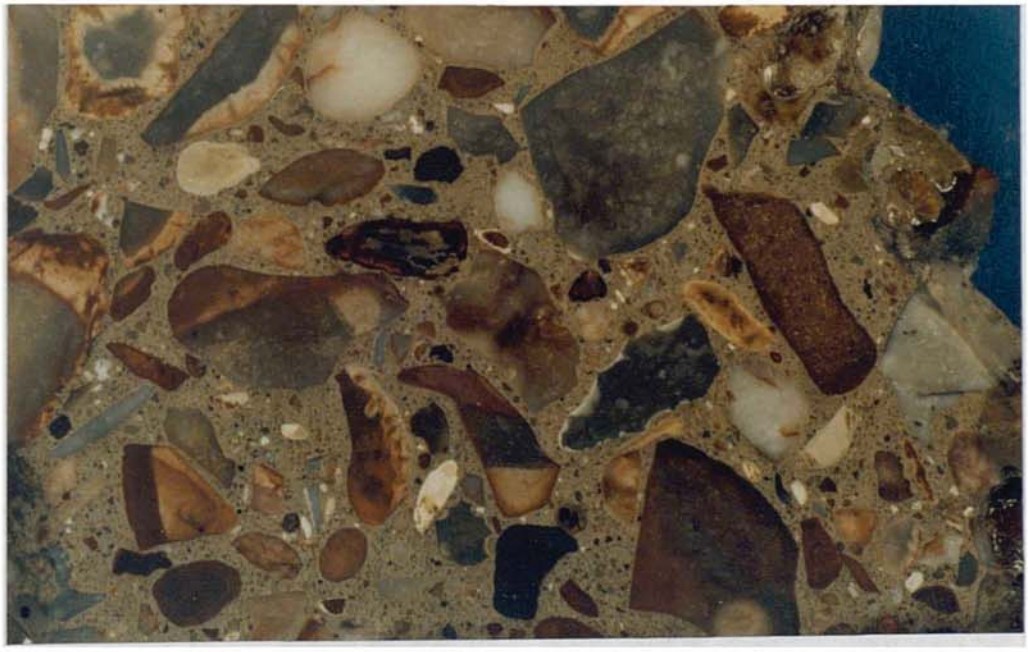

(b)

Figure 5.3 Photographs of polished cross section of (a) an unheated OPC/BFS concrete and (b) heated to 350°C (x 1.6)

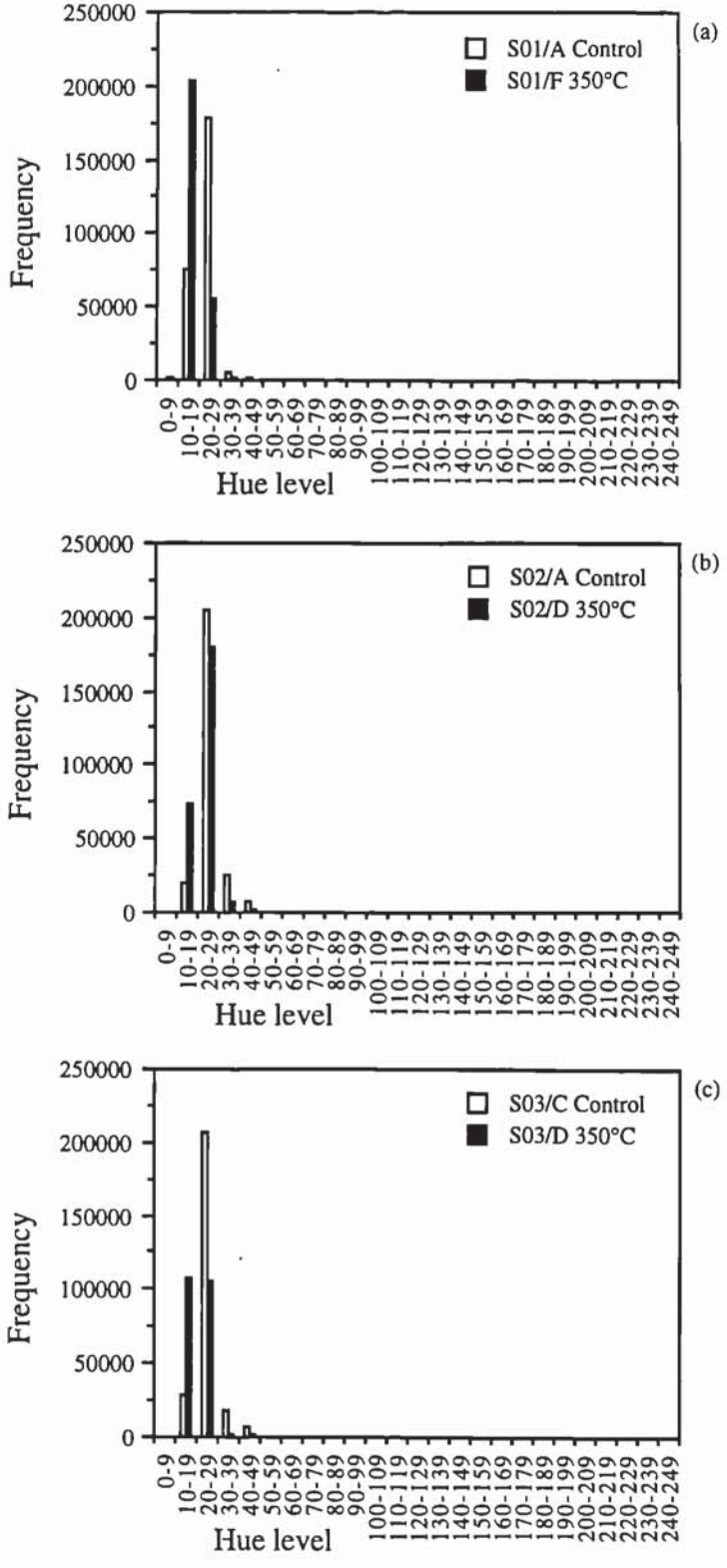

Figure 5.4 Frequency of occurrence for the levels of Hue from 0 to 255 for (a) OPC, (b) OPC/PFA and (c) OPC/BFS concrete

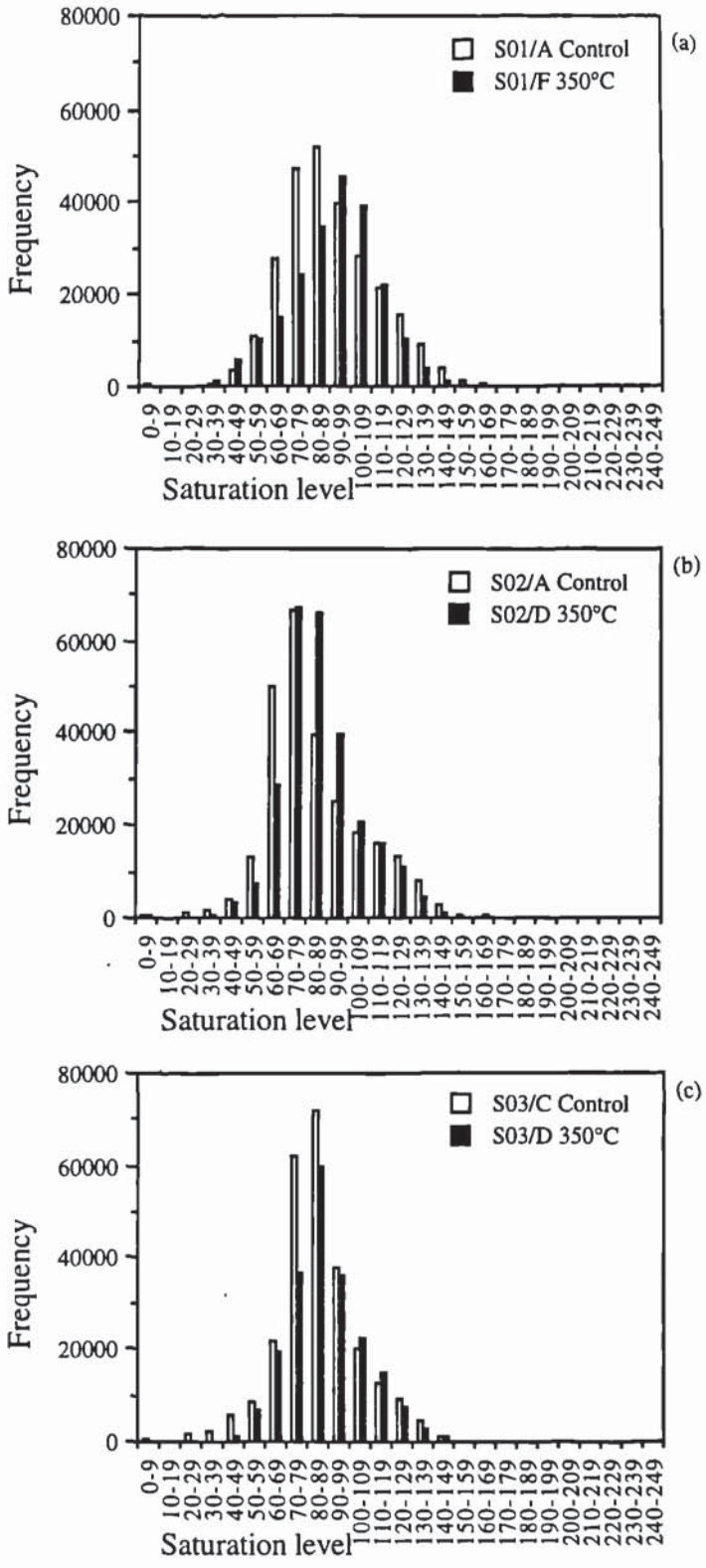

Figure 5.5 Frequency of occurrence for the levels of Saturation from 0 to 255 for (a) OPC, (b), OPC / PFA and (c) OPC / BFS concrete

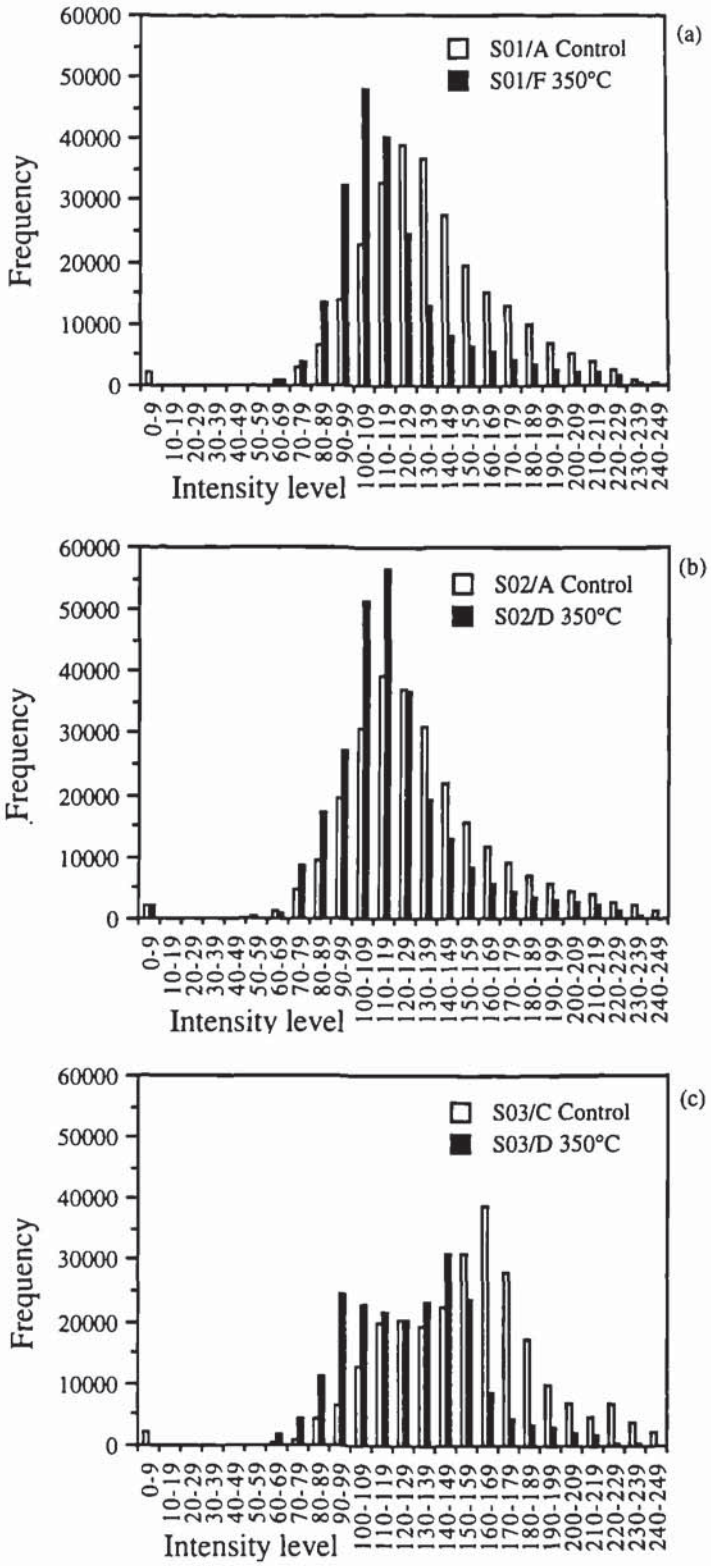

Figure 5.6 Frequency of occurrence for the levels of Intensity from 0 to 255 for (a) OPC, (b) OPC / PFA and (c) OPC / BFS concrete

(a)

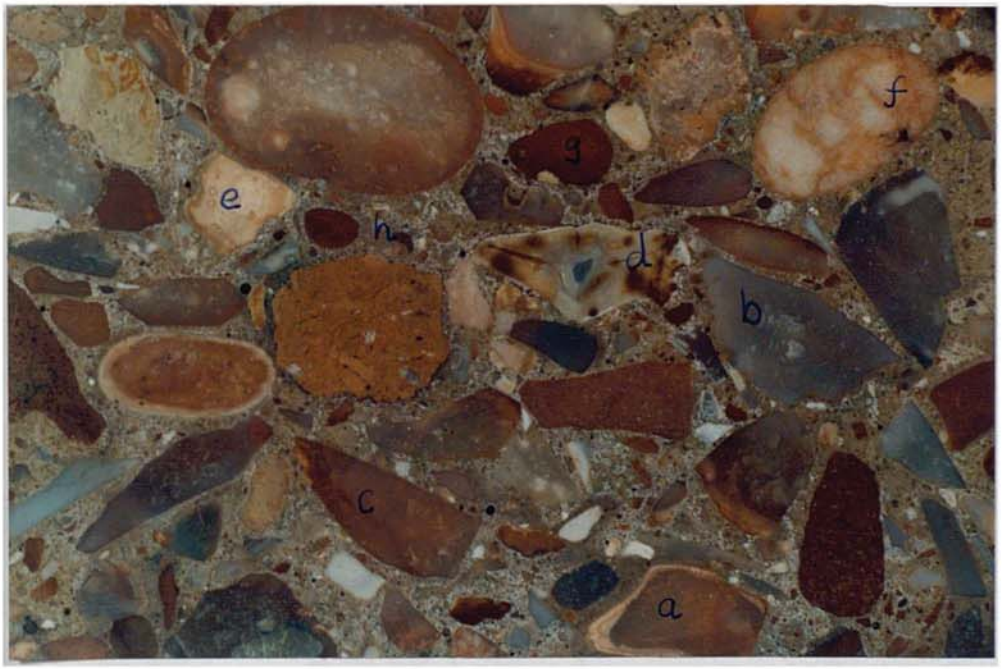

(b)

Figure 5.7 Photographs of polished cross section of (a) an unheated OPC concrete and (b) heated to 350°C with different aggregate constituents and mortar matrix identified

(a)

Figure 5.8(a) Photograph of a Blast Furnace Slag cement mortar showing a blue-green discolouration after curing for 28 days

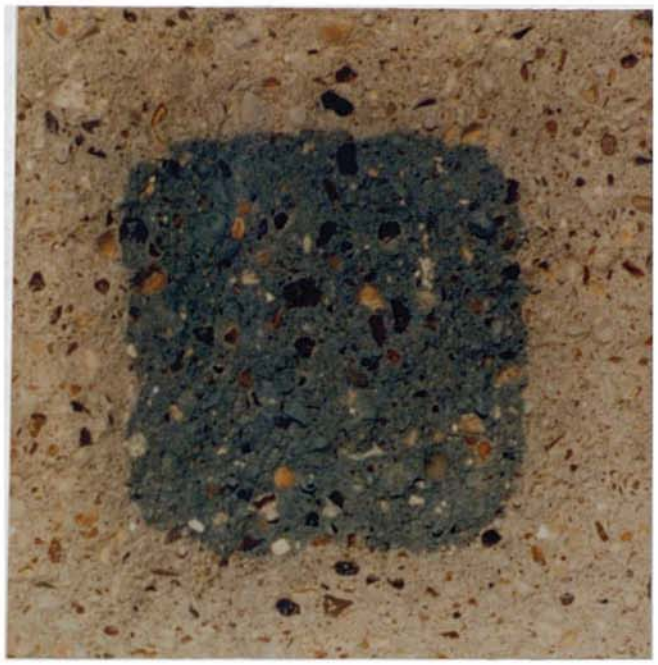

(b)

(c)

Figure 5.8 Photographs of a Blast Furnace Slag cement mortar showing a blue-green discolouration (b) & (c) after firing

(a)

(b)

Figure 5.10 Photographs of polished cross sections of OPC concrete heated to (a) 350°C (b) and 500°C (x 1.6)

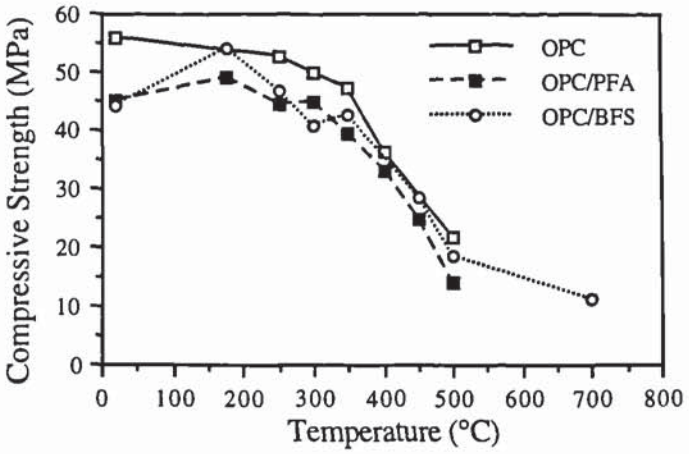

Figure 5.11 The reduction of compressive strength with increasing equilibrium temperature

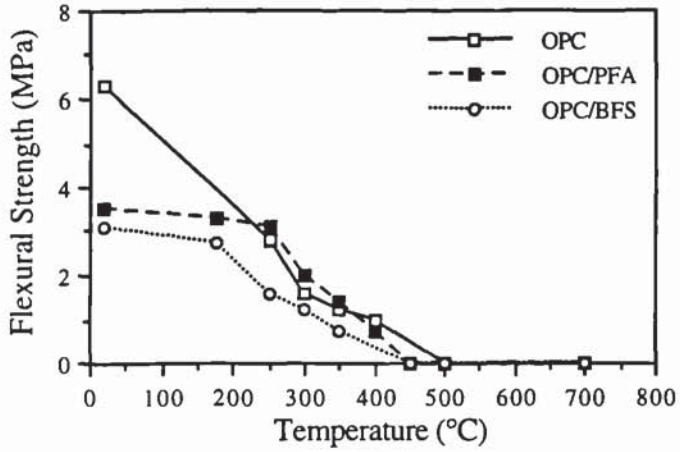

Figure 5.12 The reduction of flexural strength with increasing equilibrium temperature

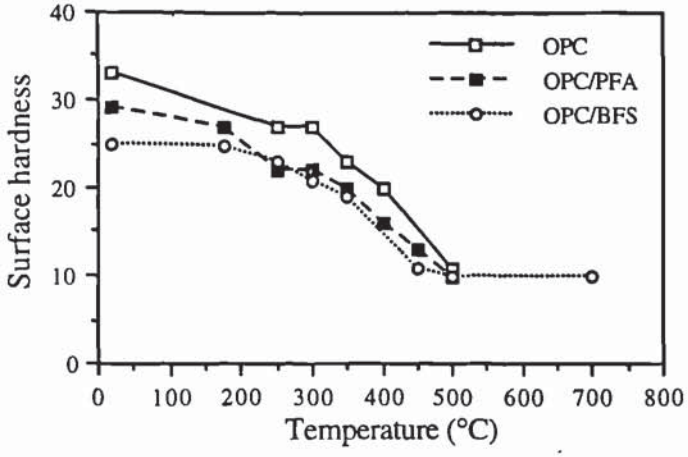

Figure 5.13 The reduction of surface hardness with increasing temperature

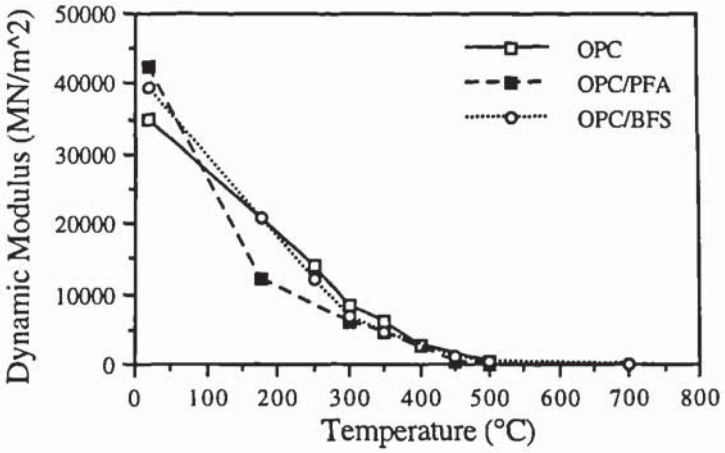

Figure 5.14 The reduction of dynamic modulus with increasing equilibrium temperature

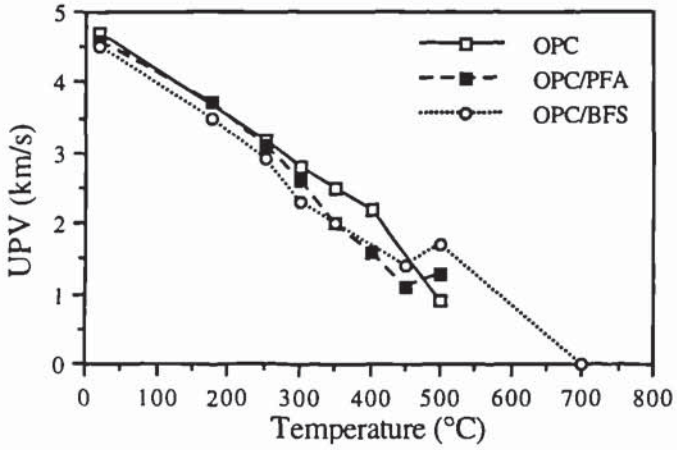

Figure 5.15 The reduction of Ultrasonic Pulse Velocity with increasing equilibrium temperature

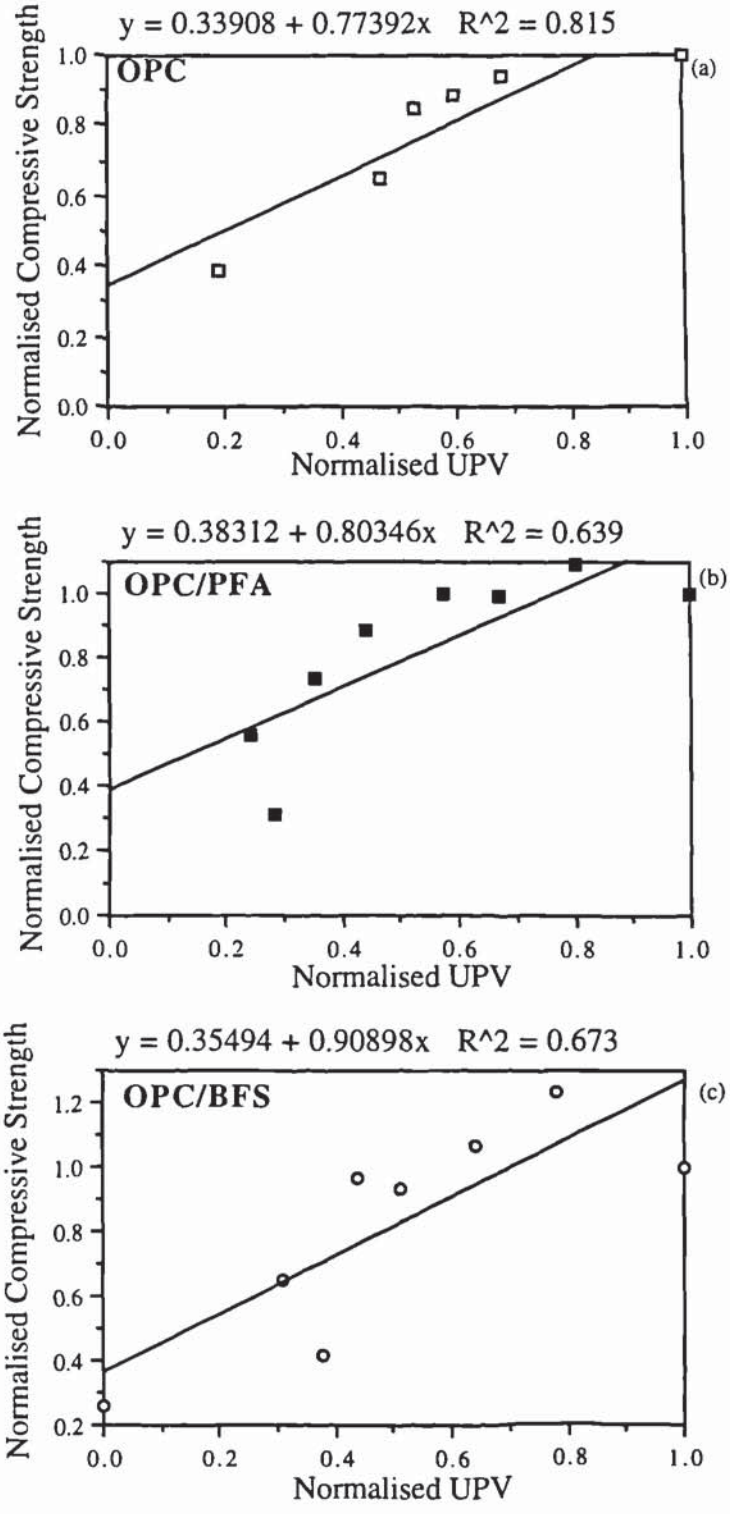

Figure 5.16 The correlation of normalised Ultra Pulse Velocity with Normalised Compressive Strength for Thames Valley aggregate concrete heated to equilibrium temperatures

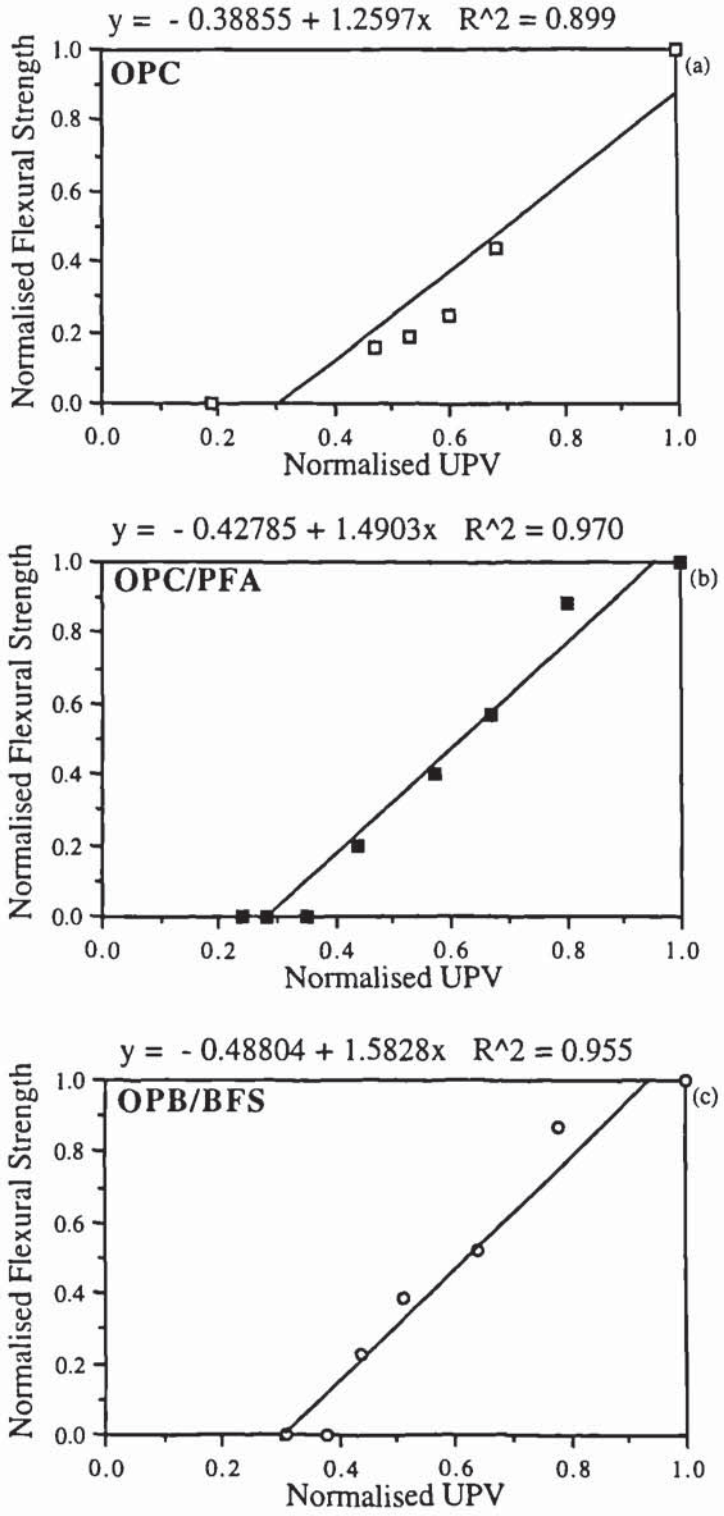

Figure 5.17 The correlation of normalised Ultra Pulse Velocity with Normalised Flexural Strength for Thames Valley aggregate concrete heated to equilibrium temperatures

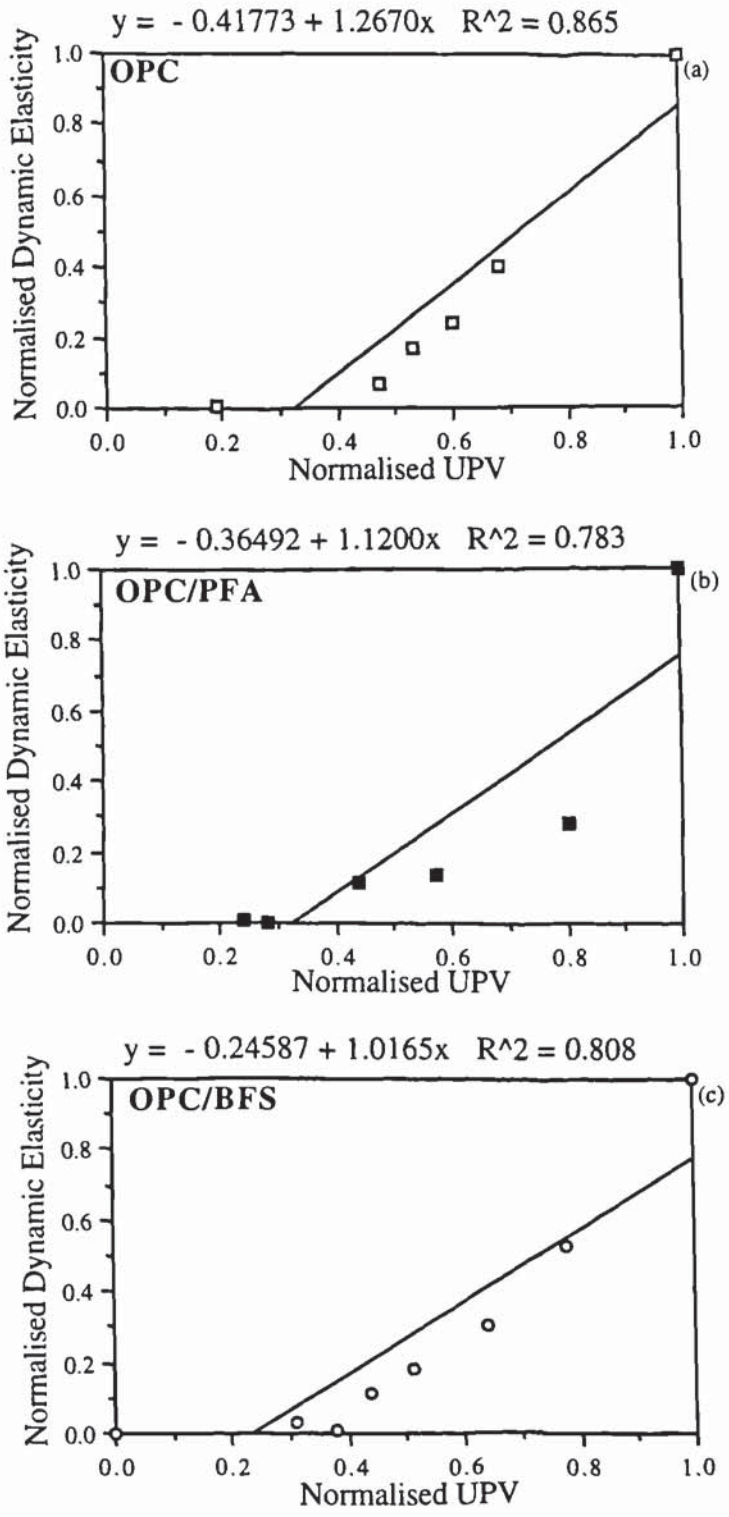

Figure 5.18 The correlation of normalised Ultra Pulse Velocity with Normalised Dynamic Modulus for Thames Valley aggregate concrete heated to equilibrium temperatures

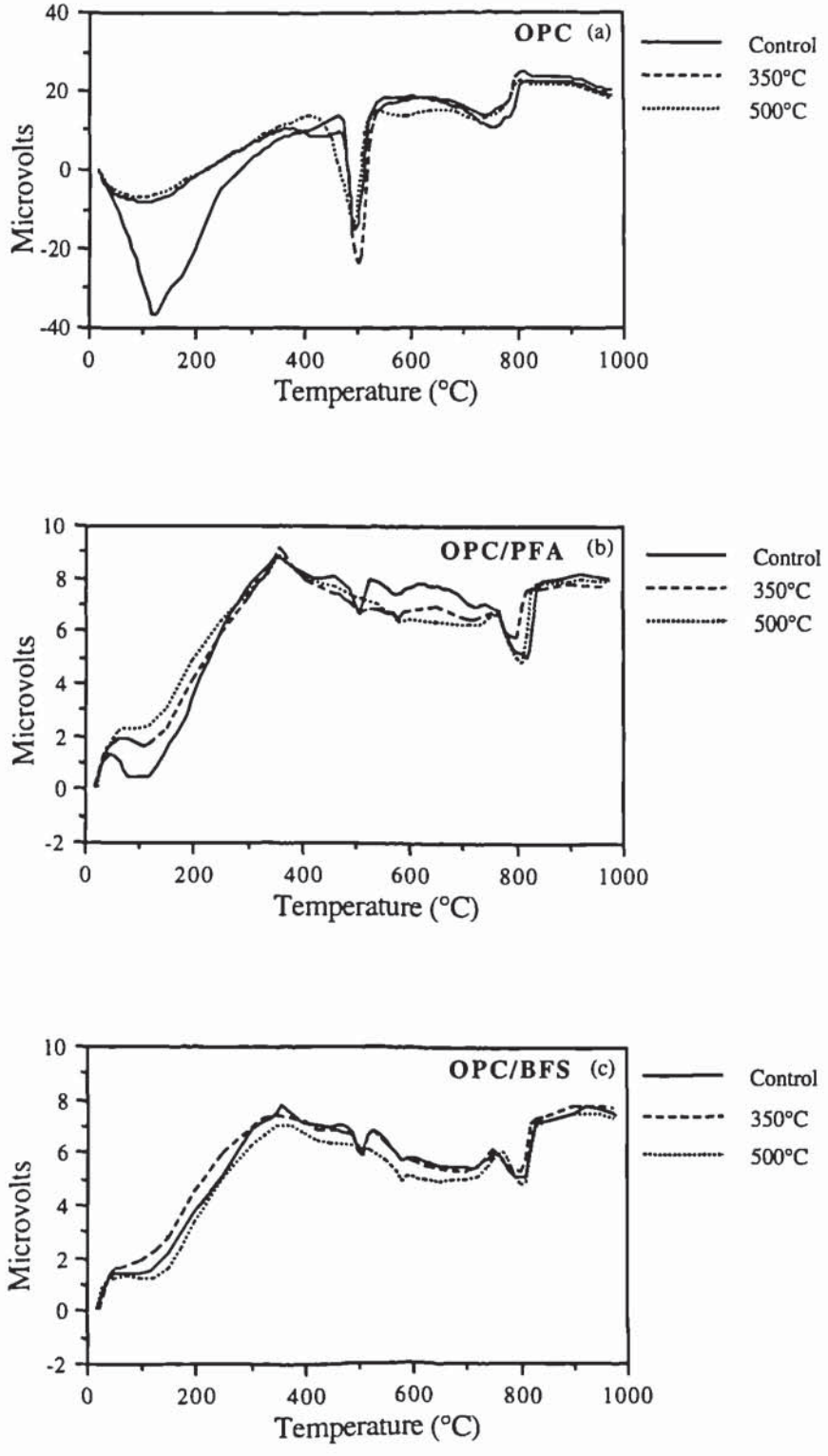

Figure 5.19 DTA curves for Thames Valley aggregate concrete heated to various equilibrium temperatures

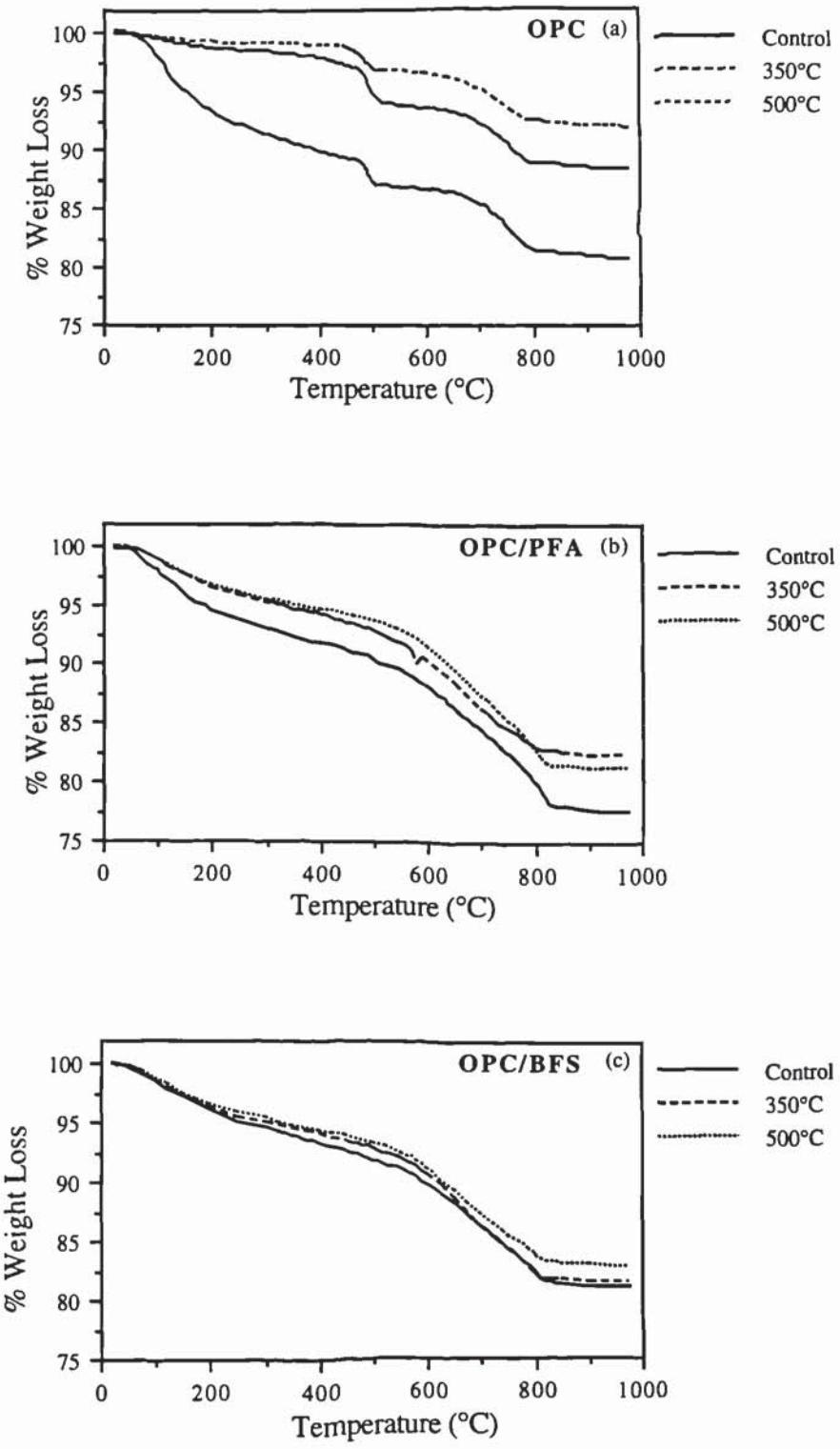

Figure 5.20 TGA curves for Thames Valley aggregate concrete heated to various equilibrium temperatures

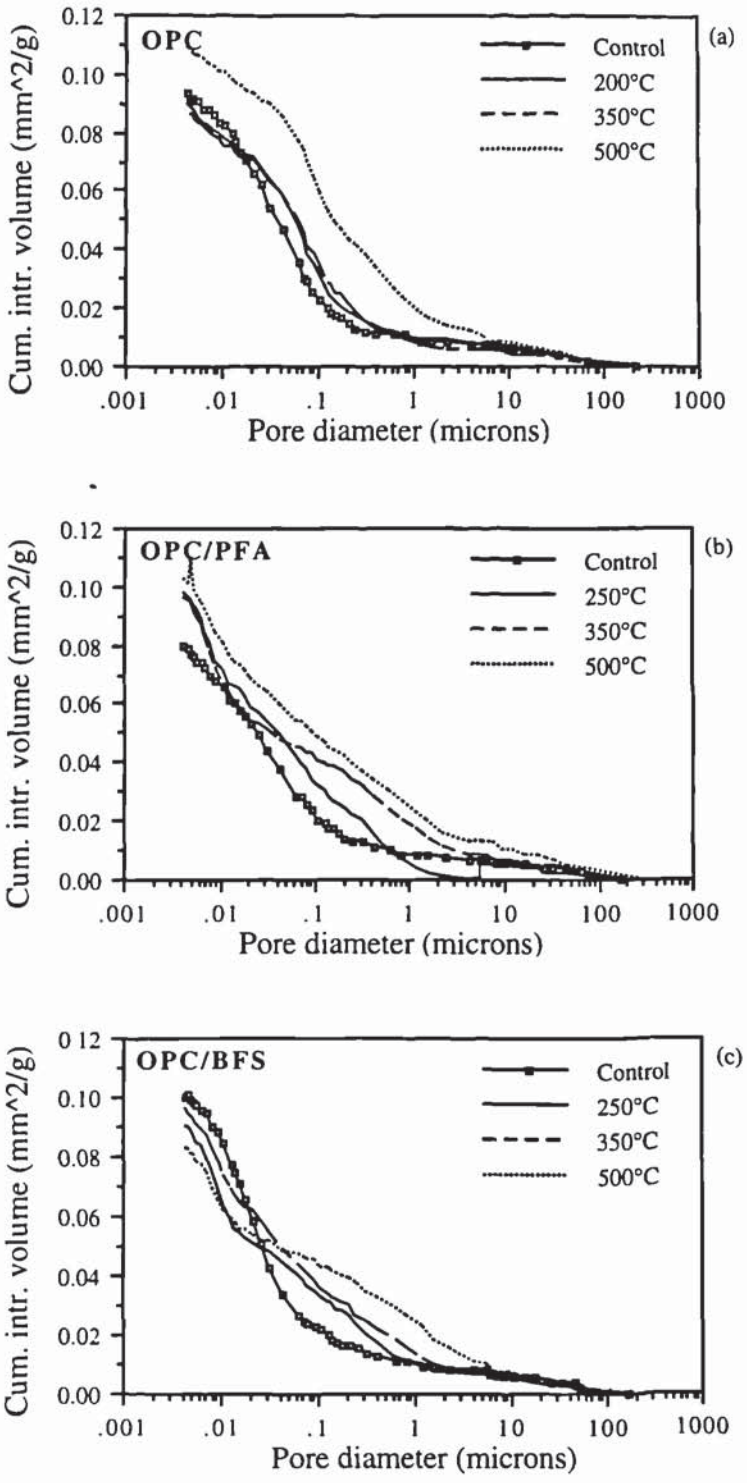

Figures 5.21 Pore size distribution curves for the Thames Valley aggregate concrete heated to various equilibrium temperatures

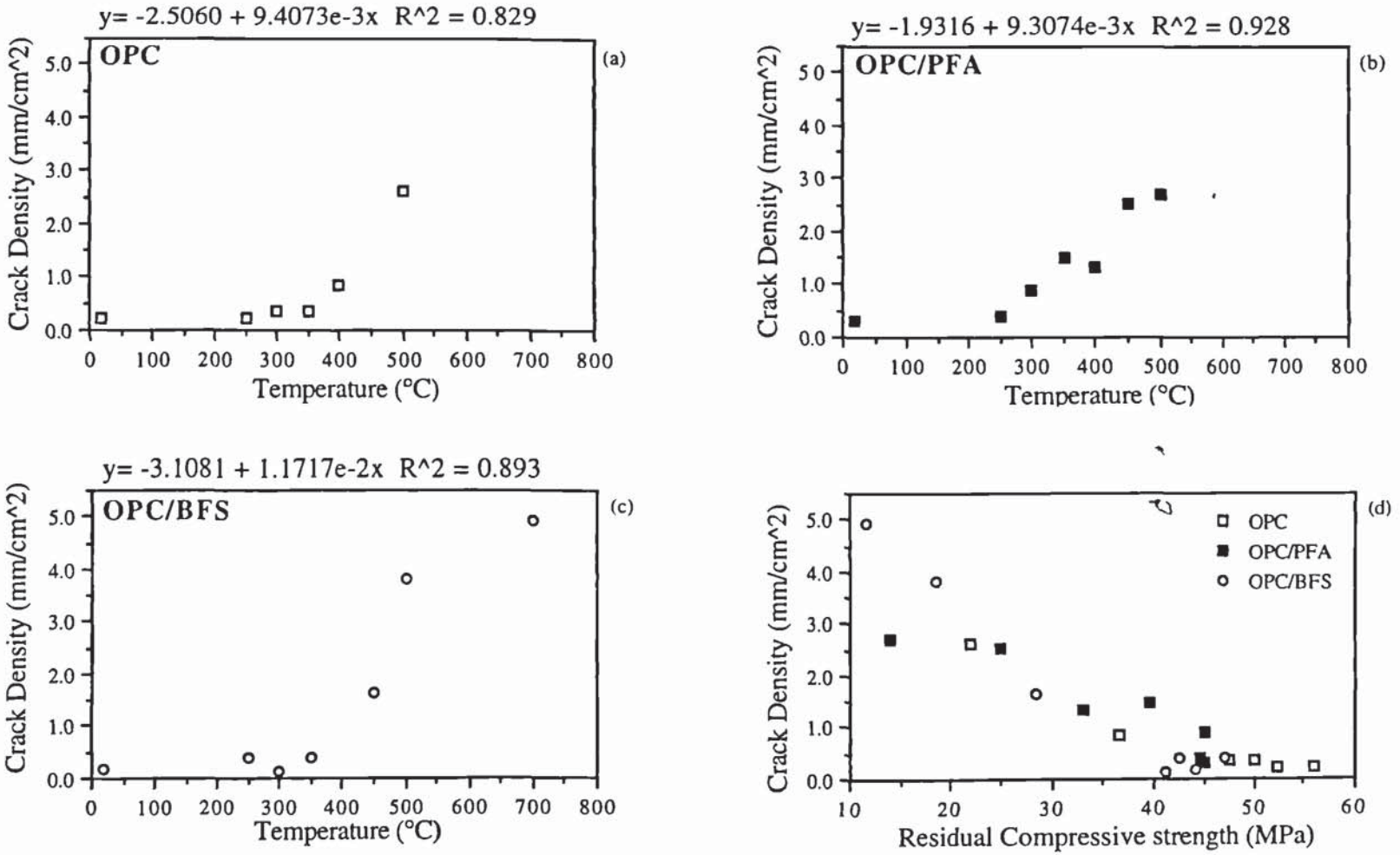

Figure 5.22 The development of crack density with increasing equilibrium temperature for a Thames Valley aggregate concrete concrete (a) OPC (b) OPC/PFA (c) OPC/BFS and (d) the correlation of crack density with residual compressive strength

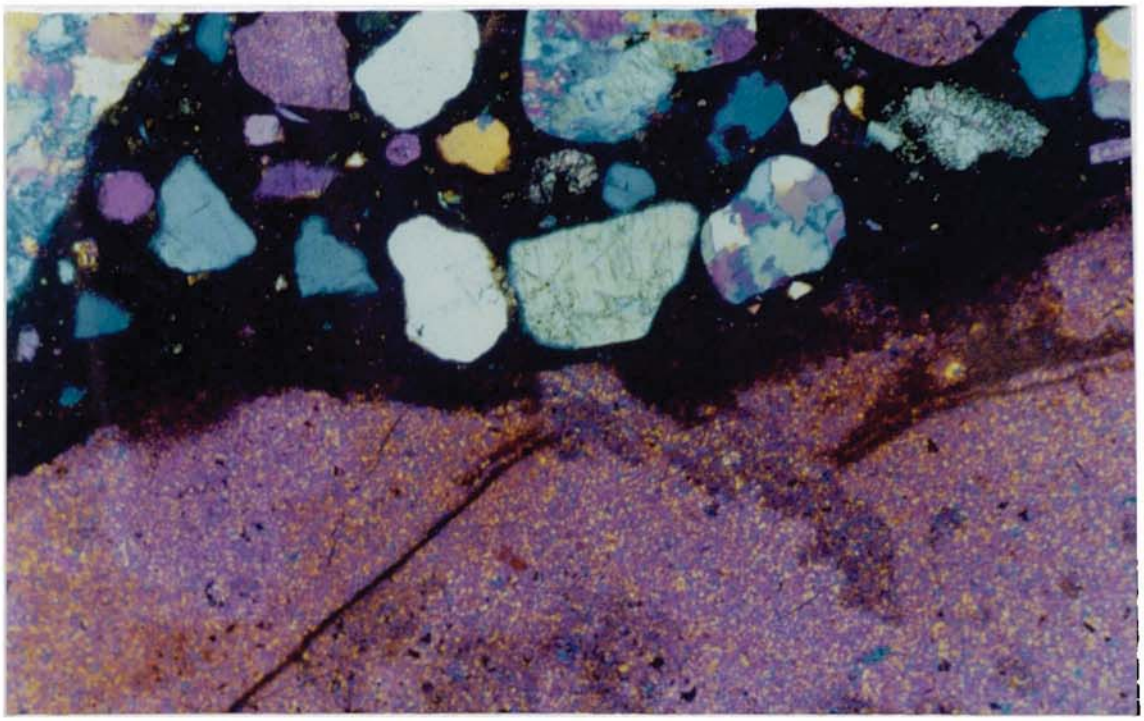

(a)

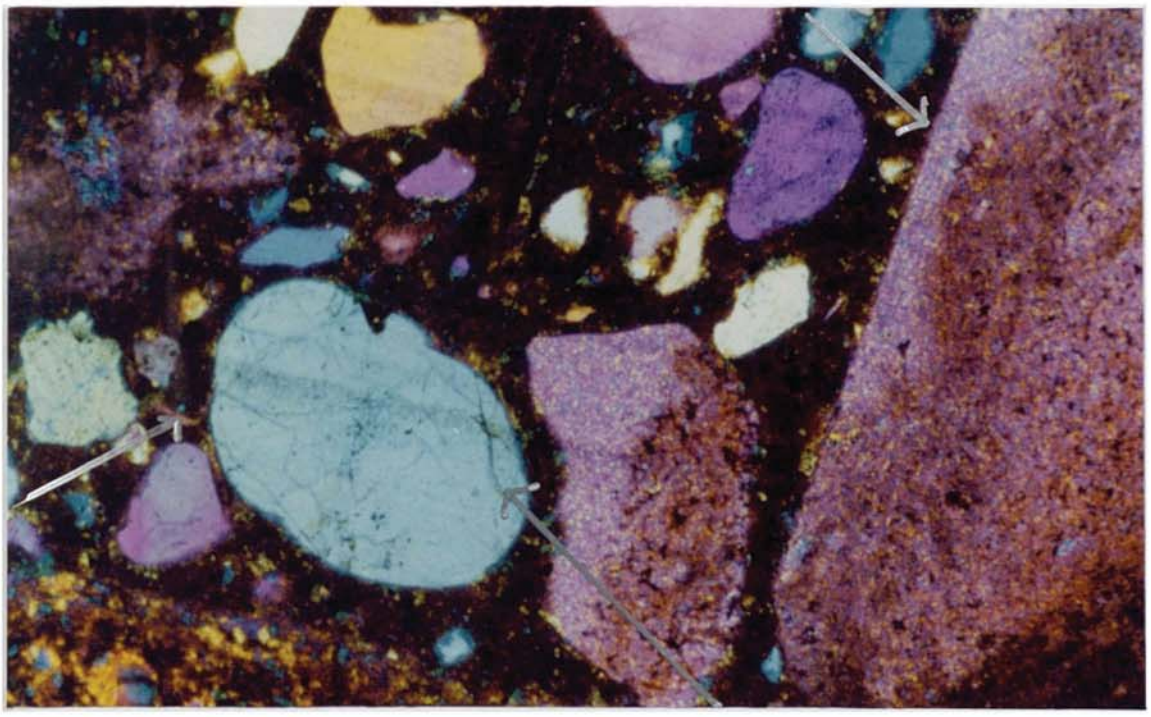

(b)

Figure 5.23 Photographs of an OPC Thames Valley aggregate concrete (a) unheated and showing minimal cracking and (b) heated to 300°C showing cracking as indicated by arrows

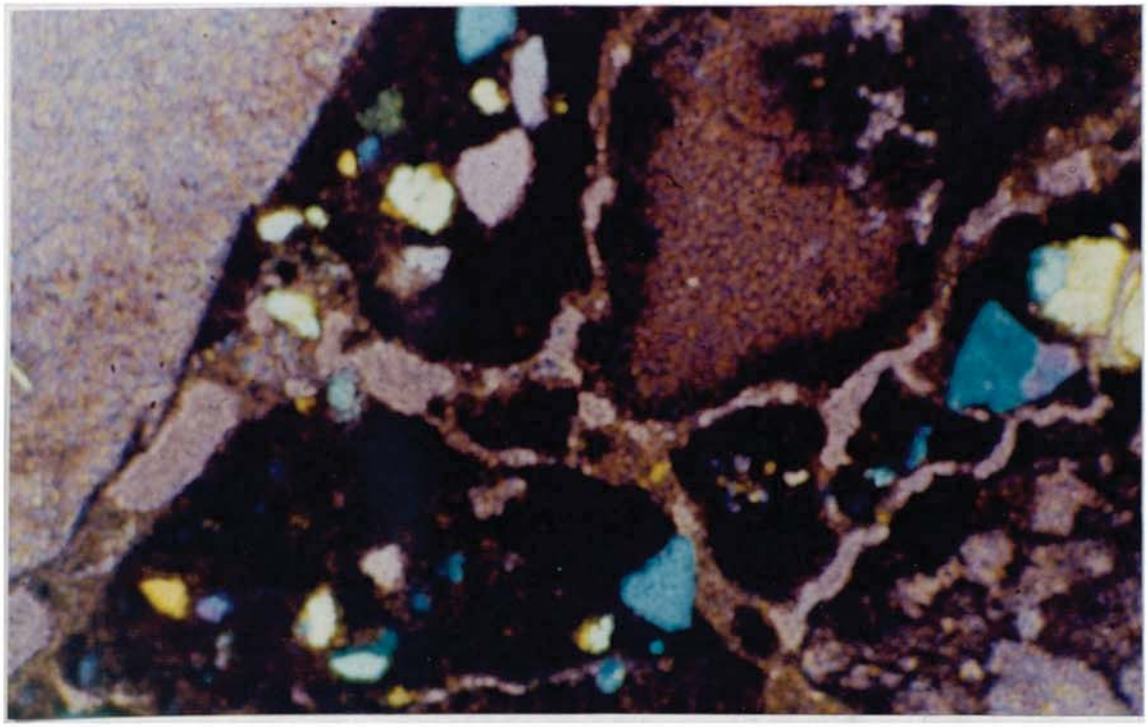

(c)

Figure 5.23(c) Photograph of an OPC Thames Valley aggregate concrete heated to 500°C showing extensive crack patterns

CHAPTER 6

RESULTS AND DISCUSSION: THE THAMES VALLEY AGGREGATE CONCRETE SAMPLES EXPOSED TO TEMPERATURE GRADIENTS

Since the measurement of hue for the equilibrium samples had proved to be the most useful for describing the colour change observed when concrete is heated, it was decided to use this method for the measurement of colour when a thermal gradient was applied to TVA concrete. Again the frequency of response was predominant in the 0-19 levels. Since the samples exposed to a thermal gradient showed a gradual colour change through the sample, hence the method of assessing the colour was altered. Areas of the sample were chosen at a width of 75 mm and these overlapped by 25 mm, to allow a more gradual change in colour to be measured.

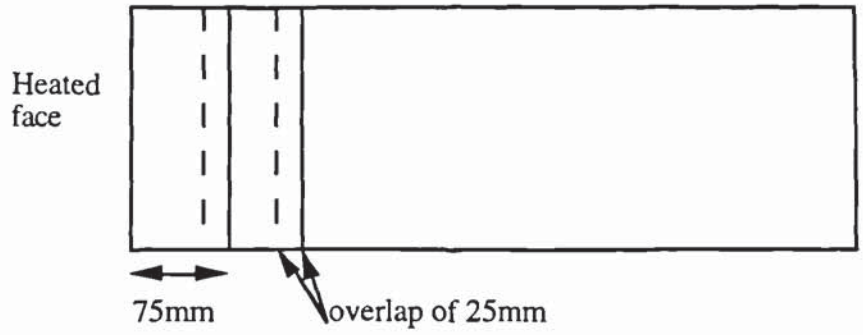

Figure 6.1 Diagram to show size of areas for colour measurement on polished sections taken from thermal gradient samples

The measurement was always started at the heated surface and moved along to areas where the concrete had not been effected by the heat. The results are expressed as frequency of occurrence of Hue in the 0-19 levels as a percentage of the total occurrence for each 75 mm column.

6.1 LOW FIRE EXPOSURE (80 kW/m^2)

The concrete was heated at the surface for approximately 1 hour. After this the furnace was switched off and the lid removed to allow the concrete to cool overnight.

6.1.1 OPC / TVA Concrete

Figure 6.2(a) (x 0.881) shows a polished cross-section of an OPC / Thames Valley aggregate concrete cylinder after heating one end face with a surface heat flux of 80 kW/m^2 for 1 hour. It can be seen that the surface section has undergone a colour change compared with the interior. The temperature distribution, Figure 6.2(b), producing this colour change shows that the temperature at the surface reached approximately 680°C and the 300°C isotherm was just over 30 mm from the exposed surface.

Figure 6.2(c) shows the measured colour change with distance from the exposed surface. Values represent measurements of hue in consecutive, partially overlapping, parallel sections, 7.5 mm wide. The red colour was at its peak up to a distance of about 25 mm. At distances of greater than 30 mm, red colour diminishes rapidly. Determination of colour at distances greater than 45 mm proved more difficult leading to erratic results. This may be as a result of the specific distribution of the gravel components in each 75 mm section, see section 5.1.4. The correlation shown is only an approximation with a possible error of +/- 5mm. In spite of the latter difficulty it is possible to define the maximum distance from the surface (25 mm) where significant reductions in compressive strength are likely to be found.

The method of sampling the bands in the sample section used for colour measurement was used for the crack density measurements, see earlier. However for the crack measurement there was no overlap of the sections. The cracking in each 75 mm band was measured in

eight different places, hence the points plotted for crack density against temperature (Figure 6.2(d) represent an average of eight measurements. It is evident that the greatest crack density is at the exposed face of the concrete and this gradually decreases as measurements were taken further away from the surface. Between 30-35 mm from the heated face the values reach a minimum of about 0.5 mm/cm^2, consistent with those normally occurring in concrete, cf. Figure 5.22(a), (b) & (c).

Thus even if the temperature distribution was not known, then from a knowledge of colour change and/or crack density, and an understanding of the relationship between these parameters and compressive strength (as shown in section 5.1.6), it is possible to define the maximum distance from the surface (in this case 30-35 mm) where significant reductions in residual compressive strength are likely to be found.

6.1.2 OPC / PFA Concrete

The surface of the OPC/PFA concrete reached approximately 625°C, Figure 6.3(b) (x 0.922) and the 300°C isotherm was found 25 mm in from the exposed face. The corresponding colour change with distance from exposed face is shown in Figure 6.3(c). The maximum development of red colour occurred at a distance of 15-20 mm from the heated surface. Colour reduction in the 10 mm surface section was a result of temperatures exceeding 500-600°C leading to a change in colour towards whitish grey. At a distance of greater than 22 mm, red colour diminishes rapidly. The measured colour levelled off at distances of greater than 25 mm which is equivalent to temperatures of less than 250°C.

6.1.3 OPC / BFS Concrete

In Figure 6.4(b) (x 1.419) the surface reached approximately 650°C and the 300°C isotherm was about 20 mm from the exposed face. Figures 6.4(c) shows the maximum development of red colour occurred at a distance of about 20 mm. After this the red colour diminished, until at distances of around 45 mm from the heated face, concrete was found that seemed to be unaffected by the heat and colour measurements for the hue in 0-19 level showed a baseline of approximately 10%.

6.2 MEDIUM FIRE EXPOSURE (110 kW/m^2)

The fire exposure of 110 kW/m^2 proved to be very detrimental to the concrete. The concrete at the heated surface became extremely crumbly and it was very difficult to work with this material to produce a polished section for colour measurement. It was therefore decided to only carry out this fire exposure test once. The concrete was heated at the surface for approximately 40 minutes. After this the furnace was switched off and the lid removed to allow the concrete to cool overnight.

6.2.1 OPC / PFA Concrete

The surface of the concrete reached in excess of 650°C, Figure 6.5(b) (x 0.908) and the 300°C isotherm was found 20 mm into the concrete from the exposed surface. Figure 6.5(c) showed the maximum development of red colour to be 20 mm away from the exposed surface. The colour reduction in the 15 mm surface section was as a result of temperatures exceeding 500-650°C, this led to change in colour towards whitish grey. Again the determination of the colour at distances greater than 45 mm was more difficult leading to erratic results.

6.3 HIGH FIRE EXPOSURE (140 kW/m^2)

Exposing the concrete to 140 kW/m^2 proved to be very destructive. The concrete was very weak and crumbly especially at the heated face. It was therefore very difficult to obtain a sample that could be used in the preparation of the polished sections. Even with impregnating the sample before cutting, the concrete fell apart and it was decided that with this amount of damage the concrete would be past repair in real life situations and colour change measurements would not be required. This test was therefore not continued.

6.4 SUMMARY

The tests described in this chapter have shown that the damage to concrete when exposed to a thermal gradient, may be characterised using crack densities and colour change measurements.

The extent of damage can be determined by measuring the colour change with distance from the exposed face. This will allow the maximum development of red colour to be determined and hence the distance where temperatures in excess of 300°C have been reached. Assessing deterioration of concrete using crack density measurements would require further understanding of the relationship with compressive strength, but with this information the maximum distance from the surface where significant reductions in strength could be identified.

(a)

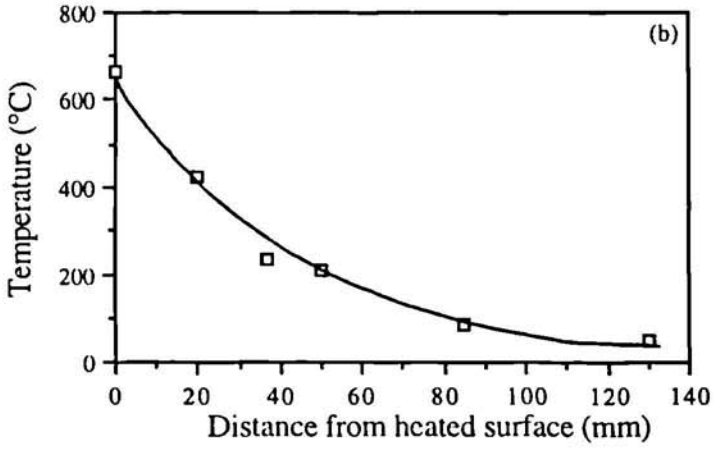

Figure 6.2 (a) Photograph of a polished cross-section of an OPC / Thames Valley aggregate concrete cylinder after heating to 80 kW/m^2 at one end face (the left) for 1 hour and the corresponding (b) temperature

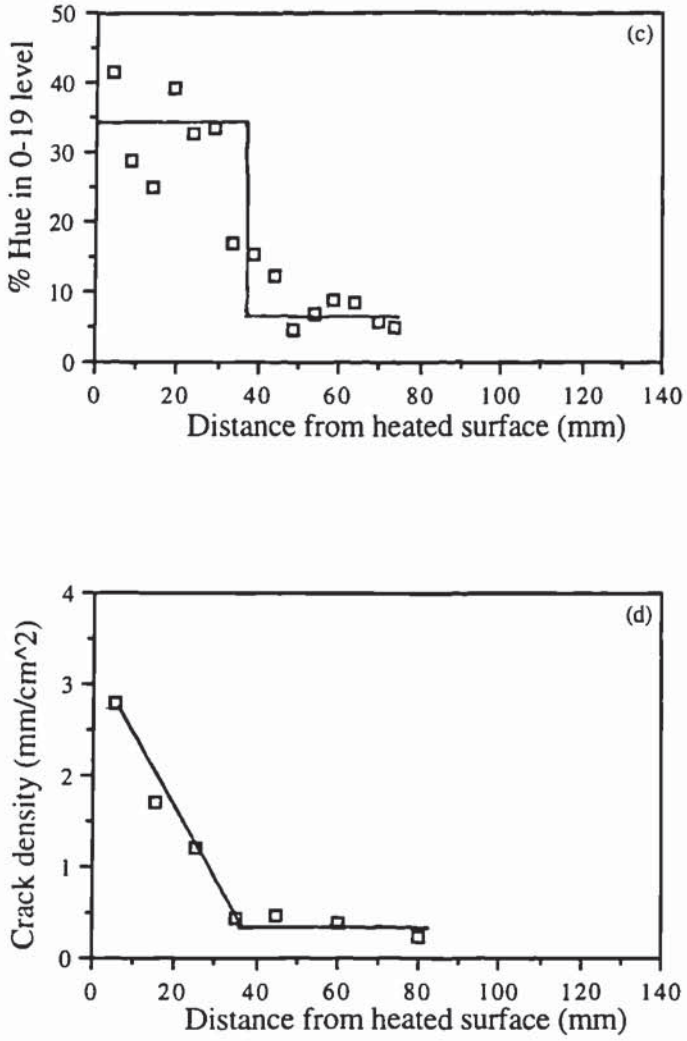

Figure 6.2 (c) Hue measurements in the 0-19 level and (d) crack density measurements for an OPC / Thames Valley aggregate concrete cylinder heated at one end face (the left) for 60 mins.

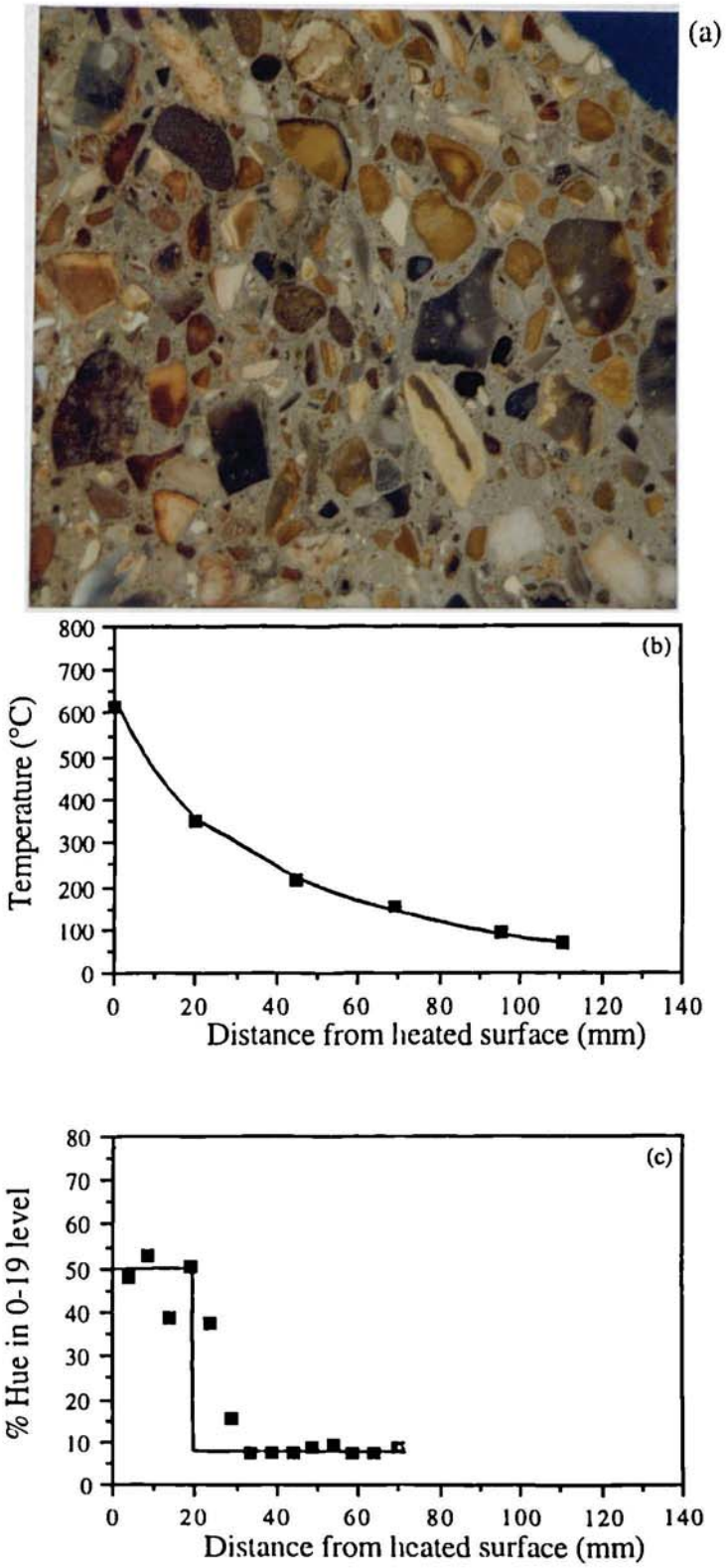

Figure 6.3 (a) Photograph of a polished cross section of an OPC/PFA Thames Valley aggregate concrete cylinder after heating to 80 kW/m^2 at one end face (the left) for 58 mins. and the corresponding (b) temperature and (c) % hue in the 0-19 levels

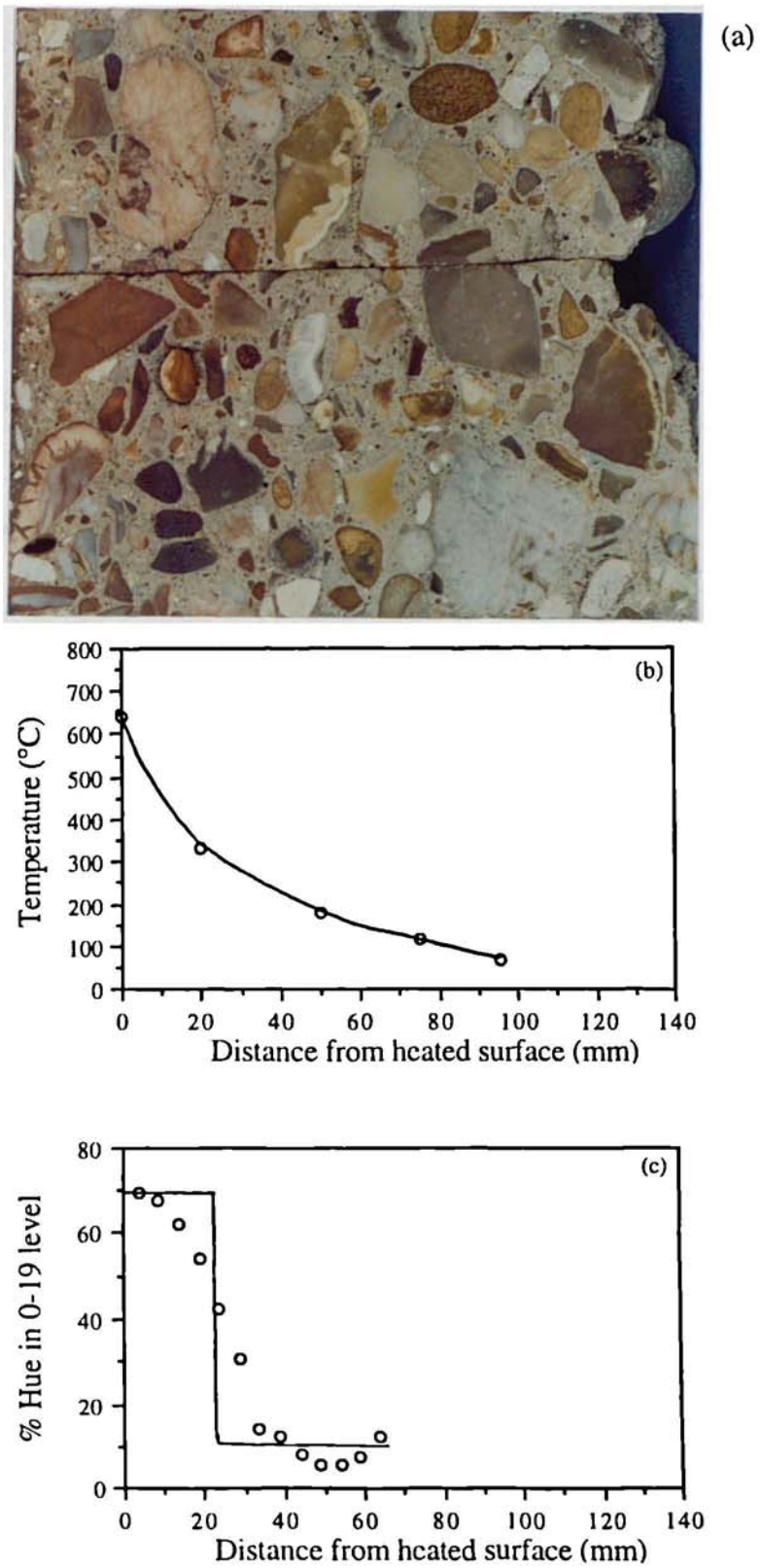

Figure 6.4 (a) Photograph of a polished cross-section of an OPC/BFS Thames Valley aggregate concrete cylinder after heating to 80 kW/m^2 at one end face for 52 mins. (the left) and the corresponding (b) temperature and (c) % hue in the 0-19 level

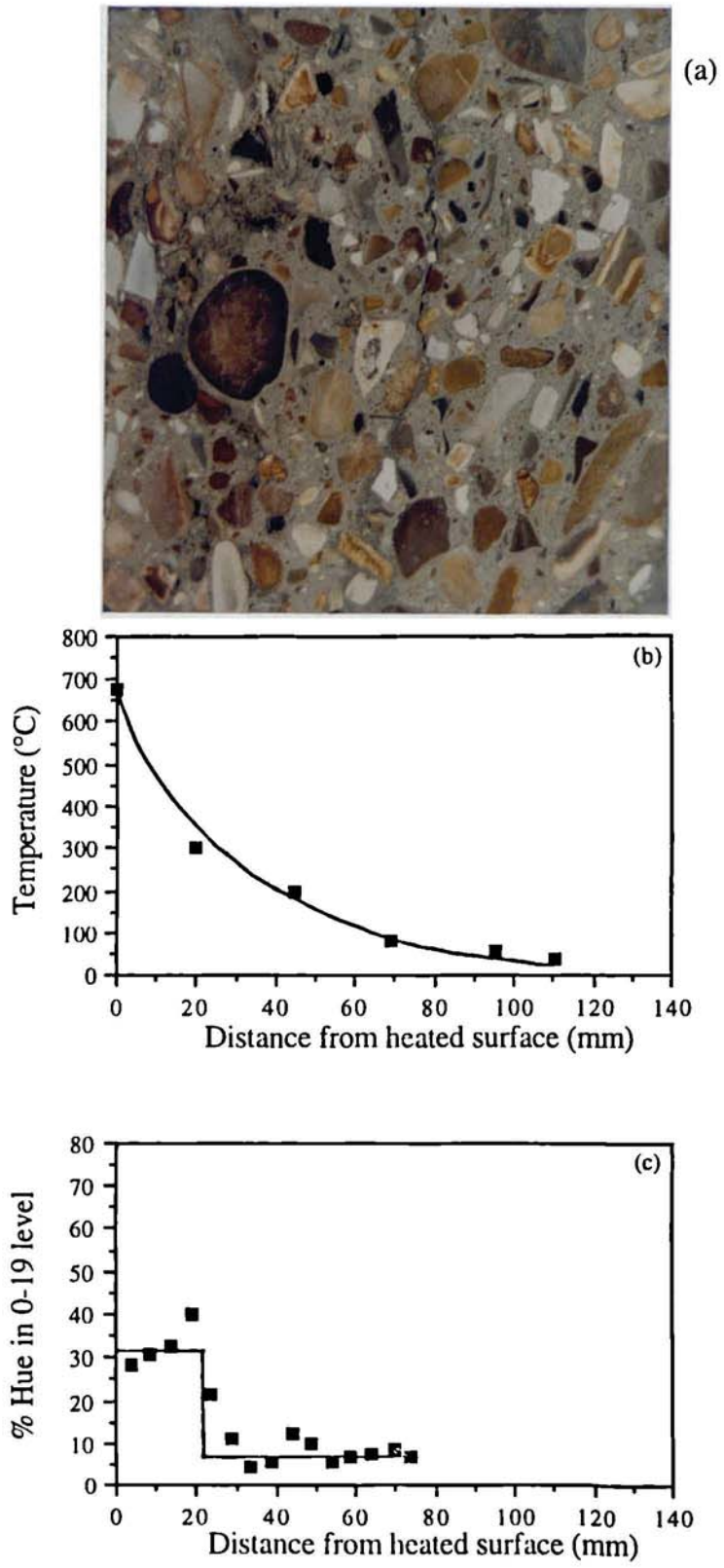

Figure 6.5 (a) Photograph of a polished cross section for an OPC/PFA Thames Valley aggregate concrete cylinder after heating at one end face (the left) for 40 mins.and the corresponding (b) temperature and (c) % hue in the 0-19 levels

CHAPTER 7

RESULTS AND DISCUSSION: THE OTHER AGGREGATE CONCRETE SAMPLES HEATED TO EQUILIBRIUM TEMPERATURES

The results presented in this chapter are for samples of concrete made with OPC and Limestone, Granite or Lytag aggregates heated to equilibrium temperatures. Results for samples of concrete made with the Thames Valley aggregate and described in Chapter 5 are included for comparative purposes.

7.1 COLOUR CHANGE

Photographs of a polished section of an unheated OPC / Limestone concrete and the same concrete heated to 350°C are shown in Figures 7.1(a) & (b) . Whilst it is evident that the colour change in the aggregate is not as distinct as in the Thames Valley aggregate concrete, after heat exposure, it is possible to see a slight change in colour of the concrete. Figures 7.3 and 7.4 show photographs of unheated concrete and concrete heated to 350°C for an OPC / Granite and OPC / Lytag aggregate concrete respectively. Again Figure 7.3 shows that the Granite aggregate does not show a large colour change but it is obvious that there has been a definite colour change in the mortar. The Lytag aggregate shows a slight lightening in colour, but no dramatic colour change occurs in the aggregate. The colour change would therefore be determined more accurately from the mortar colour changes only.

7.1.1 Hue

Figure 7.4 shows the frequency of occurrence for the 0-255 levels of hue for both control and samples heated to equilibrium temperatures of 350°C. The results for the OPC /

Thames Valley aggregate concrete have also been included for comparative purposes. It is evident that for all three alternative aggregates the frequency of response for both control and fired samples is concentrated in the 0-50 hue levels being particularly predominant in the 10-29 levels. These results are similar to those found for samples made with Thames Valley aggregate. However the shift in frequency of occurrence after heating, whilst still evident, was not as great as in the case of the Thames Valley aggregate samples.

7.1.2 Saturation

Figure 7.5 shows the frequency of occurrence for the 0-255 levels of saturation for both control and samples heated to equilibrium temperatures of 350°C. Comparing Figures 7.5(a)-(d) it can be seen that there are differences between the pattern of frequency of occurrence. However, all of the different aggregate concretes show an increase in saturation with the frequency of occurrence shifting to the right.

7.1.3 Intensity

Figure 7.6 shows the frequency of occurrence for the 0-255 levels of intensity for both control and samples heated to equilibrium temperatures of 350°C. The samples made with Limestone and Granite aggregate were similar to the samples made with Thames Valley aggregate in that the plots show a shift towards lower intensity levels after heating i.e they become darker. In contrast the plot for the samples made with Lytag aggregate show a shift in the opposite direction after heating i.e they become lighter.

7.1.4 Hue measurement for 0-19 Level for Samples Heated to Equilibrium Temperatures.

The results are shown in Figure 7.7 and give the change in the frequency of occurrence for the 0-19 hue levels and are given as a percentage of field detected over field area.

It is evident that the colour change to red is not as pronounced for the Limestone, Granite and Lytag aggregates when compared to the Thames Valley aggregate. There are smaller increases in red colour for the other aggregates in the temperature range 250-350°C. However these increases are still easily visible and the Granite develops more of a red colour than the Limestone and Lytag aggregate at the temperature of 350°C.

7.2 EFFECT UPON MECHANICAL PROPERTIES

7.2.1 Reduction in Compressive Strength

Soaking at temperatures greater than 350°C again leads to substantial reduction in compressive strength although the sample made with granite aggregate are slightly more resistant (Figure 7.8). Comparing Figures 7.7 and 7.8 the relationship between change in colour and reduction in compressive strength is not as obvious for the aggregates, Limestone, Granite and Lytag compared to gravel. Thus it may be possible to overcome this problem by eliminating the coarse aggregate during measurements and restrict the colour assessment to the mortar matrix possibly then showing more of a change at temperatures where significant strength is lost.

7.2.2 Reduction in Flexural Strength

Figure 7.9 shows that flexural strength is most effected in the temperature range 200-300°C. As discussed in section 5.2.2, results for exposure to 175°C do not exist and therefore the decrease may not be as linear as presented. Again the maximum loss of strength has occurred at lower temperatures compared to the compressive strength. Therefore the maximum development of red colour and loss in flexural strength cannot be correlated.

7.2.3 Reduction in Surface Hardness

Figure 7.10 shows that for all four types of aggregate, there is a reduction of surface hardness with increasing temperature. The reduction in surface hardness is greater after 350 C.

7.2.4. Reduction in Dynamic Modulus of Elasticity

Dynamic modulus reduces linearly with increasing temperature in Figure 7.11. It is apparent that the values for the concrete made with Granite and Limestone are higher to start with compared to the Thames valley aggregate but all decrease to less than 500 MN/m^2 for temperatures greater than 450°C.

7.2.5. Reduction in Ultrasonic Pulse Velocity

Figure 7.12 shows the pulse velocity decreases almost linearly with increasing temperature as with the different cements in chapter 5 (Figure 5.15). The aggregate type seems to have no effect on the value of pulse velocity with increasing temperatures. Using the classification from Greig (1982), in section 5.2.5 it would seem that the condition of the

concrete would become doubtful, with the compressive strength being significantly affected when heated to 200 - 250°C. However the compressive strength results in Figure 7.8 show that significant strength loss does not occur until the concrete has been heated in excess of 350°C. It therefore seems that Greig's classification slightly underestimates the resistance of the concrete to heat.

Figure 7.13 shows the correlation of normalised UPV with normalised compressive strength for cement concrete. The R^2 values are 0.815, 0.762, 0.599 and 0.689 for the Thames Valley, Limestone, Granite and Lytag concrete giving R values of 0.902, 0.873, 0.774 and 0.830. Again the R values represent reasonable correlations. However it was expected to see a significant difference for the correlations since it is the different aggregate that can effect the compressive strength. The shape of the curve for the Lytag correlation is slightly different to the others, this shows that the Lytag aggregate behaves differently to the other aggregates.

The correlations of normalised UPV with normalised flexural strength (Figure 7.14) and normalised dynamic elasticity (Figure 7.15) show little difference between the four types of aggregate. The Lytag aggregate mirrors the behaviour of the other aggregates rather than showing a marked change.

7.3 CRACK DENSITY

The effect of temperature on crack density for OPC concrete made with Thames Valley (a), Limestone (b) and Granite (c) is shown in Figure 7.16.

Looking at the photographs in Figure 7.17, it is evident that a baseline amount of cracking exists even in the control specimens, Figure 7.17(a) and 7.16(a)-(c). Cracking due to thermal cycling starts at temperatures between 300-350°C and then continues to increase

linearly, shown by the concrete in Figure 7.17(c) which has been heated to 500°C.

Increased cracking owing to the application of heat starts at 250°C for the OPC / Thames Valley and Limestone concrete and 325°C for the OPC / Granite concrete as shown by the intersection points in Figures 7.17(a), (b) & (c). The temperature for the onset of cracking for the OPC / Granite concrete is very similar to that found found for the substantial loss in compressive strength as shown in Figure 7.7. In the case of the OPC / Thames Valley and OPC / Limestone concretes cracking appears to start at a slightly lower temperature in relation to the drop in compressive strength.

Comparison of crack density with residual compressive strength at equivalent temperatures show good correlations (R^2: 0.92, 0.85, 0.88 for the Thames Valley, Limestone, Lytag aggregates respectively) as can be seen from Figure 7.13(d).

7.4 SUMMARY

The experimental investigations with OPC concrete and different aggregates have again shown that the colour change of a concrete after fire exposure can be quantified. The heating of the concrete to equilibrium temperatures has allowed a calibration standard of temperature versus colour change to be developed. However the amount of change in colour with different aggregate was less pronounced for Limestone, Granite and Lytag compared to the Thames Valley aggregate. This is probably due to the consistent colours of the Limestone, Granite or Lytag aggregates at the start compared to the mixture that exists with the Thames Valley.

The use of different aggregates with the OPC cement resulted in little difference for cracking characteristics. All three aggregate concretes, Thames Valley, Limestone and Granite, showed increased cracking at temperatures greater than 350°C. Crack densities of

around 3.0 mm/cm^2 were reached at temperatures of 500°C.

It can be therefore be concluded that the mortar characteristics of the concrete are the most important part of the concrete when assessing fire damage of concrete using this technique.

(a)

(b)

Figure 7.1 Photographs of polished cross-sections of an OPC / Limestone concrete (a) unheated and (b) heated to 350°C (x 1.6)

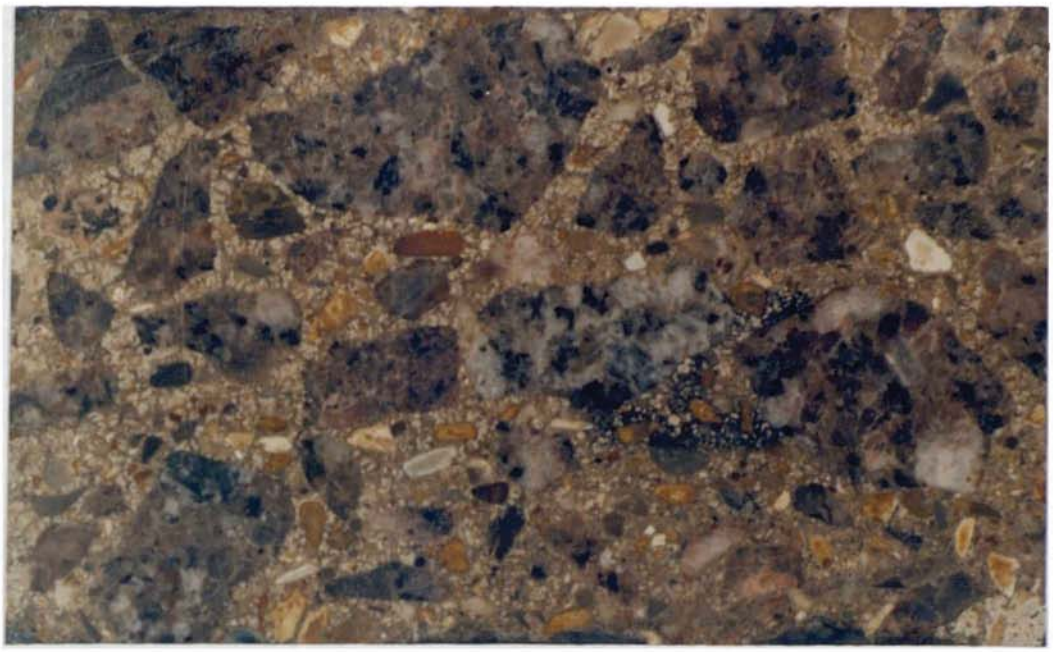

(a)

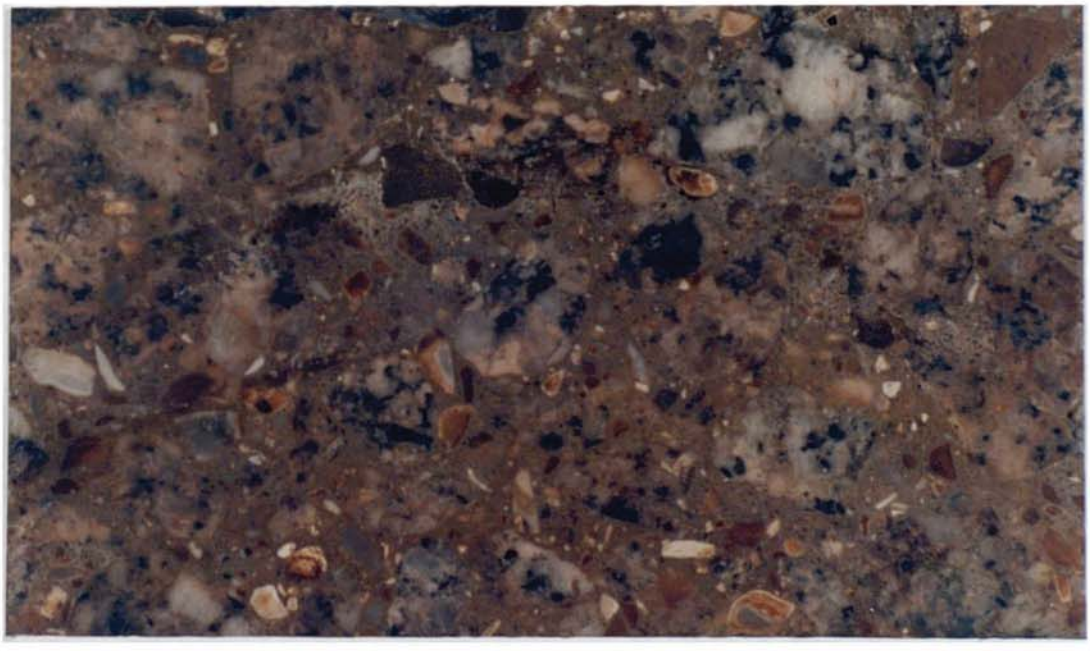

(b)

Figure 7.2 Photographs of polished cross-sections of an OPC / Granite concrete (a) unheated and (b) heated to 350°C (x 1.6)

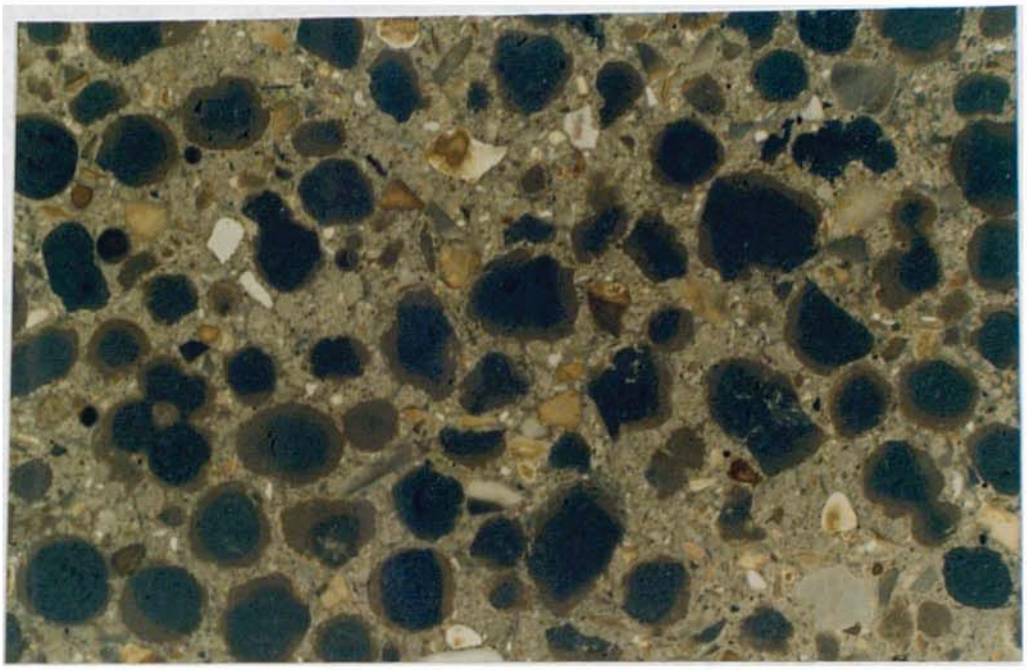

(a)

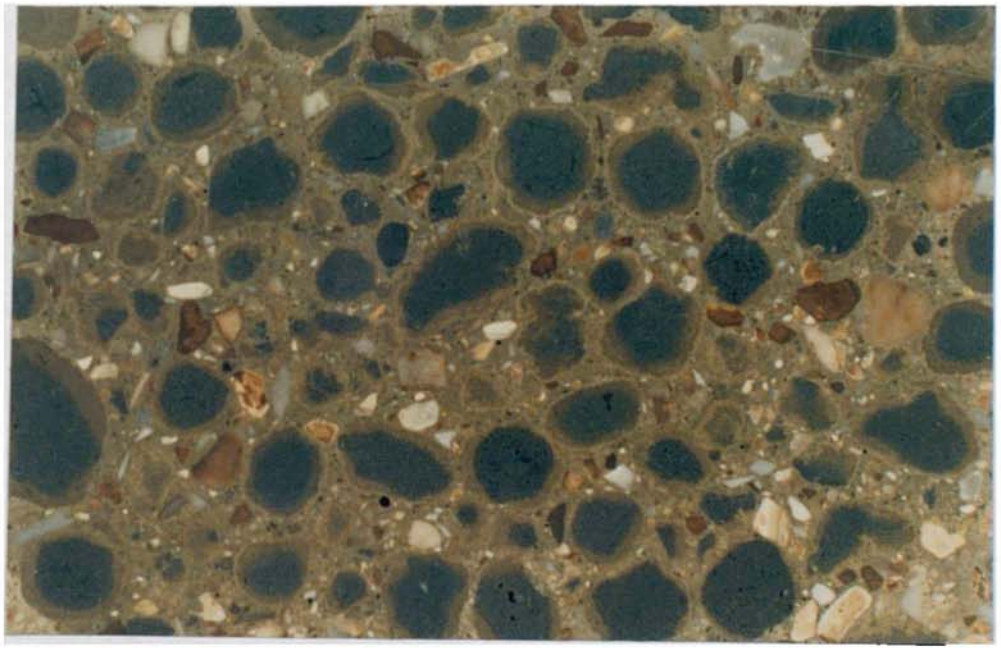

(b)

Figure 7.3 Photographs of polished cross-sections of an OPC / Lytag concrete (a) unheated and (b) heated to 350°C (x 1.6)

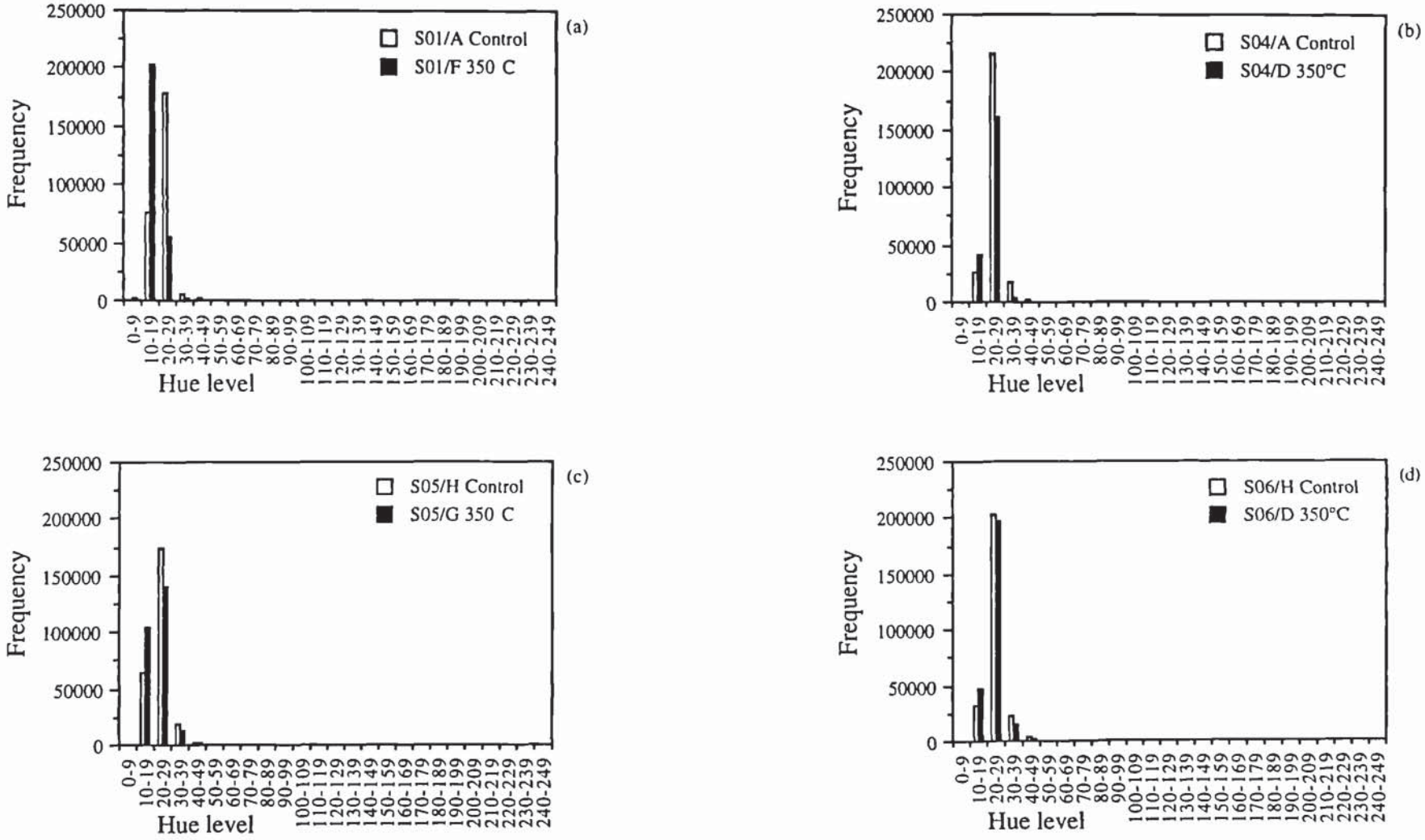

Figure 7.4 Frequency of occurence for the levels of Hue from 0 to 255 (a) Thames Valley, (b) Limestone, (c) Granite and (d) Lytag aggregate concretes

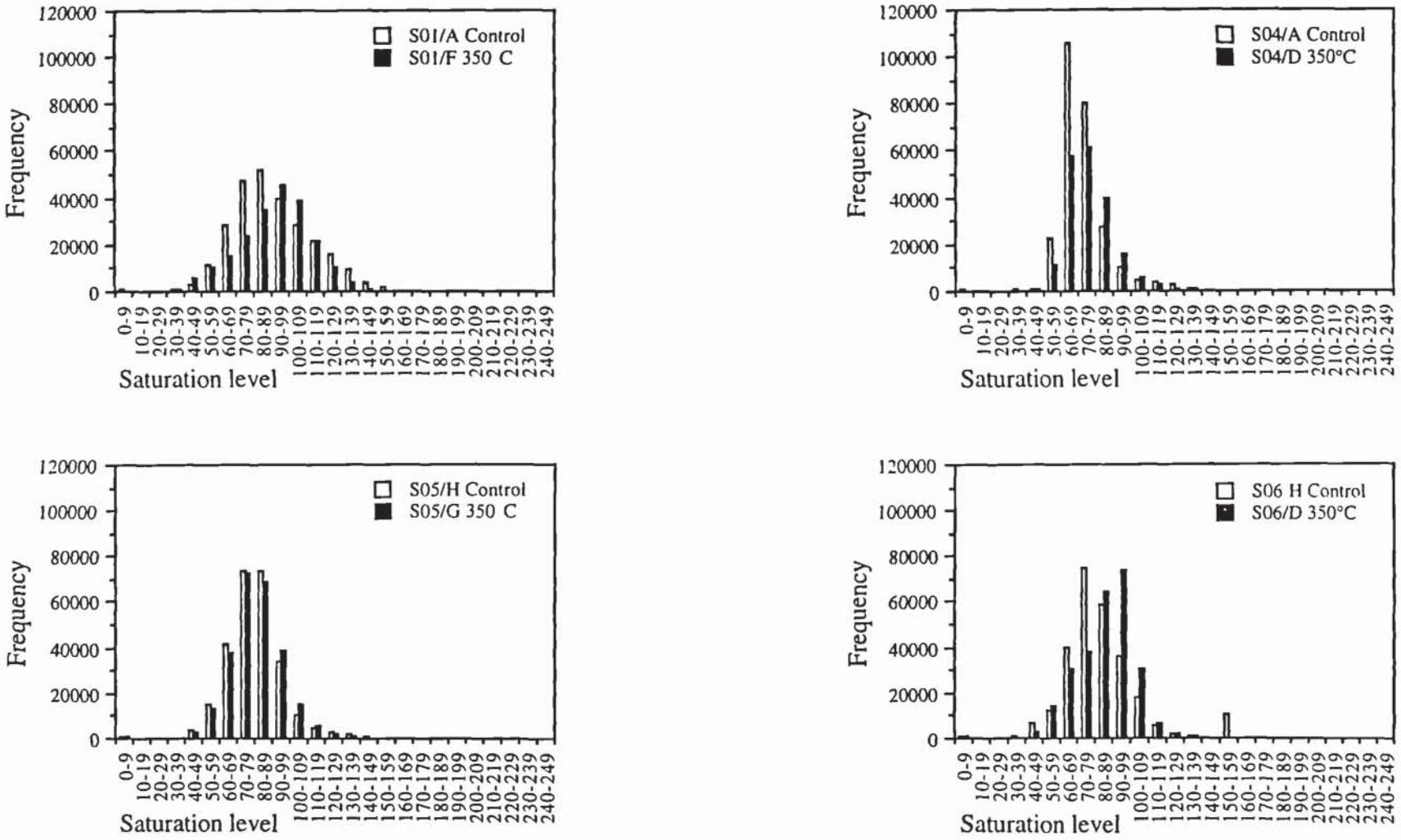

Figure 7.5 Frequency of occurence for the levels of Saturation from 0 to 255 (a) Thames Valley, (b) Limestone, (c) Granite and (d)Lytag aggregate concretes

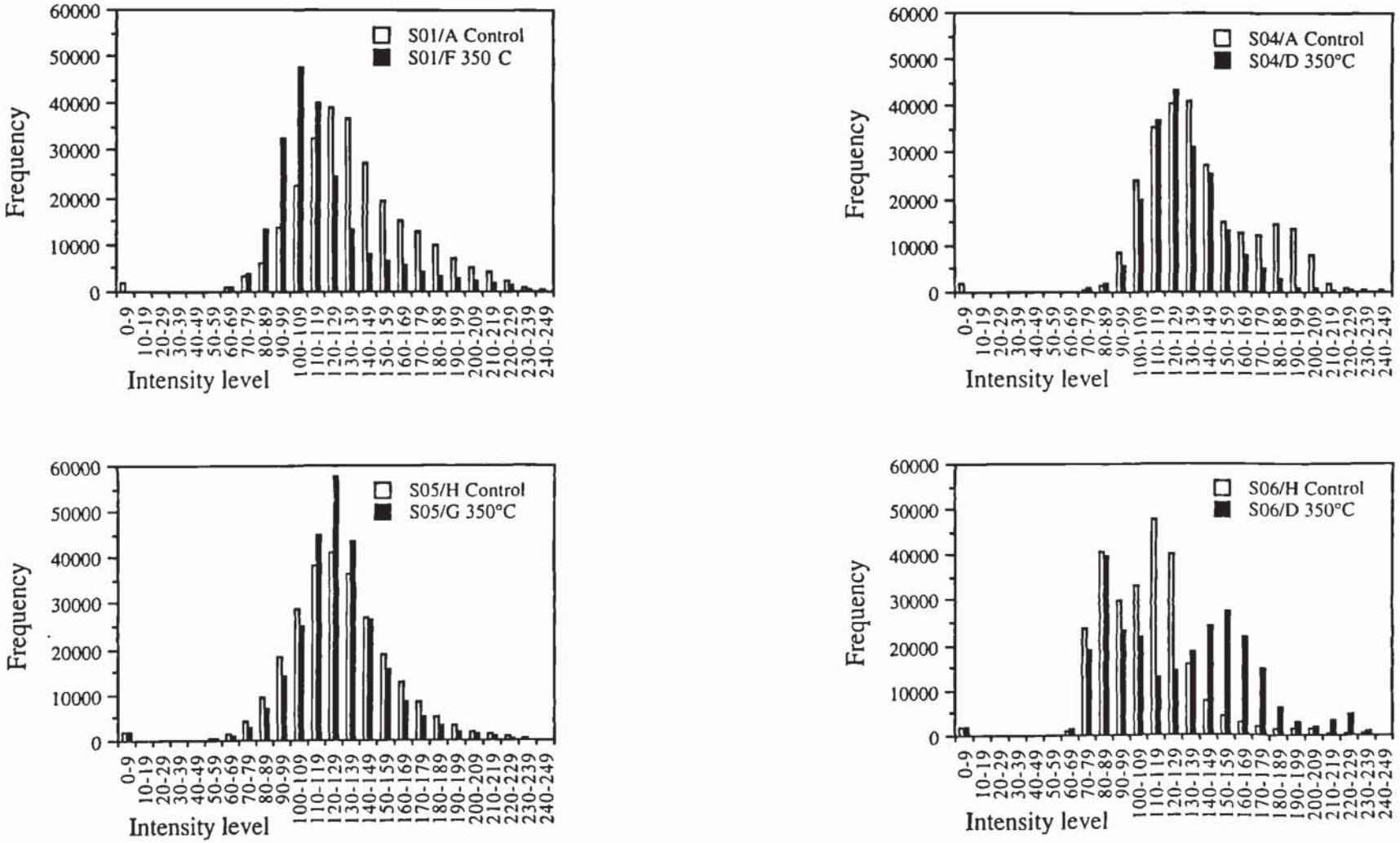

Figure 7.6 Frequency of occurence for the levels of Intensity from 0 to 255 (a) Thames Valley, (b) Limestone, (c) Granite and (d) Lytag aggregate concretes

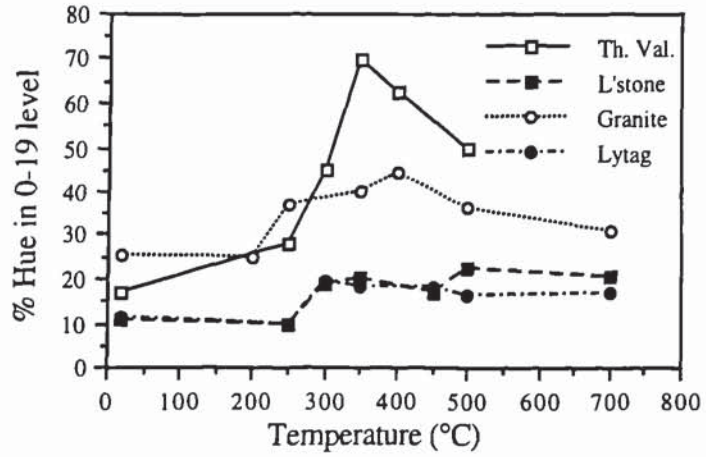

Figure 7.7 Hue measurements in 0-19 level for samples heated to equilibrium temperatures

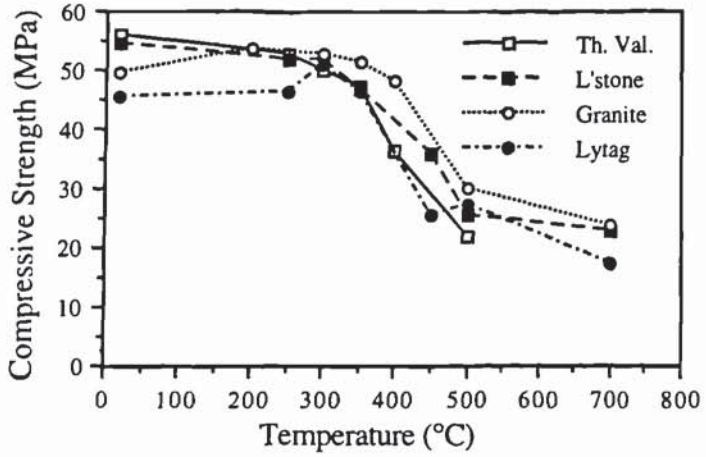

Figure 7.8 The reduction of compressive strength with increasing equilibrium temperature

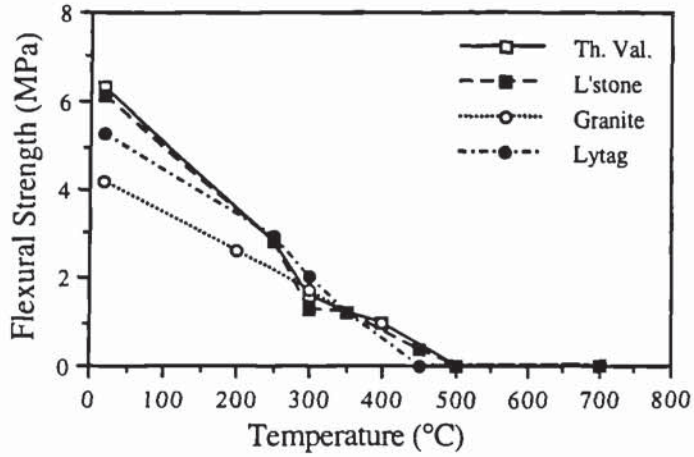

Figure 7.9 The reduction of flexural strength with increasing equilibrium temperature

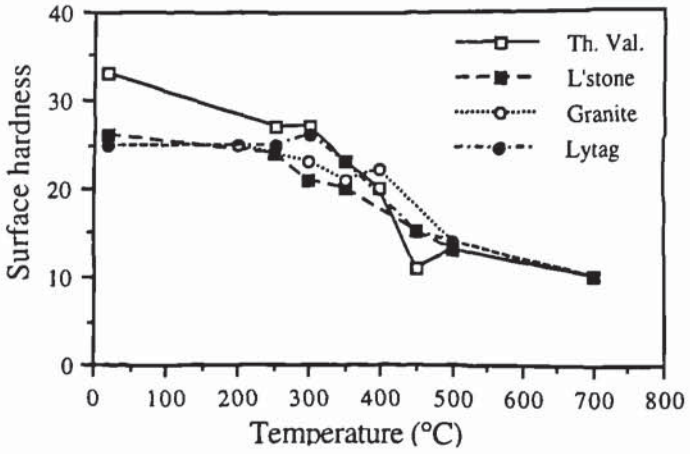

Figure 7.10 The reduction of surface hardness with increasing equilibrium temperature

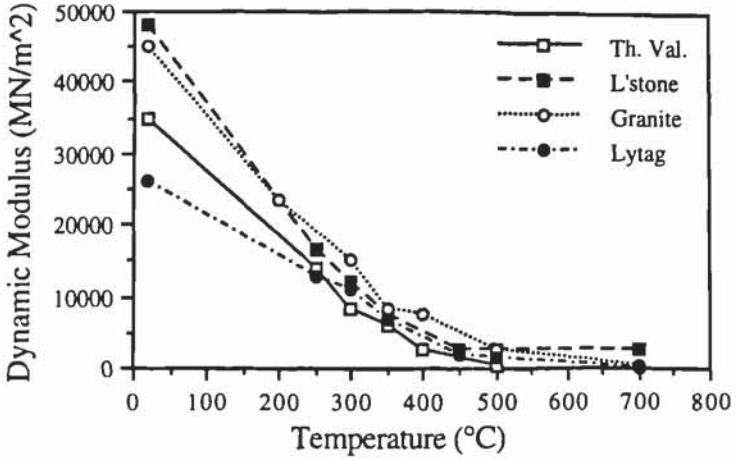

Figure 7.11 The reduction of dynamic modulus with increasing equilibrium temperature

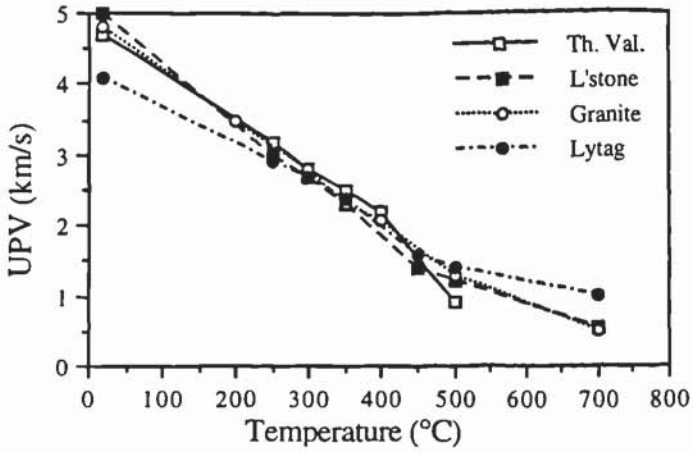

Figure 7.12 The reduction of Ultrasonic Pulse Velocity with increasing equilibrium temperature

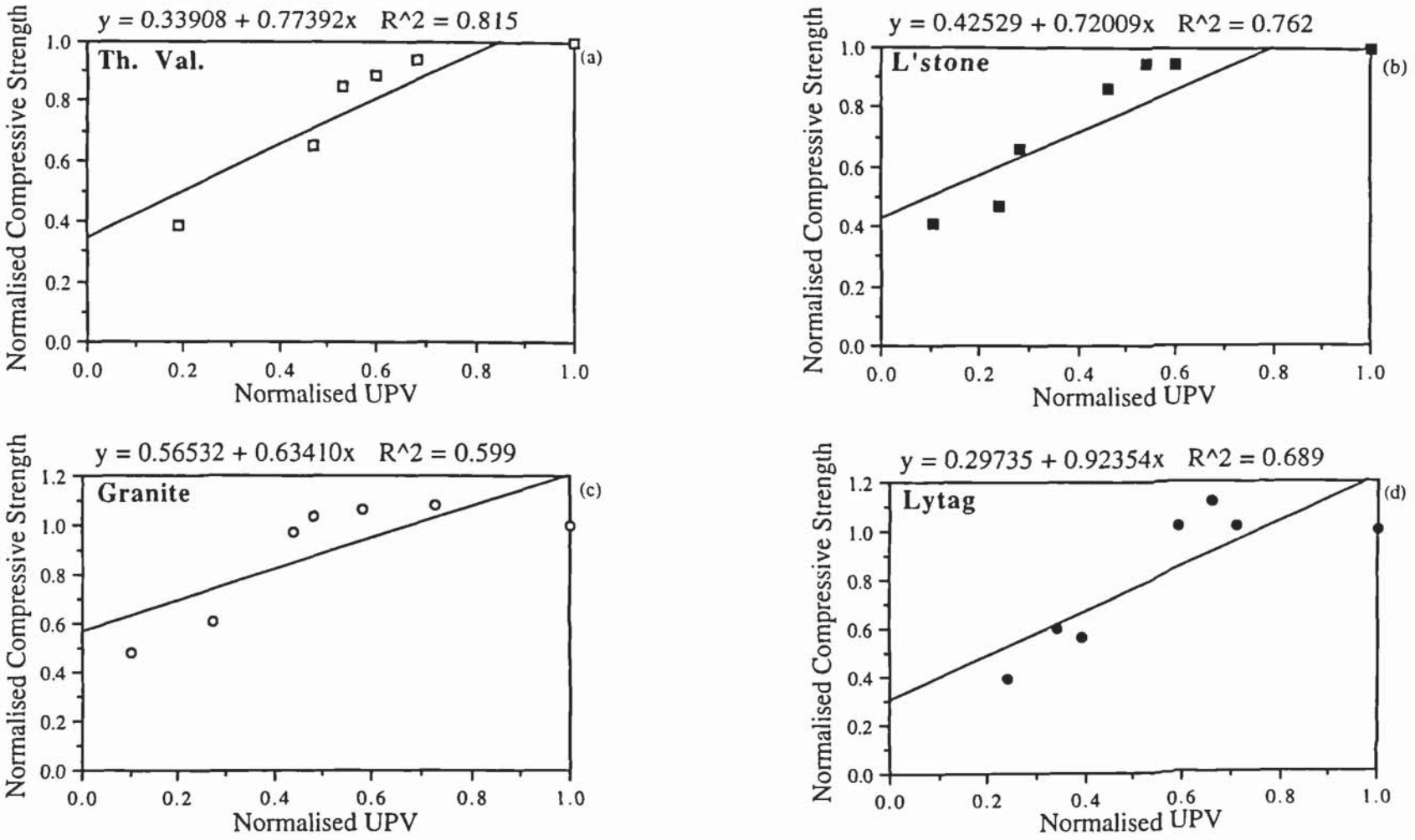

Figure 7.13 The correlation of normalised Ultrasonic Pulse Velocity with normalised Compressive Strength for OPC concrete heated to equilibrium temperatures

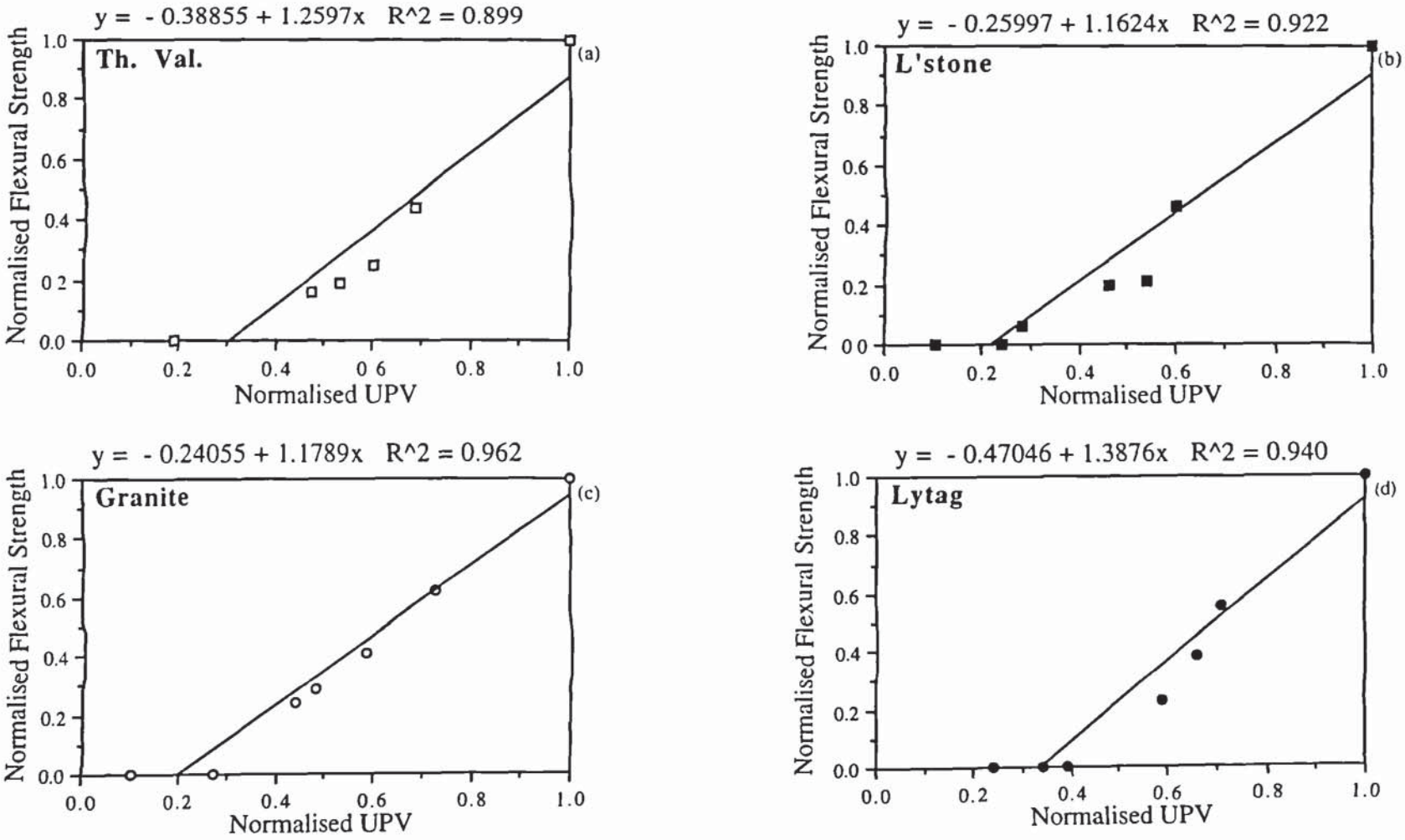

Figure 7.14 The correlation of normalised Ultrasonic Pulse Velocity with Flexural Strength for OPC concrete heated to equilibrium temperatures

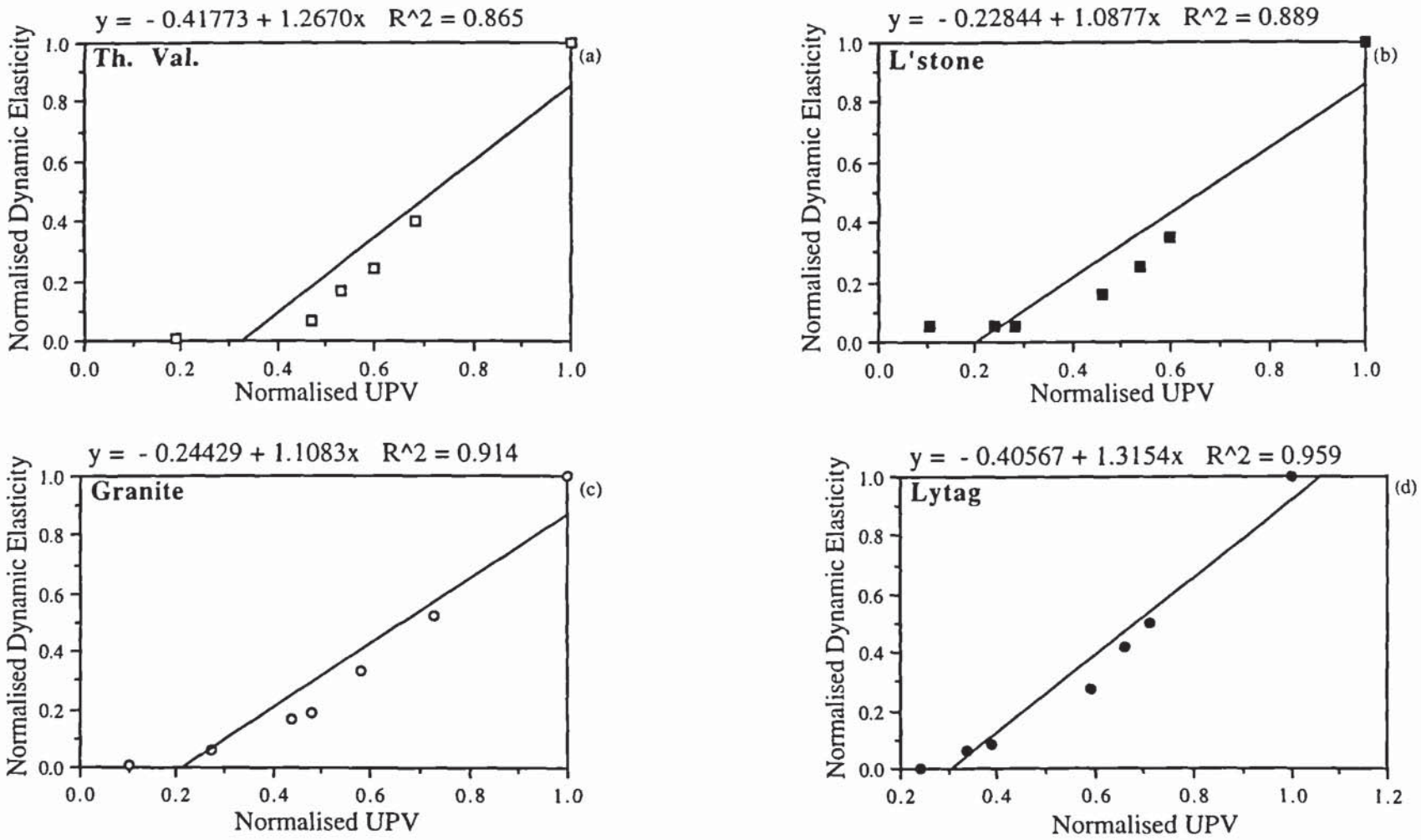

Figure 7.15 The correlation of normalised Ultrasonic Pulse Velocity with normalised Dynamic Modulus for OPC concrete heated to equilibrium temperatures

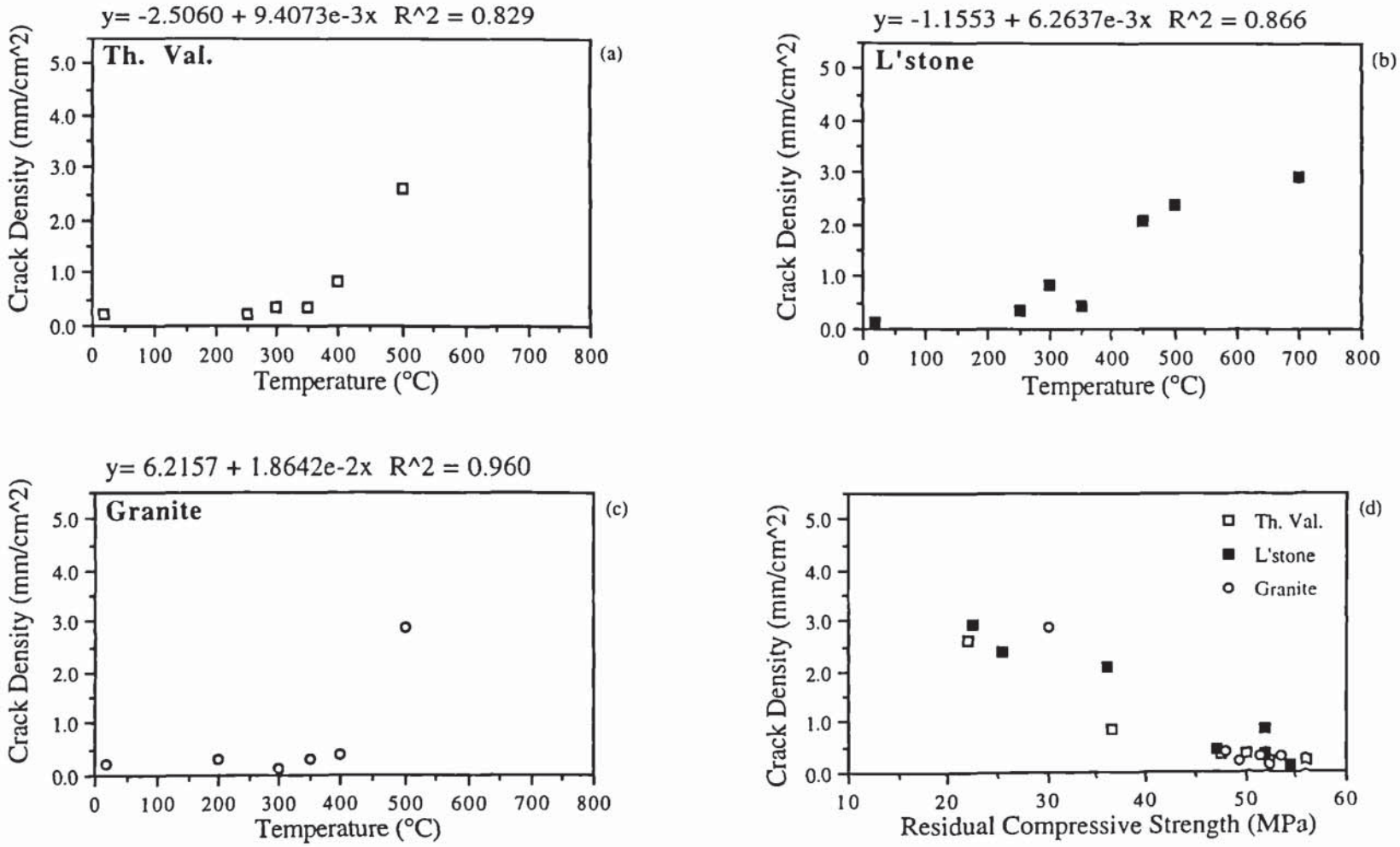

Figure 7.16 The development of crack density with increasing equilibrium temperature for an OPC concrete (a) Thames Valley, (b) Limestone, (c) Granite aggregate and (d) the correlation of crack density with residual compressive strength

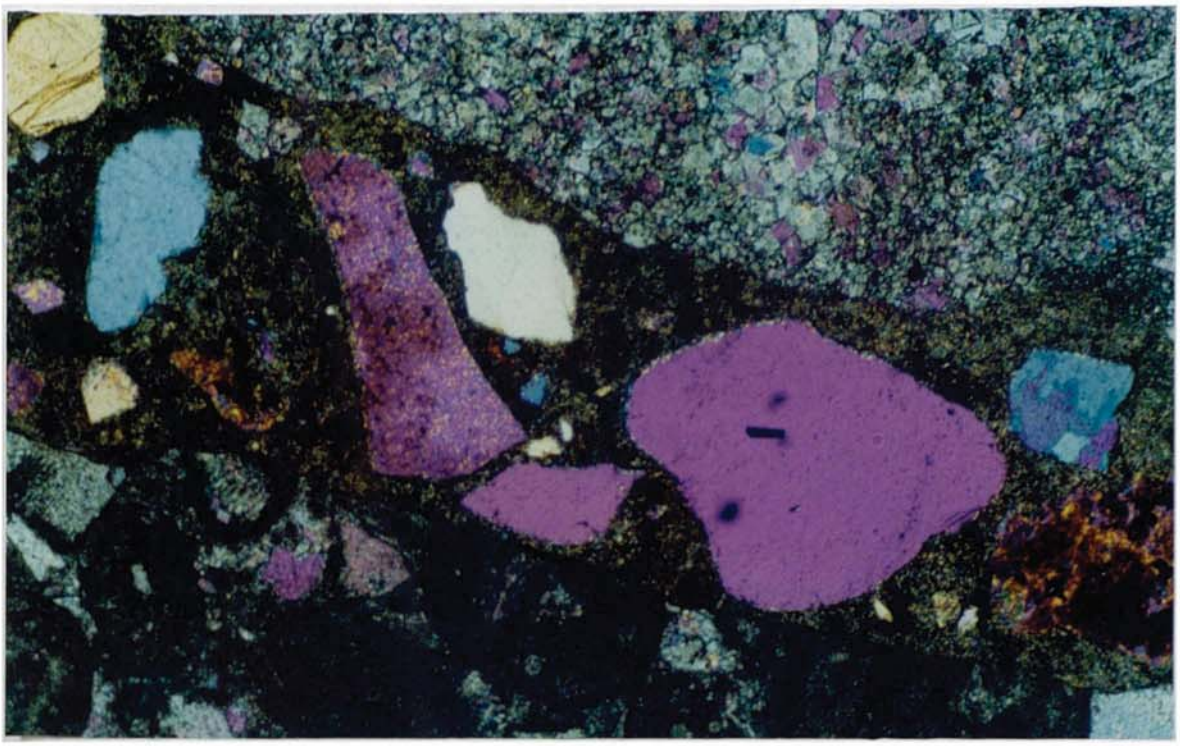

(a)

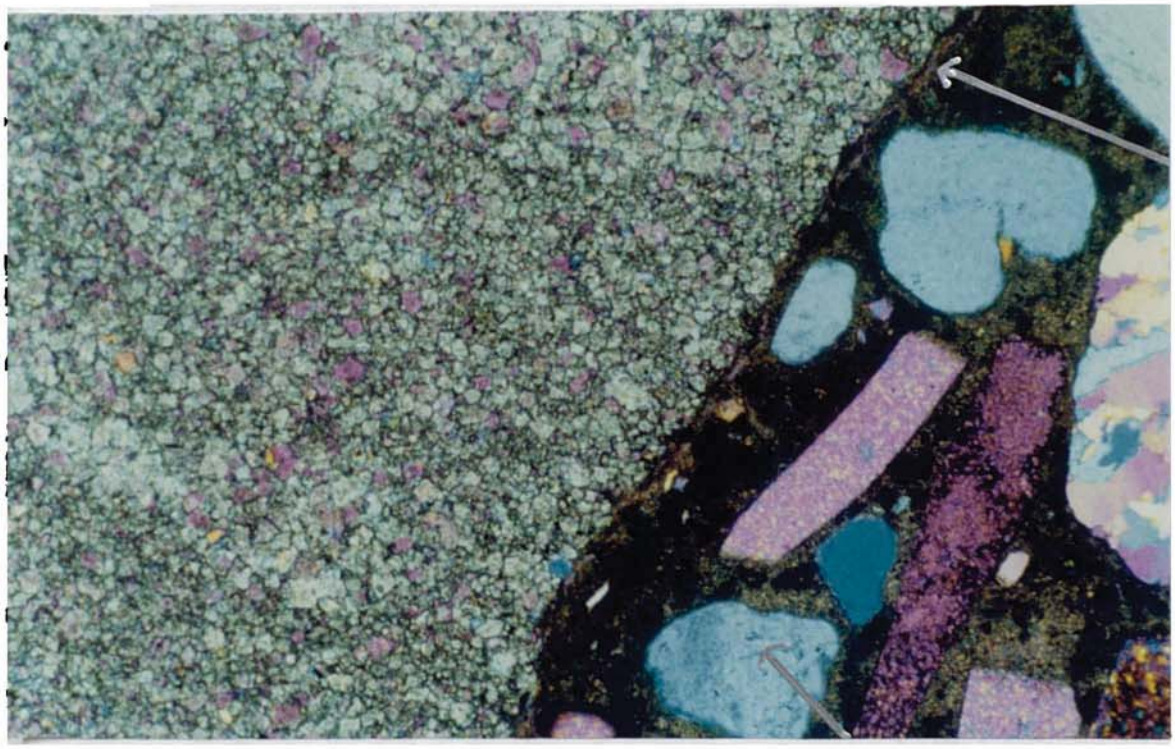

(b)

Figure 7.17 Photographs of an OPC Limestone aggregate concrete (a) unheated and showing minimal cracking and (b) heated to 300°C showing cracking as indicated by arrows

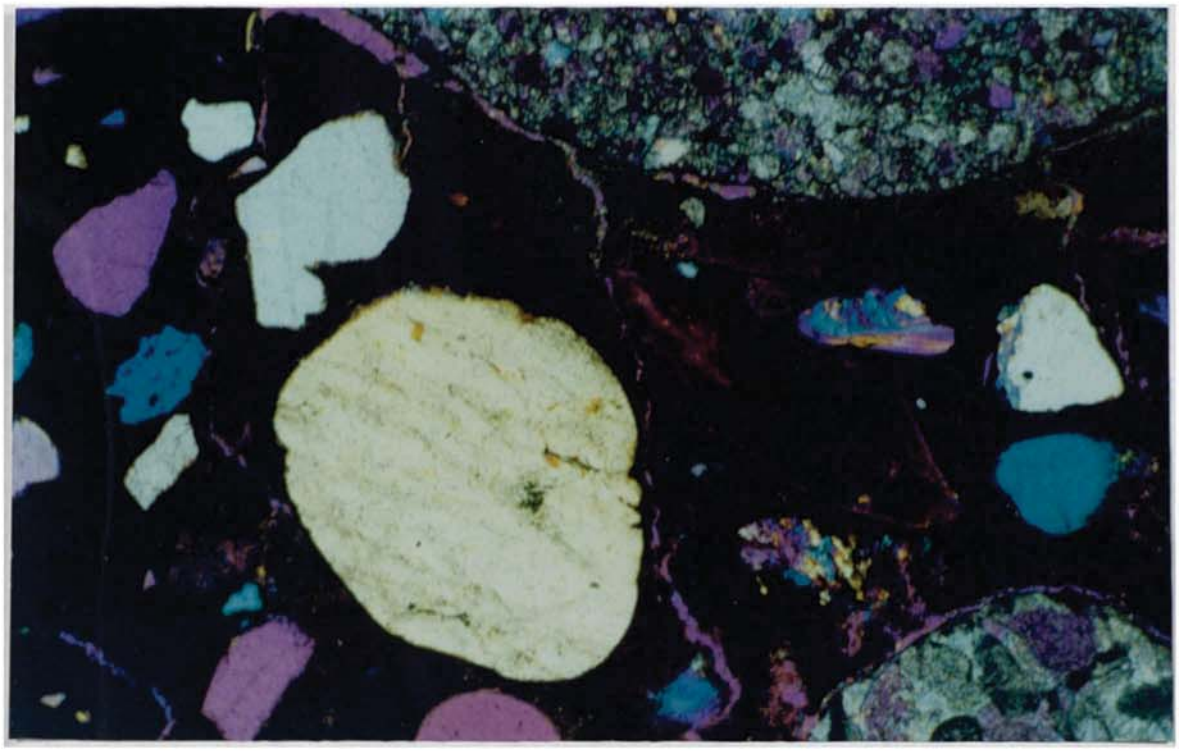

(c)

Figure 7.17(c) Photograph of an OPC Limestone aggregate concrete (c) heated to 500°C showing extensive crack patterns

CHAPTER 8 SUPPLEMENTARY TESTS

8.1 APPLIED COMPRESSION DURING HEATING

Small cylinders with either no load or a pre-load of 0.3 times the cylinder strength were heated to around 380°C and cooled. Crack density measurements were taken on both longitudinal and traverse sections.

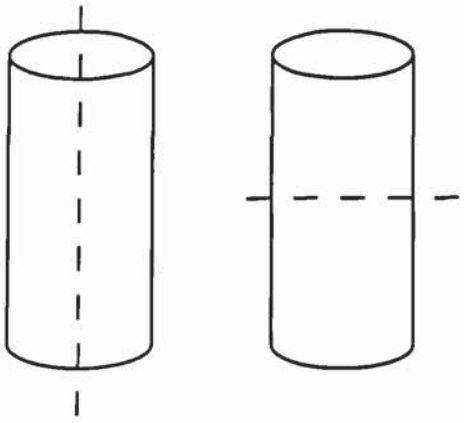

Figure 8.1 Diagram to show sampling position for polished cross-sections on cylinders

The results are given in Table 8.1:

Table 8.1 Crack density measurements made in the longitudinal and traverse sections after heating to 380°C with and without an applied load

	Crack density (mm/cm^2)	
	Longitudinal	Traverse
Control (no load, heated)	2.44	4.64
Loaded (0.3, heated)	2.40	5.76

The crack density in the transverse direction increased by 25% for the pre-loaded specimen compared with the unloaded specimen. In the longitudinal direction both specimens gave essentially similar results.

Purkiss & Bali (1988) have suggested that the application of compressive stress during the heating of concrete samples could reduce strength loss and loss in elastic modulus. They reported that the phenomenon was not known but was likely to be as a result of crack formation. Other literature (Khoury *et al.*, 1989) also suggest this theory as a possible reason for the reduction in the loss of strength.

Overall the results suggest that the application of compressive load are not inhibiting traverse crack formation but it is unclear what is happening in the longitudinal sections. Since this is the first set of work to be carried out where crack measurements have actually been quantified, an immense amount of work is now required to develop the crack measuring process further and research the possible explanations of compressive stress inhibiting crack formation and hence allowing a lower reduction in compressive strength to occur than what would have been expected.

8.2 AUTOGENOUS HEALING OF CRACKS

The thin sections were taken from the same positions as of those cylinders in 8.1 so that the control results could be used as a comparison for the samples re-immersed in water for 3 and 14 days. The results are as follows:

Table 8.2 Crack density measurements made in the longitudinal and traverse sections after heating to 380°C and then re-immersed in water for 0, 3 and 14 days

	Crack density (mm/cm^2)	
	Longitudinal	Traverse
Control	2.44	4.64
3 day immersion	2.58	5.33
14 day immersion	2.66	4.46

Khoury *et al.* (1989) has suggested that re-immersing samples after exposure to high temperatures may allow a crack healing process to occur which is indicative of improved compressive strengths that have been measured.

The results shown in Table 8.2 show no evidence for the autogenous healing of cracks in this work.

8.3 HEATING TO PRODUCE SPALLING

In furnace tests for columns, spalling caused by the corners (or a face) parting from the core is often observed in the late stages of testing, provided explosive spalling has not occurred earlier (Connolly, 1995). It is generally accepted that this is caused by the corner expanding faster than the core due to temperature gradients and the concrete at midheight deforming laterally and eventually spalling (Connolly, 1995). The magnitude is likely to be dependent upon the amount of restraint offered by the core and the cover. During a column test, Figure 8.2(a) the interface will be adjacent to the links as there will be some loss of bond. As the two ends of the spalled concrete are held in position, i.e. for a

sample that is being loaded, the only point of deflection is sideways at the centre, Figure 8.2(b).

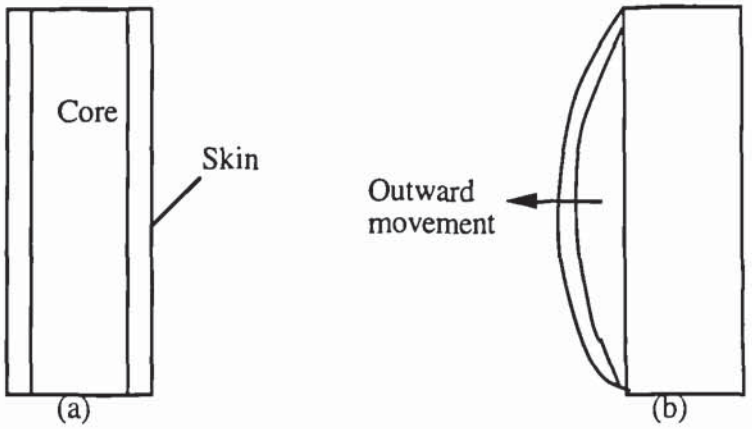

Figure 8.2 Diagram to show the effects of a column test (a) when no spalling has occurred and (b) with a sideways deflection for a column that has been restrained at both ends

Even for unloaded samples the skin still attempts to expand more than the core and breaks away at the free ends due to symmetry where there is no positional restraint. Therefore the test specimens crack patterns at those points produce similar crack patterns as columns give in the centre. Generally the more reinforcement in a concrete column then the more restraint offered by the central core.

It was attempted to replicate the process of corner spalling on unloaded specimens by heating prisms reinforced by four longitudinal bars. Two types of reinforcement were used, 6mm diameter plain mild steel and 8mm diameter high tensile steel. The reinforcement was arranged in a cage within the concrete beams with a minimum concrete coverage of 25mm. Two beams with each reinforcement were heated for 30 minutes. These tests produced severe cracking at the ends of the specimens for both types of reinforcement, Figure 8.3. The amount of cracking increased as the amount of reinforcement was increased. The crack pattern along the test beam can be seen in Figure 8.4.

Figures 8.5 (a), (b) & (c) also show evidence for another type of spalling - aggregate spalling. The aggregate appears to have popped out at the surface. Figures 8.5(a), (b) & (c) show flint aggregates of differing iron contents all splitting at the aggregate face.

8.4 SUMMARY

From the very limited amount of work that has been completed for the above supplementary tests, it is apparent that there are possibilities of further work to confirm initial findings. The application of compression may be inhibiting crack formation and could therefore make concrete more fire resistant. However this could exacerbate spalling by reducing the pathways for moisture loss and hence bigger cracks form.

Figure 8.3 Photographs to show severe cracking at the ends of test beams

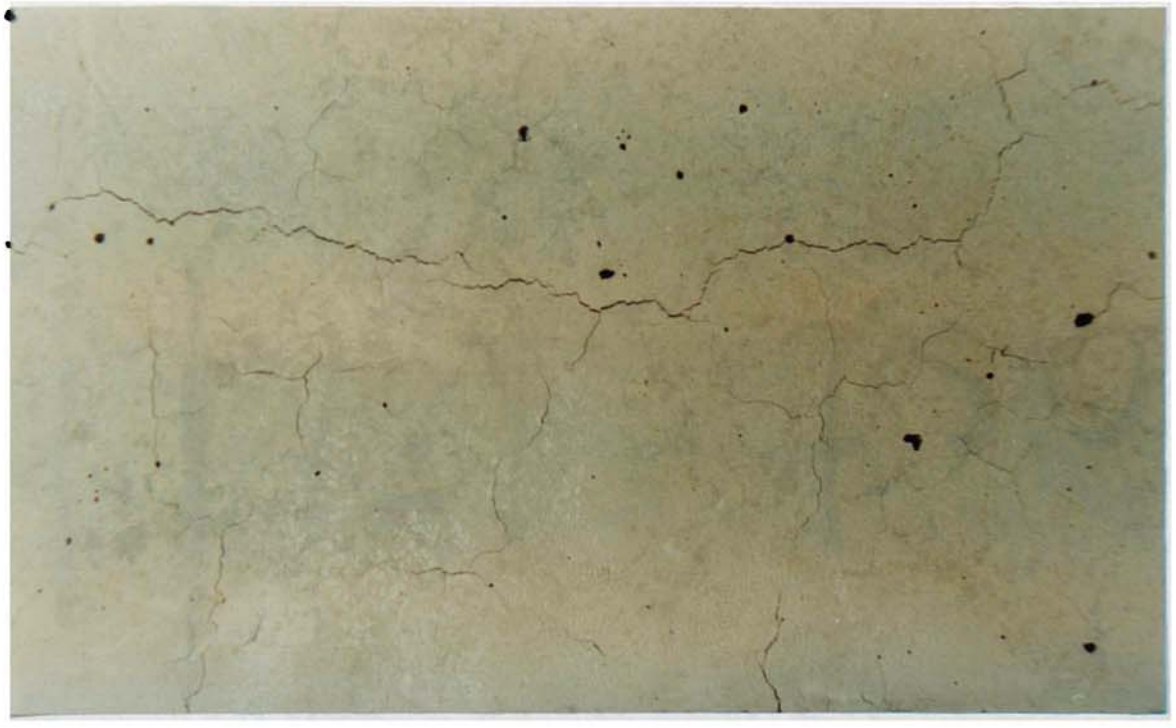

Figure 8.4 Photographs to show cracking along a test beam

(a)

(b)

Figure 8.5 Photographs to show (a) & (b) aggregate spalling on a test beam

(c)

Figure 8.5(c) Photograph to show aggregate spalling on a test beam

CHAPTER 9 GENERAL DISCUSSION, CONCLUSIONS & FURTHER WORK

9.1 GENERAL DISCUSSION AND CONCLUSIONS

The objectives of the work, as listed in Chapter 1 - Introduction, were to provide :

(a) Quantification (rather than purely visual assessment) of colour change as an indicator of the thermal history of concrete.

(b) Quantification of the nature and intensity of crack development as an indication of the thermal history of concrete, supporting and in addition to, colour change observations.

(c) Further understanding of changes in the physical and chemical properties of aggregate and mortar matrix after heating.

(d) An indication of the relationship between cracking and non-destructive methods of testing e.g. UPV and Schmidt hammer.

The extent to which these objectives have been met are considered below.

Objective (a):

The results show that colour image analysis can be used to quantify the colour changes found when concrete is heated. Such measurements may be used to determine the thermal history of concrete by providing information regarding the temperature distribution that existed at the height of a fire. In addition it was found that the development of red colour coincides with significant reduction in compressive strength.

However, actual colours observed depended on the types of cement and aggregate that were used to make the concrete. With some aggregates such as Limestone, Granite and Lytag it may be better to concentrate on analysis of the colour changes occurring in the mortar matrix, rather than an average colour change for the sample as a whole.

Objective (b):

It has been demonstrated that petrographic techniques may be used to determine the nature and density of cracks developing at elevated temperatures. Furthermore, values of crack density correlate well with measurements of residual compressive strength. Small differences in the temperature for onset of increased crack density were observed with the different cements and which may be attributed to changes in porosity. Use of different aggregates with the same cement had little effect on cracking characteristics (see Section 7.3). These latter observations suggest that it is the mortar characteristics, either bulk or at the aggregate interface, which is more important rather than the type of aggregate.

Objective (c):

Concretes made with blended cements tended to produce small differences in physical and chemical properties which were not evident with concretes made with unblended cements. There is some evidence to suggest that a coarsening of pore structure in blended cements may lead to onset of cracking at lower temperatures. The use of DTA/TGA was of little use in assessing the thermal history of concrete made with blended cements.

Objective (d):

Good correlations were found between compressive strength and the Schmidt Hammer test. Significant reduction in surface hardness can be used as a indicator that the level of cracking in the concrete has increased.

Ultrasonic Pulse Velocity failed to detect the significant deterioration after temperatures in excess of 350°C were reached for any of the concretes.

With regard to dynamic modulus of elasticity, greatest reductions in E_d were observed after heating to temperatures of up to 250°C with smaller reductions at higher temperatures. Thus whilst it may provide some guide to thermal history there is no sharp discontinuity at temperatures associated with strength reduction.

Supplementary Investigations:

From a very limited study of the application of compression during heating results suggested that there may be a redistribution of crack pattern.

Similarly, a limited study revealed no evidence to suggest autogenous healing of cracks after immersing fired samples in water.

Corner spalling and sloughing off, as observed in columns, was effectively reproduced in tests on small scale specimens and the crack distributions were observed although no firm conclusions made.

9.2 SUGGESTED PROCEDURES FOR SITE INVESTIGATION

Taken together it has been shown that the two new techniques, colour change and crack density, can provide further useful information for the evaluation of fire damaged concrete. They may be used to establish the thermal history and extent of deterioration. In addition petrographic analysis could also provide information on the quality of the original concrete.

From the current investigations the following sequence of procedures are suggested for the investigation of fire damaged concrete structures.

- Take cores from suspect and known undamaged areas. Use standard techniques such as Schmidt Hammer in similar areas.

- Make a visual inspection of the cores.

- If a red / pink colour is observed, measure it and the colour of undamaged concrete. From the colour change estimate the temperature to which the sample has been exposed.

- If no colour change is present but the concrete is suspect, measure the crack density and then determine the temperature exposure and assess deterioration. Crack densities in excess of 1 mm/cm^2 would be suspicious.

- Use petrographic analysis to provide further information on the quality of the original concrete such as cement content and w/c ratio.

Whilst it is considered that such procedures could be implemented now it is felt that further work along the lines recommended in the following section should be carried out before a Standard Procedure is issued.

9.3 FURTHER WORK

(i) An in depth investigation of colour changes occurring in the mortar matrix and individual components of the aggregate in order to identify those showing maximum difference before and after heating. These should be carried out on samples heated to equilibrium temperatures.

(ii) In the case of samples subjected to heating at one face (a thermal gradient) more work on identifying the boundary between material exhibiting significant colour change and natural material colour is required. For instance use could be made of the statistical analysis as derived by Kriging and discussed in Isaaks (1989).

(iii) Devise optimum method of sample preparation. For instance the thickness of the sample taken prior to impregnation should be investigated. As cracks may be discrete rather than continuous (see section 4.6.4) then with thinner samples there is more chance of the resin to reach all cracks.

(iv) Research into area of thin section preparation. The drying of samples removes the evaporable water. Perhaps soaking them in alcohol first so that after firing whilst waiting for preparation they would not absorb any water. After coming out of the alcohol, they are put into the oven ready for preparation. This may be useful for similar work related to thesis because of the discrepancies of the control samples were not usually dried at 105°C, but at 50°C during thin section preparation.

(v) Following (iii) use of fluorescent resin may be more successful in that crack measurement could be made automatically by measuring fluorescence. This would avoid the more tedious method employed in the current investigations.

(vi) Further work to look at crack widths, as this work has concentrated on crack length. But a better approach to measuring the cracks would need to be developed before this was tackled.

(vii) Published papers are bound at the back of the thesis. In addition others are in preparation for both refereed journals and publications for site engineers and insurance investigators. It has become evident that whilst considering publication that some method of colour matching between actual samples and colour prints may be necessary. Use of digital image capturing techniques should reduce problems with this.

(viii) In view of the increased use of high strength concrete it may be appropriate to test the applicability of these methods to this material.

REFERENCES

ACI Committee 226 (1987) Ground granulated blast-furnace slag as a cementitious constituent in concrete, American Concrete Institute Materials Journal, **Vol. 84**, 327-42.

Abrams, M.S. (1971) Compressive strength of concrete at temperatures to 1600°F, In Temperature and Concrete, American Concrete Institute SP No. 25-2, 33-58.

Ahmed, A. E., Al-Shaikh, A. H. & Arafat, T. I. (1992) Residual compressive and bond strengths of limestone aggregate concrete subjected to elevated temperatures, Magazine of Concrete Research, **Vol. 44**, No. 159, 117-25.

Bali, A. (1984), The transient behaviour of plain concrete at elevated temperatures, PhD Thesis, University of Aston in Birmingham.

Berger-Shunn, A. & Saltman, M. (1994) Practical colour measurement, a primer for the beginner, a reminder for the expert, Wiley.

Bessey, G.E. (1950) Investigations to buildings fires : Part 2 - Visible changes in concrete and mortar exposed to high temperature, National Building Studies Technical Paper No.4 HMSO London, 6-18.

BS 476: Pt 20: 1987, Method for the determination of the fire resistance of elements of construction (general principles), British standards Institute, London.

BS 1881: Pt 102: 1983, BS 1881 Methods of testing concrete, Pt 102 Method for determination of slump, British Standards Institute, London.

BS 1881: Pt 107: 1983, BS 1881 Methods of testing concrete, Pt 107 Method for determination of density of compacted fresh concrete, British Standards Institute, London.

BS 1881 : Pt 116: 1983, BS 1881 Methods for testing concrete, Pt 116 Method for the determination of the compressive strength of concrete cubes, British Standards Institute, London.

BS 1881: Pt 118: 1983, BS 1881 Methods for testing concrete, Pt 118 Method for determination of flexural strength, British Standards Institute, London.

BS 1881: Pt 202: 1986, BS 1881 Methods for testing concrete, Pt 202 Recommendations for surface hardness testing by rebound hammer, British Standards Institute, London.

BS 1881: Pt 203: 1986, BS 1881 Methods for testing concrete, Pt 203 Recommendations for measurement of ultrasonic pulses in concrete, British Standards Institute, London.

BS 1881: 209: 1990, BS 1881 Methods for testing concrete, Pt 209 Recommendations for the measurement of dynamic modulus elasticity, British Standards Institute, London.

Bungey, J.H. (1989) Testing of concrete in structures, Surrey University Press.

Carette, G.G., Painter, K.E. & Malhotra, V.M. (1982) Sustained high temperature effect on concrete made with normal portland cement, normal portland cement and slag, or normal portland cement and pulverised fuel ash, Concrete International, July 198241-51.

Chew, M.Y.L. (1993a) The assessment of fire damaged concrete, Building and Environment, **Vol. 28**, No. 1, 97-102.

Chew, M.Y.L. (1993b) Effect of heat exposure duration on thermoluminescence of concrete, American Concrete Institute Materials Journal, Title no. 90-M34, 319-22.

Clulow, F.W. (1972) Colour - its principles and their applications, London, Fountain.

Concrete Society Working Party (1990) Assessment and repair of fire-damaged concrete structures, Concrete Society Technical Report No. 33, Concrete Society (Replaces Report 15, 1978).

Connolly, R.J. (1995) The spalling of concrete in fires, PhD Thesis, Aston University, Birmingham.

Cruz, C.R. and Gillen, M. (1980) Thermal expansion of Portland cement paste, mortar and concrete at high temperatures, Fire and Materials, **Vol. 4**, No. 2, 66-70.

Davis, H.S. (1967) Effects of high temperature exposure on concrete, Materials Research and Standards, **Vol. 7**, No. 10, 452-59.

Diederichs, U. & Schneider, U. (1981) Bond strength at high temperatures, Magazine of Concrete Research, **Vol. 33**, No. 115, 75-84.

Dougill, J. W. (1971) The effect of high temperatures on concrete with reference to thermal spalling, PhD Thesis, Imperial College, London.

Fischer, R. (1970) On the behaviour of cement mortar and concrete at high temperatures, Deutscher Ausschuss für Stahlbeton, Heft 214, W. Ernst und Sohn, Berlin, Germany.

Greig, N. (1982) Recommended guide-lines for fire damage assessment in structures, Cement and Concrete Association (50442).

Harada, T., Takeda, J., Yamane, S. & Furamura, F. (1972) Strength, Elasticity and Thermal properties of concrete subjected to elevated temperatures, American Concrete Institute SP 34, 377-406.

Harmathy, T.Z. & Berndt, J.E. (1966), Hydrated Portland Cement and Lightweight concrete at elevated temperatures, American Concrete Institute Journal, Title no. 63-4, 93-112.

Henstock, D. (1995) Investigation into the visual effects of heat on blended cement mortar, B Eng. Research project, Aston University.

Hsu, T.T.C. & Slate, F.O. (1963) Tensile bond strength between aggregate and cement paste or mortar, American Concrete Institute Journal, Title No. 60-25, 465-85.

Illston, J.M. (1994) Construction Materials - Their nature and behaviour, 2nd Edition, Chapman and Hall, London.

Ingburg, S.H. (1929) Influence of mineral composition of aggregates on fire resistance of concretes, ASTM Proceedings, **Vol. 29**, 824-29.

Isaaks, H. & Mohan Srivastava, R. (1989) An introduction to applied geostatistics, Oxford University Press.

Kaplan, M.F. & Roux, F.J.P. (1972) Effect of elevated temperatures on the properties of concrete for the containment and shielding of nuclear reactors, American Concrete Institute SP 34, Paper 24.

Kasami, H., Okuno, T. & Yamane, S. (1975) Properties of concrete exposed to sustained elevated temperatures, Transactions of the 3rd International Conference on Structural Mechanics in Reactor Technology, London, 1-5 September, **Vol. 3**, Part H 1/5.

Khoury, G.A., Sarshar, R., Sullivan, P.J.E. & Grainger, B.N. (1989) Factors effecting the compressive strength of unsealed cement paste and concrete at elevated temperatures up to 600°C, Submitted to the 2nd International Workshop on 'Mechanical behaviour of concrete under extreme thermal and hygral conditions.

Khoury, G.A., Grainger, B.N. & Sullivan, P.J.E. (1986) Strain of concrete during first cooling to 600°C under load, Magazine of Concrete Research, **Vol. 38**, No. 134, 3-12.

Kornerup, A. & Waneseker (1963) Methuen handbook of colour.

Lie, T.T. (1972) Fire and Buildings, Architectural Science Series, Applied Publishers, Ripple Road, Barking, Essex, England.

Lie, T.T. (1968) Fire resistance of Buildings, National Research Council of Canada, Ottawa, Technical Translation No. 1334.

Malhotra, H.L. (1956) The effect of temperature on the compressive strength of concrete, Magazine of Concrete Research, **Vol. 8**, No. 23, 85-94.

Mohamedhai, G. T. G (1986) Effect of exposure time and rates of heating and cooling on residual strength of heated concrete, Magazine of Concrete Research, **Vol. 38**, No. 136, September, 151-8.

Morley, P. D. & Royles, R. (1983) Response of the bond in reinforced concrete to high temperatures, Magazine of Concrete Research, **Vol. 35**, No. 123, June, 67-74.

Nassif, A. Y., Burley. E. & Rigden. S (1995) A new quantitative method for assessing fire damage to concrete structures, Magazine of Concrete Research, **Vol. 47**, No. 172, September, 271-8.

Neville, A.M. (1995) Properties of Concrete, 4th Edition, Longman Scientific and technical, Harlow.

Philleo, R. (1958) Some physical properties of concrete at high temperatures, American Concrete Institute Journal Proceedings, **Vol. 29**, No. 10, 857-64.

Placido, F. (1980) Thermoluminescence test for fire damaged concrete, Magazine of Concrete Research, **Vol. 32**, No. 111, 112-16.

Purkiss, J.A. (1996) Fire Safety Engineering - Design of Structures, Butterworth - Heinemann, Oxford.

Purkiss, J.A. & Bali, A. (1988) The transient behaviour of concrete at elevated temperatures up to 800°C, 10th Ibausil (Weiner), Hochscuhle für Architektur und Bauwesen, section 2/1, 245-63.

Riley, M.A. (1991) Possible new method for the assessment of fire-damage concrete, Magazine of Concrete Research, **Vol. 43**, No. 155, 87-92.

Rotasy, F.S., Weiss, R. & Wiedermann, G. (1980) Changes of pore structure of cement mortars due to temperature, Cement and Concrete Research, **Vol. 10**, No. 2, 157-64.

Saemann, J.C. & Washa, G.W. (1957) Variation of mortar and concrete properties with temperature, American Concrete Institute Journal, Title No 54-20, **Vol. 29**, No. 5, 385-95.

Schneider, U. (1989) Repairability of fire damaged structures (CIW W14 Report), Fire Safety, Vol. 16 (4), 251-336.

Schneider, U. (1986) Properties of Materials at High Temperatures - Concrete, 2nd edn, RILEM Report, Gesamthochschule Kassel, Germany.

Smith, L.M. (1983) The assessment of fire damage to concrete structures, PhD. Thesis, Paisley College of Technology.

Sullivan, P.J.E. (1979) The effects of temperature on concrete, F.D. Lydon (ed.), Developments in concrete technology, Applied Science Publisher Ltd., London, Chapter 1, 1-49.

Sullivan, P.J. & Poucher, M.P. (1971) The influence of temperature on the physical properties of concrete in, mortar in the range 20°C to 400°C, American Concrete Institute Journal, SP 25, Paper 4, 103-135.

Sullivan, P. J. E. (1970) The structural behaviour of concrete at elevated temperatures, PhD, University of London.

Watkeys, D.G. (1955) Non-destructive testing of concrete subject to fire attack, MSc. (Eng.) Thesis, University of London.

Weigler, H. & Fischer, R. (1972) Influence of high temperatures on strength and deformations of concrete, International Seminar on Concrete for Nuclear Reactors, American Concrete Institute SP34-26, 481-93.

Winslow, D.N. & Diamond, S. (1970) A Mercury Intrusion Porosimetry study of evolution of porosity in Portland Cement, Journal of Materials, **Vol. 5**, No. 3, 564-85.

Zoldners, N.G. (1960) Effect of high temperatures on concrete incorporating different aggregates, ASTM Proceedings, **Vol. 60**, 1087-108.

Appendix 1

Source and Composition of Cements

Ordinary Portland Cement (OPC)

Aston standard 4

Blue Circle Industries PLC, Blue Circle Cement

Cauldon Business Unit, Nr Stoke on Trent, Staffs.

Pulverised Fuel Ash (PFA)

Boral Pozzolanic Lytag

Cleveland House, Cleveland Road, Hemel Hempstead, Herts..

Source - Fiddlers Ferry

Ground Granulated Blast Furnace Slag (BFS)

Frodingham Cement Company, Appleby Group Limited

Brigg Road, Scunthorpe, South Humberside.

Chemical Compositions

	wt. %		
	OPC	PFA	BFS
SiO_2	20.2	48.2	35.51
Al_2O_3	5.6	38.2	12.59
Fe_2O_3	2.6	8.02	0.58
CaO	64.3	1.45	40.09
MgO	1.3	0.66	9.11
MnO			0.48
Na_2O	0.1	0.98	
K_2O	0.76	2.85	
LOi	0.80		
TiO_2		0.79	0.7
SO_3	3.2	0.52	0.15

Appendix 2

Source and Analysis of Aggregates

A2.1. Thames Valley coarse aggregate

Hatfield Quarry, St. Albans sand and gravel company Ltd.

Delamare Road, Chestnut, Waltham Cross, Herts.

Description - 20-5mm Shingle

Quantitative Analysis

	%
Flint	76
Quartzite	10
Quartz	11
Sandstone	2

Other of less than 1 % included Midstone, Spherulitic Quartz, Jasper, Weatherhead, Basalt.

Sieve Analysis

Sieve size(mm)	% Passing	Specification
37.5	100	100
28.0	100	
20	98	90-100
14	70	40-80
10	40	30-60
5	7	0-10

A2.2. Carboniferous Limestone aggregate

RMC Western Roadstone Limited, Avon Wickwar Quarry

The Downs Road, Wickwar, Wotton under edge, Gloucester.

Sieve Analysis

Sieve size (mm)	% Passing	Specification
37.5	100	100
20	99.6	95-100
10	42.0	30-60
5	4.8	0-10
0.75	1.0	

Chemical Composition

SiO_2	3.25
CaO	44.50
MgO	8.20
Loss of ign.	43.56
Al_2O_3	-
Fe_2O_3	0.49

Carbonate content

$CaCO_3$	78.80
$MgCO_3$	16.94
Silicates	4.24

A.2.3. Granite aggregate

Redlands Aggregates Limited, Central Region, Mountsorrel Quarry

Mountsorrel, Loughborough, Leics.

Chemical Composition

	% Dry Basis
LOI	0.75
Fe_2O_3	2.29
SiO_2	72.5
TiO_2	0.36
CaO	2.66
K_2O	3.70
Al_2O_3	13.5
MgO	1.09
Na_2O	3.00

A.2.4. Lytag

Supamix

Griff Lane, Griff Clara, Nuneaton, Warwickshire.

Description - 12 mm LYTAG

A.2.5. Sand

Hall Aggregates, Kingsmead Quarry Thames Valley.

Description - Medium zone sand

Sieve Analysis

Sieve size (mm)	% Passing
2.36	87
1.18	77
0.6	64
0.3	28

Appendix 3

Mix Designs and Quality Control

Series 1 - OPC / Thames Valley (S01)

Ref	A	F+G	H+I	J+K	LMN	OPQ	R	S	T	U
Cem. mat	OPC	OPC	OPC	OPC	OPC	OPC	OPC	OPC	OPC	OPC
Cem. content (kg)	296	304	302	302	302	302	301	298	302	301
Coarse agg. (20-5mm) (kg)	1247	1280	1273	1273	1273	1273	1266	-	1279	1273
Coarse agg. (10-5mm)(kg)	-	-	-	-	-	-	-	995	-	-
Fine agg (kg)	623	640	637	637	637	637	633	815	641	638
w/c ratio	0.70	0.66	0.66	0.66	0.66	0.66	0.66	0.76	0.66	0.66
Water (L/m^3)	206	199	198	198	198	198	197	226	200	199
F.W.D. (kg/m^3)	2374	2422	2410	2410	2410	2410	2397	2334	2422	2410
Initial slump (mm)	48	55	40	35	45	50	50	40	30	35
28 day C. Strength (N/mm^2)	45.5	-	-	-	43.5	45.5	49.5	29.4	-	-

Series 2 - OPC / PFA / Thames Valley (S02)

Ref	A	C+D	E+F	G+H	I+J	KLM	NOP	Q
Cem. mat	OPC/ PFA	OPC/ PFA	OPC/ PFA	OPC/ PFA	OPC/ PFA	OPC/ PFA	OPC/ PFA	OPC/ PFA
Cem. content (kg)	289	302	301	300	296	301	301	304
Coarse agg. (20-5mm)(kg)	1227	1280	1281	1275	1255	1278	1277	1279
Fine agg. (kg)	611	638	638	635	625	637	637	638
w/c ratio	0.63	0.63	0.63	0.62	0.62	0.62	0.60	0.61
Water (L/m^3)	182	190	190	187	184	187	181	184
F.W.D. (kg/m^3)	2309	2409	2410	2397	2359	2403	2397	2403
Initial slump (mm)	50	40	55	70	50	60	45	45
28 day C. Strength (N/mm^2)	33.5	-	-	-	34.5	37.5	37.0	38.5

Series 3 - OPC / BFS / Thames Valley (S03)

Ref	A+B	C+D	E+F	G+H	I
Cem. mat.	OPC/ BFS	OPC/ BFS	OPC/ BFS	OPC/ BFS	OPC/ BFS
Cem. content (kg)	300	300	296	296	299
Coarse agg. (20-5mm)(kg)	1272	1270	1258	1258	1267
Fine agg. (kg)	634	633	627	627	631
w/c ratio	0.64	0.65	0.65	0.65	0.65
Water (L/m^3)	191	194	192	192	194
F.W.D. (kg/m^3)	2397	2397	2372	2372	2391
Initial slump (mm)	65	50	50	45	40
28 day C. Strength (N/mm^2)	-	34.0	-	-	33.5

Series 4 - OPC / Limestone (S04)

Ref	A+B	C+D	E+F	G+H
Cem. mat.	OPC	OPC	OPC	OPC
Cem. content (kg)	312	311	311	311
Coarse agg. (20-5mm)(kg)	1264	1257	1256	1259
Fine agg. (kg)	711	707	706	708
w/c ratio	0.66	0.64	0.65	0.65
Water (L/m^3)	205	198	201	201
F.W.D (kg/m^3)	2491	2473	2473	2479
Initial slump (mm)	60	35	50	40
28 day C. Strength (N/mm^2)	49.0	-	-	53.0

Series 5 - OPC / Granite (S05)

Ref	A+B	C+D	E+F	G+H
Cem. mat.	OPC	OPC	OPC	OPC
Cem. content (kg)	300	303	300	302
Coarse agg. (20-5mm)(kg)	1213	1225	1215	1222
Fine agg. (kg)	682	689	684	687
w/c ratio	0.65	0.64	0.64	0.64
Water (L/m^3)	195	193	192	193
F.W.D. (kg/m^3)	2391	2410	2391	2404
Initial slump (mm)	65	45	45	55
28 day C. Strength (N/mm^2)	45.5	-	-	-

Series 6 - OPC / Lytag (S06)

Ref	A+B	C+D	E+F	G+H
Cem. mat.	OPC	OPC	OPC	OPC
Cem. content (kg)	306	307	305	306
Coarse agg. (20-5mm)(kg)	668	668	665	666
Fine agg. (kg)	777	777	774	776
w/c ratio	0.75	0.75	0.78	0.77
Water (L/m^3)	230	230	237	234
F.W.D. (kg/m^3)	1981	1981	1981	1981
Initial slump (mm)	30-50 shear	30	100 coll-apse	40 true
28 day C. Strength (N/mm^2)	39.5	-	-	40.3

Appendix 4

Mechanical Results

Ref.	C. Strength (MPa) 60 Day	UPV (Km/s)	Flexural (N/mm^2)	Schmidt Hammer	Dy. E (MN/ mm^2)
Series 1 - OPC / Thames Valley					
Av. (con)	56	4.7	6.3	33	
S01/A (con)	54.5	4.6	7.1	33	35000
S01/J (con)	57.5	4.7	5.4	32	
S01/I (250°C)	52.5	3.2	2.8	27	14000
S01/G (300 C)	50.0	2.8	1.6	27	8500
S01/F (350°C)	47.5	2.5	1.2	23	6000
S01/H (400°C)	36.5	2.2	1.0	20	2500
S01/K (500°C)	22.0	0.9	0	11	500
Series 2 - OPC / PFA / Thames Valley					
Av. (con)	45.0	4.6	3.5	29	
S02/A (con)	45.0	4.6	3.7	29	42500
S02/J (con)	45.0	4.5	3.3	28	
S02/H (175°C)	49.0	3.7	3.1	27	
S02/G (250°C)	44.5	3.1	2.0	22	12000
S02/E (300°C)	45.0	2.6	1.4	22	6000
S02/D (350°C)	39.5	2.0	0.7	20	4500
S02/C (400°C)	33.0	1.6	0	16	
S02/I (450°C)	25.0	1.1	0	13	500
S02/F (500°C)	14.0	1.3	0	0	0

Ref.	C. Strength (MPa) 60 Days	UPV (Km/s)	Flexural (N/mm^2)	Schmidt Hammer	Dy.E (MN/ $mm^{2)}$
Series 3 - OPC / BFS / Thames Valley					
S03/C (con)	44.0	4.5	3.1	25	39500
S03/E (175°C)	54.0	3.5	2.7	25	21000
S03/B (250°C)	47.0	2.9	1.6	23	12000
S03/A (300°C)	41.0	2.3	1.2	21	7000
S03/D (350°C)	42.5	2.0	0.7	19	4500
S03/H (450°C)	28.5	1.4	0	11	1000
S03/G (500°C)	18.5	1.7	0	0	500
S03/F (700 C)	11.5	0	0	0	0
Series 4 - OPC / Limestone					
Av (con)	54.5	5.0	6.1	26	
S04/A (con)	53.5	5.0	6.4	23	
S04/H (con)	54.5	5.0	5.7	28	48000
S04/B (250°C)	52.0	3.0	2.8	24	16500
S04/C (300 C)	52.0	2.7	1.3	21	12000
S04/D (350 C)	47.0	2.3	1.2	20	7500
S04/E (450°C)	36.0	1.4	0.4	15	2500
S04/G (500°C)	25.5	1.2	0	13	2500
S04/F (700°C)	22.5	0.7	0	10	2500

Ref.	C. Strength (MPa) 60 Days	UPV (Km/s)	Flexural (N/mm^2)	Schmidt Hammer	Dy. E (MN/mm^2)
Series 5 - OPC / Granite					
Av (con)	49.0	4.8	4.2	25	
S05/A (con)	46.5	4.8	4.2	26	45000
S05/H (con)	51.5	4.7	4.2	24	
S05/B (200°C)	53.5	3.5	2.6	25	23500
S05/C (300°C)	52.5	2.8	1.7	23	15000
S05/G (350°C)	51.5	2.3	1.2	21	8500
S05/D (400°C)	48.0	2.1	1.0	22	7500
S05/E (500°C)	30.0	1.3	0	14	2500
S05/F (700 C)	23.5	0.5	0	10	500
Series 6 - OPC / Lytag					
Av (con)	45.5	4.1	5.3	25	26000
S06/A (con)	45.0	4.1	5.5	24	28000
S06/H (con)	45.5	4.0	5.1	25	25000
S06/B (250 C)	46.5	2.9	2.9	25	13000
S06/C (300 C)	51.0	2.7	2.0	26	11000
S06/D (350°C)	46.5	2.4	1.2	23	7000
S06/E (450°C)	25.5	1.6	0	15	2000
S06/F (500°C)	27.5	1.4	0	14	1500
S06/G (700°C)	17.5	1.0	0	10	0

Appendix 5

Papers Published and submitted from the study

Appendix 5 contains four papers published in advance of this thesis based on results obtained during the research programme.

These are :

1. Guise, S.E., Short, N.R. and Purkiss, J.A. (1996) Colour analysis for assessment of fire damaged concrete, Proceedings of the International Conference Concrete in the Service of Mankind, Concrete Repair, Rehabilitation and Protection, University of Dundee, Scotland, 24-28 June 1996, pp 53-63, Edited by R. K. Dhir & M. R. Jones, E & FN Spoon.

2. Short, N.R., Guise, S.E., and Purkiss, J.A. (1996) Assessment of fire damaged concrete using colour analysis, Interflam 96', Proceedings of the 7th International Fire Science and Engineering Conference, Cambridge, 26-28 March 1996, pp 927-31, Interscience Communications, London.

3. Guise, S.E., Short, N.R. and Purkiss, J.A. (1996) Petrographic and colour analysis for assessment of fire damaged concrete, Proceedings of the 18th Conference on Cement Microscopy, Houston, Texas, 21-25 April, 1996, ICMA, Texas, 1996, pp 365-72. Eds. L Jany, A Nisperos and J Bayles, International Cement Microscopy Association, Ducanville, Texas, 1996.